



エンドミル加工における加工誤差予測のための複合モデリング

メタデータ	<p>言語: English</p> <p>出版者:</p> <p>公開日: 2022-12-19</p> <p>キーワード (Ja): 加工誤差, 複雑な加工現象, 小ロット生産, 柔軟弾性体エンドミル加工, モデルベース加工誤差制御, 統計的アプローチ</p> <p>キーワード (En): Machining error, Complex machining phenomenon, Small-lot production, Elastomer end-milling, Statistical approach</p> <p>作成者: アディレーク, チャイナワカル</p> <p>メールアドレス:</p> <p>所属:</p>
URL	https://doi.org/10.15118/00010867

Compositional Modelling for Machining Error Prediction in End-milling Process

*A dissertation submitted in partial fulfillment
of the requirements to*

MURORAN INSTITUTE OF TECHNOLOGY



for the degree of

DOCTOR OF ENGINEERING

In the Advanced Production Systems Engineering

Chainawakul Adirake

Doctoral Program, Graduate School of Engineering
September 2022

博士学位論文

エンドミル加工における加工誤差予測のための 複合モデリング



室蘭工業大学大学院 工学専攻

先端生産システム工学コース

チャイナワクル アデイレーク

令和4年9月

“Passion, Mission, Profession, Vacation”

A reason for being

IKIGAI

生き甲斐



侘寂

WABI-SABI

Impermanent and Imperfect

“Nothing lasts, nothing is finished, and nothing is perfect”

Declaration

I hereby declare that this dissertation was composed by myself. The work contained herein is my own except where explicitly stated otherwise in the text. And that this work has not been submitted for any other degree or professional qualification except as specified text. I confirm that the work submitted is my own, except where work that has formed part of jointly-authored publications has been included. My contribution and those of the other authors to this work have been explicitly indicated as specified text. I confirm that appropriate credit has been given within this dissertation where reference has been made to the work of others.

Chainawakul Adirake
Manufacturing Engineering Laboratory (MEL)
Muroran Institute of Technology
Hokkaido, JAPAN
September 2022

Acknowledgement

First of all, I would like to express my sincere gratitude to the Royal Thai Government for science and technology scholarships, the Royal Thai Government authorities' development scholarship program, funded by the Office of Civil Service Commission (OCSC), and partner organizations, the Office of Educational Affairs, Royal Thai Embassy of Japan.

Importantly, I am extremely highly grateful to my esteemed advisor, Prof. TERAMOTO Koji (教授: 寺本 孝司), for his invaluable supervision, continuous support, and patience during my Ph.D. program. His excellent experience has encouraged me entirely throughout the time in my academic research, career, and daily life during the Covid-19 situation, which was difficult. Furthermore, I gratefully to Prof. KAZAMA Toshiharu (教授: 風間 俊治) and Prof. FUJIKI Hiroyuki (教授: 藤本 裕行) for being my advisors with their immense knowledge, support, and guidance for thoughtful comments and suggestions in this dissertation.

Furthermore, I would like to thank my great tutor Mr. NAKAO (中尾さん) for his helpful and always support for all my activities and troubles. Likewise, thanks to Mr. HIBINO (日比野さん), Mr. HIRATA (平田さん), Ms. UEDA (上田さん), and Ms. WU (呉さん) for their kindness in helping with the language barrier. I also appreciate my fellow international friends for entire of their consistent support. I would also like to thank Mr. ARAKI (荒木さん), Mr. WU (呉さん), and Mr. KATSUBE (勝部さん) for their experiments and programming on technical support in my research. I sincerely thank you for Arai Yoshio Memorial Foundation (荒井芳男記念財団) and KAKENHI Grant (科学研究費) Number 19K04119 for their research fund support.

I am fortunate to have been a part of the Manufacturing Engineering Laboratory (MEL) member and would like to thank all the members for their kind help and support that have made my study and life in Japan a wonderful time. Moreover, thank you to every Thai student in Muroran for their living help, suggestion, and sharing of gleeful moments. I would also like to thank you for the entire support of the Office of Educational Affairs officers, the Royal Thai Embassy of Japan, and the International Relations Center of Muroran Institute of Technology.

My sincere acknowledgment is extended to my colleagues and members in the Tools and Die Engineering division, the Industrial Engineering department, the Faculty of Engineering, the Human Resource Department, and elsewhere in the Rajamangala University of Technology Lanna. For their providing encouragement and offering an opportunity for my study abroad.

Finally, I would like to express my deepest gratitude to my beloved family, wife, and son for their love and care which was a source of motivation throughout my studies. Without their tremendous understanding and encouragement over the past few years, it would be impossible for me to complete my study.

Chainawakul Adirake
Manufacturing Engineering Laboratory (MEL)
Muroran Institute of Technology
Hokkaido, JAPAN
September 2022

チャイナワクル アディレーク
生産加工学研究室
室蘭工業大学
北海道、日本国
令和 4 年 9 月

Abstract

Machining is a method that important to the manufacturing process in the industry. Productivity and product quality are always concerned with significant issues in manufacturing technologies. Modern manufacturing aims to improve the machining accuracy and efficiency of parts and products. However, machining variables involve the complex machining phenomena that usually generates process limitations and reduces product quality. Machining error is one of responsiveness in complex machining phenomena. It has directly influenced by varying cutting conditions, workpiece shape, material characteristics, cutting force, and workpiece deformation. Therefore, a reliable method for predicting machining errors is essential to solving these requirements.

Small-lot production has attracted attention in the new tendency of manufacturing. Due to the changing consumer behavior, the personalized, high-quality, and technology trends require the service of direct-to-consumer manufacturing. Product prototype and mould making for mass production are regarded as small-lot production that suitably serves by milling process. On the other hand, end-milling is also a capable method for direct operating on parts or products with a large variety of materials. This method does not require expensive and time-consuming preparation. This research deals with a machining error modelling for the end-milling of elastomer material because it's uniquely elastic deformation, crack generation, and difficult to control machining error. Conventional control method of machining error in elastomer end-milling has been studied with a limitation because most machining services of the elastomeric parts are based on enterprise-dependent dexterities or know-how. Therefore, this material has been selected to be a case study in this research.

In order to secure machining accuracy and control the phenomenon, this dissertation proposes the machining error models through a systematic framework for machining error modelling. In the framework, the candidates of model variables are evaluated based on the preliminary experiments. Candidate variables are the cutting conditions and physical state variables such as workpiece deformation and cutting force. The proposed models are constructed by conventional data-centric approach, mechanistic knowledge-based approach, and principal component analysis (PCA) based statistical approaches. The correlation

coefficient and multiple regression method are employed to compute the model's coefficient and form the linear regression model. Three different models: the conventional cutting condition model, mechanistic model, and statistical model are constructed. At the statistical model construction, a proposed systematic procedure to determine the effective variable is utilized. Afterward, the models are investigated by using larger experimental cases as the evaluation experiment. From the experimental results, the models could generate a comparison between calculated and measured machining errors. In addition, the statistical model provides relatively good agreement. Therefore, it could be confirmed the proposed machining error modelling.

Keywords: Machining error, Complex machining phenomena, Small-lot production, Elastomer end-milling, Conventional control method, Mechanistic knowledge-based, Statistical approach

概要

機械加工は、製造業における部品製造プロセスとして重要な加工方法です。生産性と製品品質は、常に製造技術の重要な課題として考えられてきました。現代の製造業は、部品や製品の加工精度と効率を向上させることを求められています。機械加工プロセスには、複雑な加工現象が含まれ、多くの場合ではプロセスの制約が発生し、製品の品質が低下します。加工誤差は、複雑な加工現象の代表的なもののひとつであり、切削条件、工作物形状、材料特性、切削抵抗、工作物変形などの変化に影響されます。したがって、これらの要件を解決するには、加工誤差を予測するための信頼できる方法が不可欠です。

新たな製造業のトレンドとして、小ロット生産が注目されています。消費者の行動の変化により、個人化された高品質の製品が求められる傾向が高まり、消費者と直結した製造サービスが提案されています。また、大量生産のための製品試作や金型製作も、エンドミル加工によって実現される小ロット生産といえます。エンドミル加工は、多種多様な材料を使用した部品や製品を直接加工するための有効な方法です。この加工方法は、費用と時間のかかる金型の準備を必要としません。この研究では、柔軟弾性体のエンドミル加工における加工誤差モデリングを扱います。これは、柔軟弾性体が独特の弾性変形特性と亀裂の発生形態を有し、加工誤差の制御が難しいためです。柔軟弾性体エンドミル加工における加工誤差の従来の制御方法は、柔軟弾性体部品の機械加工サービスを提供する企業のノウハウに依存し、体系的な研究は十分なされていません。したがって、本論文は、提案する加工誤差モデル化手法の対象として柔軟弾性体のエンドミル加工を対象とすることにしました。

加工精度を確保し、加工プロセスを制御するために、本論文では、加工誤差モデリングのための体系的なフレームワークをもとにした加工誤差モデルの構築手法を提案します。提案するフレームワークでは、モデル変数の候補は予備実験に基づいて評価されます。候補となるモデル変数は、切削条件と、工作物の変形や切削抵抗などの物理的状態変数です。提案されたモデルは、従来のデータ中心のアプローチ、経験的な知識を基にしたアプローチ、および主成分分析 (PCA) を基にした統計的アプローチによって構築されます。モデルの係数を計算し、線形回帰モデルを形成するために、相関係数と重回帰法が採用されています。従来の切削条件ベースモデル、経験的モデル、統計ベースモデルの 3 つの異なるモデルが構築されます。統計モデルの構築では、有効変数を決定するために提案された体系的な手順が利用されます。その後、評価実験としてより大きな実験事例を用いてモデルの妥当性を評価し

ます。実験結果は、提案手法により構築されたモデルを用いて計算された加工誤差と測定された加工誤差の比較に用います。比較の結果として、提案手法を基にした統計ベースモデルは実験結果と最も良好な一致を示しました。以上の結論として、提案された加工誤差モデリング手法の妥当性を確認することができました。

キーワード：加工誤差、複雑な加工現象、小ロット生産、柔軟弾性体エンドミル加工、モデルベース加工誤差制御、統計的アプローチ

Contents

Declaration	i
Acknowledgement	ii
Abstract	iii
Contents	iv
List of Figures	v
List of Tables	vi
List of Abbreviations	vii
1. Introduction	1
1.1 Background of Research	1
1.1.1 Manufacturing processes in modern production	1
1.1.2 Machining Error in End-milling Process	4
1.1.3 Machining Error in Elastomer End-milling	6
1.2 Purpose and Outcomes of Dissertation	8
1.3 Structure of Dissertation	8
2. Literature Review	11
2.1 Small-lot Manufacturing	11
2.2 Machining Error	12
2.2.1 Machining Process Classification	12
2.2.2 Conventional Machining Process	13
2.2.3 Machining Accuracy and Surface Quality	14
2.2.4 Cutting Phenomena	14
2.2.5 Orthogonal Cutting Model	16
2.2.6 End-milling Process	17
2.2.7 Cutting Force and Deformation in Milling	18
2.3 Elastomer End-milling	22
2.3.1 Cutting Force and Deformation Studies in Elastomer Milling	23
2.3.2 Machining Error Studies in Elastomer End-milling	25

2.4	Statistics Implementation	34
2.4.1	Principle Component Analysis	34
2.4.2	Correlation Coefficient	35
2.4.3	Multiple Regression Analysis	36
3.	Framework for Machining Error Modelling	38
3.1	A Framework of Machining Error Modelling	39
3.2	Evaluation of Machining Error Model	42
4.	Compositional Machining Error Prediction Model	44
4.1	Experimental Setup and Configurations	46
4.2	Preliminary Experiment	47
4.3	Conventional Cutting Conditions Model	48
4.4	Mechanistic Model	49
4.5	Statistical Model	50
4.6	Machining Error Calculation	57
4.6.1	Model Coefficient Calculation	58
4.6.2	Multiple Regression Calculation	58
5.	Evaluation Experiment and Results Discussion	62
5.1	Evaluation Experiment	62
5.2	Machining Error Prediction Results	63
5.2.1	Machining Error of Conventional Model	64
5.2.2	Machining Error of Mechanistic Model	65
5.2.3	Machining Error of Statistical Model	66
5.3	Results Discussion	67
6.	Conclusion and Further Aspect	68
6.1	Conclusion	68
6.2	Further Aspect	69
	Bibliography	70
	Appendix	76
	Publication	87

List of Figures

1-1	Factors and contributions of machining phenomena	5
1-2	Error generation phenomenon in elastomer	6
1-3	Structure of the dissertation	10
2-1	Machining process classification	12
2-2	Conventional machining operation	13
2-3	Cutting Phenomena	16
2-4	Orthogonal cutting model	17
2-5	Process of up-milling and down-milling	18
2-6	Merchant's circle diagram	19
2-7	Instantaneous cutting force in end-milling	21
2-8	Interrelationship of cutting force in end-milling	21
2-9	Elastomer end-milling simulation model	23
2-10	Systematic model construction procedure	24
2-11	Workpiece with marker film for machining observation	29
2-12	Behavior observation during machining	29
2-13	Tracking screen using software analyzer	30
2-14	Schematic of machining error measurement	31
2-15	Machining and measurement configuration	31
2-16	Machined workpiece on a metallic base	32
2-17	Measurement area for machined workpiece	32
2-18	Processed surface shape evaluation	33
2-19	Machining error measurement	33
3-1	A mapping function of compositional modelling	38
3-2	Framework of machining error modelling	40
3-3	Evaluation of machining error model	43
4-1	Instruments setup schematic	46
4-2	Actual experimental setup	47
4-3	Example of program coding for PCA approach	52
4-4	Standardization of target data (factor_analysis.csv)	52

4-5	Calculation of principal component score	52
4-6	A plot of principal component score	53
4-7	All principal component score plot	53
4-8	Contribution rate from PCA	54
4-9	Cumulative contribution rate of main components	54
4-10	The eigenvalues of main components	55
4-11	Eigenvectors for each principal component condition	55
4-12	Coordinated eigenvectors of variables related to PC1 and PC2	56
4-13	Principal Component observed variable contribution	56
4-14	Normal probability of the conventional model	59
4-15	Normal probability of the mechanistic model	60
4-16	Normal probability of the statistical model	61
5-1	Measured machining error comparison of the conventional model	64
5-2	Measured machining error comparison of the mechanistic model	65
5-3	Measured machining error comparison of the statistical model	66
B-1	Normal probability of the conventional model for preliminary	79
B-2	Preliminary machining error comparison of the conventional model	80
B-3	Normal probability of the mechanistic model for preliminary	81
B-4	Preliminary machining error comparison of the mechanistic model	81
B-5	Normal probability of the statistical model for preliminary	82
B-6	Preliminary machining error comparison of the statistical model	83

List of Tables

1-1	Main types of manufacturing processes and their sub types	2
2-1	Experimental instruments, materials and their specification	26
4-1	Machining conditions for preliminary experiment	47
4-2	Machining error prediction model's variable coefficients	58
4-3	Multiple regression analysis of the conventional model	59
4-4	Multiple regression analysis of the mechanistic model	60
4-5	Multiple regression analysis of the statistical model	61
5-1	Machining conditions for evaluation experiment	63
5-2	Comparison of machining error	67
A-1	Machining error obtained from preliminary experiments	76
A-2	Machining error obtained from evaluation experiments	77
B-1	Multiple regression analysis of the conventional model for preliminary	79
B-2	Multiple regression analysis of the mechanistic model for preliminary	80
B-3	Multiple regression analysis of the statistical model for preliminary	82
C-1	PCA source code using Python	84

List of Abbreviations

α	:	Rake angle (in Chapter 2)
α	:	Coefficient of the conventional cutting conditions model (in Chapter 4)
β	:	Clearance angle (in Chapter 2)
β	:	Coefficient of the mechanistic model (in Chapter 4)
γ	:	Coefficient of the statistical model (in Chapter 4)
δ	:	Objective variable (in Chapter 2)
δ	:	Machining error (in Chapter 4)
θ	:	Tool rotation angle
λ	:	Eigenvalue of A
ϕ	:	Shear angle
A	:	Width of workpiece
ADM	:	Additive Manufacturing
ANOVA	:	Analysis of Variance
$a(\theta)$:	Axial depth of cut
b_0	:	Constant (intercept)
b_p	:	Regression coefficients
D	:	Depth of cut
DoC	:	Depth of cut
df	:	Degree of freedom
Eq.	:	Equation
F	:	Friction force at chip-tool interface (in Chapter 2)
F	:	Feed rate of cutting (in Chapter 4)
F	:	F-test statistic (in Chapter 4)
$F_{aj}(\theta)$:	Tool axial force
F_m	:	Direction of force
F_n	:	Normal force
$F_{rj}(\theta)$:	Tool radial force
$F_{tj}(\theta)$:	Instantaneous cutting forces of the cutting edge tangential force
F_s	:	Shear force

FEM	:	Finite Element Methodology
Fig	:	Figure
f	:	Force
f_x	:	Cutting forces at a surface generation moment of x direction
f_y	:	Cutting forces at a surface generation moment of y direction
H	:	Height of workpiece
$h(\theta)$:	Cut thickness
j_{th}	:	Cutting edge number
K_{rc}, K_{re}	:	Cutting coefficients of cutting force in end-milling
K_{tc}, K_{te}	:	Cutting coefficients of cutting force in end-milling
L	:	Length of workpiece
L_c	:	Contact length
l_{sl}	:	Sliding length
l_{st}	:	Sum of sticking
M/C	:	Machining
M.E.	:	Machining Error
MS	:	Mean square
MTO	:	Make to order
N	:	Normal rake face
n	:	Total number of data
PC1	:	First principal component
PC2	:	Second principal component
PC	:	Principal Component
PCA	:	Principal Component Analysis
P-value	:	Probability value of obtaining test results of observed data
p	:	Dimension in the multiple regression analysis
R	:	Pearson's correlation (in Chapter 2)
R	:	Rotational speed of spindle (in Chapter 4)
RPM	:	Revolution per minute

r	:	Correlation coefficient of x and y
SS	:	Sum of square
S_x	:	Standard deviation of x
S_y	:	Standard deviation of y
S_{xy}	:	Covariance of x and y
t	:	Thickness (in Chapter 2)
t_{Stat}	:	T-test statistic
t_c	:	Deformed chip
W	:	Width of cut
WoC	:	Width of cut
WP	:	Workpiece
X, x	:	X-axis direction
X^{\rightarrow}	:	Eigenvector of A
x_i, y_i	:	i^{th} data value
x_p	:	Explanatory variables
\bar{x}	:	Average of x
Y, y	:	Y-axis direction
\bar{y}	:	Average of y
Z	:	Z-axis direction

1. Introduction

This chapter will provide an initiative to the study by first discussing the research background and context, followed by the purpose of the research and its outcome. Afterward, the structure of the dissertation will be expressed.

1.1 Background of Research

1.1.1 Manufacturing processes in modern production

Manufacturing is a critical part of any economy, whether still developing or already advanced. This sector has been at the top of the changing global trends over the recent decades. As a continuously competitive circumstance, several developing economies emerged as prominent manufacturing nations. Their demand decreased during a recession, and employment in manufacturing fell rapidly in advanced economies. Consumers' requirements have become increasingly diverse. The manufacturers must decide to enhance their services to modernize production and respond to those specific needs. The popularization of these specialty manufacturers has been part of a growing trend that drew the maker closer to the consumer than ever before. Consumers are now searching out the products they desire rather than just taking from the manufacturers' offers. Due to the changing behavior of consumers and economic tendencies, the Covid-19 pandemic, the rising cost of labor, the growth of e-commerce and mobile technology will lead more attention to small-lot production, batch production, or direct-to-consumer manufacturing. The product life cycle will be shorter. Consumers are drawn more towards personalized, high-quality goods with a mark of craftsmanship and an environmentally friendly approach to production. [1-2]

As the continuing revolution of the manufacturing industry and the role of technology are increasing, the variety of tools and materials could deliver products to the customer faster. Many significant trends are shaping manufacturing in the present day, for example; [3-4]

- **Increased Focus on Skills** - the opportunity to learn new knowledge and skills to fill the gap in the industry increased the level of expected skills

- **Additive Manufacturing** - three-dimensional objects and shapes are created by adding layers opposed to the more traditional subtractive manufacturing. This method allows manufacturers rapidly produce prototypes for their designers and engineers. Its recent affordability has been a great driver of its growth and its role in helping smaller suppliers take more control of their manufacturing
- **Advanced Automation** - artificial intelligence, sensors, and vision systems are just a couple of ways that basic automated systems can be transformed into advanced automation with a lot of technology available today at a very reasonable price
- **Smart Machinery** - machine-to-machine communication is part of data-driven manufacturing. Besides, the Internet of Things is expected to provide data analytics and inventory data to companies in real-time

Regarding the mentioned trends above, there are many conventional manufacturing methods consisting of forming, joining, coating, casting, moulding, machining, and 3D printing with the subtypes of each process as shown in **Table 1-1**. [5-6]

Table 1-1 Main types of manufacturing processes and their sub types

Main Type	Sub Type	Description	Advantage & Limitation
Forming	Forging, Stamping	A manufacturing process uses suitable	It can be processed with
	Bending, Shearing,	stresses such as compression, tension,	high precision but cannot
	Grinding	or shear to deform the material and get the desired shape. This process involves deformation and displacement of material leads to no material removal or loss of material.	process with complex shapes.
Joining	Welding, Soldering,	A joining or assembling process is part	Necessary for assembly
	Adhesive Joining,	of every production process where two	works. Needed high level
	Brazing, Fastening,	or more parts are combined together to	of skills for welding
	Mechanical Assembly	get the required product.	Health risks from welding fume.
Coating	Powder Coating,	A method of covering the part surface	Necessary for protecting
	Sputter Deposition,	with powder or zinc or other chemicals	products from corrosion.
	Electroplating	to protect it from corrosion, wear, and other defects. It is also to improve the material electrical conductivity or magnetic response.	Risk of asthma and skin irritation, and skin sensitization.

Table 1-1 Main types of manufacturing processes and their sub types (cont.)

Main Type	Sub Type	Description	Advantage & Limitation
Casting	Centrifugal Casting,	A process that pours liquid metal into a mould containing the hollow shape of the desired outcome.	Suitable to provide a basic shape and size to the product, but mostly it cannot provide complex shapes, intricate details and smooth surfaces in mass production.
	Die and Mould Casting,		
	Sand Casting,		
	Shell Moulding		
Moulding	Injection Moulding,	A manufacturing process that uses a rigid frame to shape hot liquid or ductile raw material. It is mostly used to manufacture plastic products.	Suitable for mass production but unsuitable for small-lot production because it will take cost and time.
	Blow Moulding,		
	Extrusion Moulding,		
	Rotational Moulding,		
	Thermoforming, Powder Metallurgy		
Machining	Milling, Turning,	A manufacturing process is used to cut a piece of raw material into the desired shape and size with the help of a controlled material removal process. These processes are based on a common theme known as subtractive manufacturing and are used for all genres of products, especially metal products.	Compatible with various materials, shapes, and small-lot production or prototype. The error involved many factors as machining error.
	Drilling, Shaping,		
	Honing, Finishing		
Additive Manufacturing	3D Printing, Rapid Prototyping, Direct Digital Manufacturing, Additive Fabrication	A manufacturing process which is reversible to subtractive manufacturing of machining. It can build 3D objects by adding layer-upon-layer of material, whether the material is plastic, metal, or concrete.	This technology is growing at speed due to its high efficiency and accuracy.

Ordinary manufacturing is traditional mass production in which molding became important role-playing. Manufacturing repetitive parts and components with common shapes or even complex shapes are required time and cost-consuming mould. On the other hand, a product prototype, job shop manufacturing, and batch production are suitable with rapid production for cost reduction. However, 3D printing or additive manufacturing involves the genre of

materials limitations it can process. Therefore, some small-lot production or specific products such as mould making (core and cavity), personal dental, and medical parts needed the machining methods. [7-9]

1.1.2 Machining Error in End-milling Process

The modelling of machining operations has been evolving as a necessary engineering tool for simulating the operational physics ahead of costly production trials of parts used in the industry [22]. For achieving an accurate machining process, the model-based approaches are sought as an alternative method of trial-and-error concepts. These notions are interesting and investigated by researchers in many recent years. These lofty scrutinizes indicate that a model-based approach must be promising. For these reasons, predictive models are constantly being developed by estimating predicted machining errors with experimental results.

In traditional machining, material removal is accompanied by the formation of chips, the machining process is an essential source of innovation and significantly contributes to research and development, increasing productivity and quality of products. Machining accuracy affects product quality, caused of the significant process parameters. The parameters involved material removal volumes that influence the process precision. These obtained effective outcomes such as an affected layer, surface roughness, and machining error. A machining prediction model is required to reduce the cost and time of machining. Nonetheless, good surface quality is indispensable.

Direct machining to raw materials is desirable for small-lot production in order to avoid the cost and time consuming of mould production. The typical conventional researches of machining processes are investigation of the single physical phenomenon affected by physics-based factors such as cutting force, vibration, thermal expansion. However, considering influences from the multiple physical phenomena is also necessary. In these phenomena, more determinants than single physical aspect involved the machining error, surface roughness, and other contributions consisting of the cutting force, workpiece deformation, chip separation, and machining conditions. In order to find the direct relations between machining conditions and the target values that correspond to the complex phenomena, by considering the single and multiple phenomena, there are previous researches that attempted to investigate machining process modelling prediction. **Figure 1-1** shows the relation of factors and contributions that influenced machining phenomena. [10-13]

Complex machining phenomena are affected by varying determinants such as cutting conditions, workpiece shape, and material characteristics. There are three categories of approaches for investigating the phenomena included physics-based, data-centric, and mechanistic. Firstly, based on computational mechanics such as Finite Element Method (FEM) analysis. Second, utilize statistics to find direct relations between machining conditions and values that represent phenomena. Finally, combine empirical knowledge and appropriate numbers of preliminary experiments. Recently, the second approach has become dramatic for accurately predicting in order to find direct information to control complex phenomena. However, it is unable to be applied against machining because it requires huge amount of learning data set which is difficult to prepare for a variety of wildly different workpiece shapes and different machining methods.

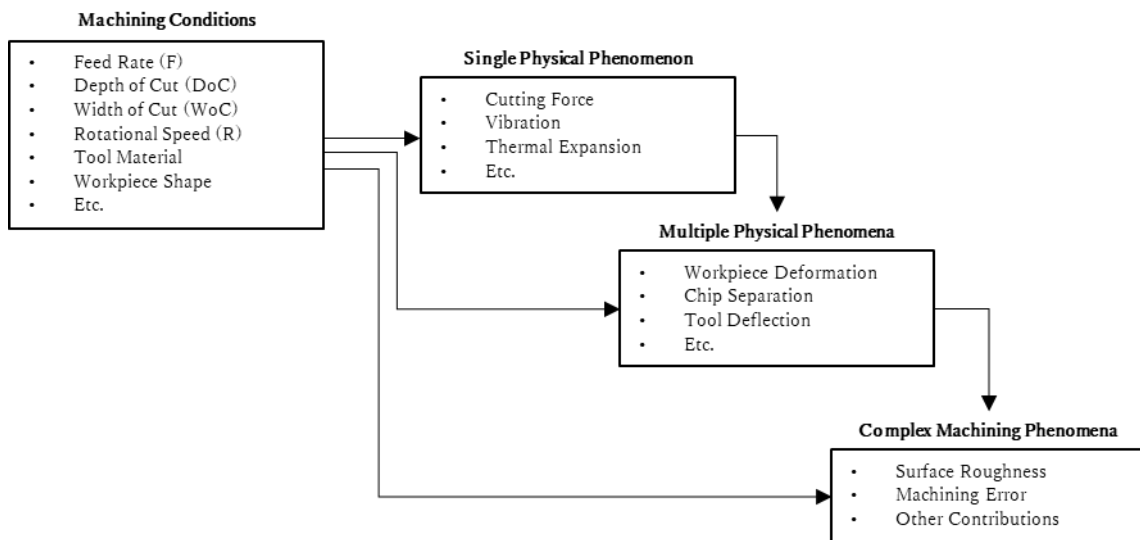


Fig. 1-1 Factors and contributions of machining phenomena

In order to eliminate the error from the machining process, it is necessary to secure machining accuracy. These essential parameters affect complex machining phenomena. For this reason, various machining scenarios are studied and proposed by researchers. A compositional machining simulation framework [14-16] presented the possibility of generating machining errors with predictive methods for standard metal cutting processes. It is planned to assume that the workpiece has good rigidity and perfect shape transfer. Low rigidity and different fracture mechanisms lead to large machining error. Regarding a physics-based approach, the analysis of workpiece deformation, chip separation, the cutting force has become seriously

studied in soft materials [17-20]. Recently, a mechanistic approach was proposed for model-based prediction of machining error in elastomer end-milling [21]. On the other hand, the data-centric method has become mainly investigated because of the expectation to find direct information to control the phenomena. Machine learning has become popular role-playing to assist in terms of data analytics and statistical methods. However, big data sets and massive preparations are needed. In addition, machine learning also requires time and resources because there are complicated methods. Therefore, the proper modelling with the minimum preparation has eagerly required for predicting complex phenomenon such as machining error, surface roughness, and workpiece quality. A systematic construction of compositional model based on the statistical evaluation is a promising approaches because aggregated models of aspect models which correspond to each single phenomenon are expected to represent characteristics of complex phenomenon.

1.1.3 Machining Error in Elastomer End-milling

Studying basic problems that have obvious limitations compared to a real-world problem has several benefits. This dissertation mainly aimed to propose a framework for complex machining phenomena and error generation modelling. In order to confirm a proposed systematic procedure of evaluation framework, error modelling of elastomer end-milling is investigated as an extraordinary than the other conventional materials case study.

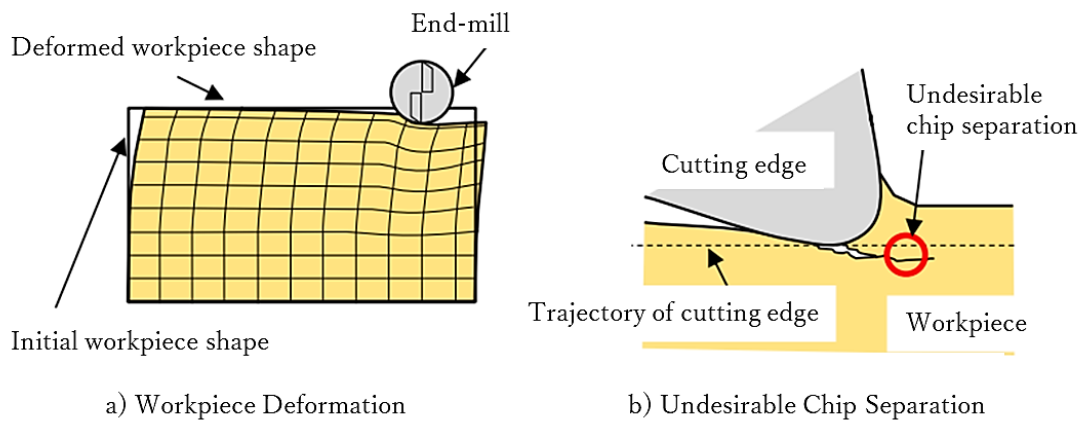


Fig. 1-2 Error generation phenomenon in elastomer

A basis on the modeling of machining error in elastomer end-milling, a basic error generation process of elastomer end-milling is analyzed to clarify possible error-related factors. There are

two basic error generation phenomena which deteriorate the machine accuracy. **Figure 1-2** shows the workpiece deformation at surface generation and imperfection of shape transfer by undesirable chip separation. According to feed per tooth in elastomer end-milling, it usually limited very small because of the limitation of workpiece holding and workpiece deformation. Except the special machining situation such as employing diamond tool, surface generation processes in elastomer end-milling with usual cutting tool become a mixed situation for rubbing and tearing off as illustrated in **Fig. 1-2(b)**. However, analyses of the elastomer end-milling are required to consider chip separation with both of geometrical non-linearity and material non-linearity under the solid contact environment. The numerical calculations with the high non-linearity often cause numerical instability. Therefore, more stable method is necessary to employ. Furthermore, determination of chip separation criterion in elastomer cutting has not been solved [23-24].

The elastomer end-milling commence attracted considerable attention because of its excellent characteristics, uniquely elastic deformation, and difficulty controlling machining error. Although the standard metal machining processes are planned by assuming rigid workpiece and perfect shape transfer, elastomer's characteristics consist of low rigidity and different fracture mechanism causing large machining errors. Concerning the workpiece deformation, measurement and elastic analyses in elastomer end-milling have been investigated [25] with a similar method to metal end-milling [19]. However, there is limited research about the shape transferring error of elastomer because the chip separation mechanism of elastomer is quite different from the mechanism of metals [20, 26]. The unique mechanical properties of elastomers, particularly the large elongation to fracture and low thermal conductivity, can greatly affect chip formation during machining [27]. This research proposes the continuing developed model as the empirical model for machining error in elastomer end-milling prediction models with complex machining phenomena. From the mentioned framework, preliminary experiments have been designed and considered for constructing the error models. A conventional machining error model has been generated from the cutting conditions. A second model simulated physical state value and mechanistic knowledge-based has been created as a mechanistic model. Finally, the statistical model which a hybrid of the correlated variables between cutting conditions and mechanistic knowledge has been constructed as an empirical statistics-based model. Afterward, these created models are investigated by evaluating the predicted machining error with larger experimental results by comparing calculated machining error and measured error from actual cutting experiments.

1.2 Purpose and Outcomes of Dissertation

The principal purpose of this dissertation is to propose a machining error modeling framework and empirical machining error prediction models in the case of elastomer end-milling as a case study. In order to confirm a proposed systematic procedure, the study attempts to focus on the following;

- 1) To propose a modelling framework and investigate the systematic-procedure of machining error modelling
- 2) To construct the machining error prediction models in diversified conditions
- 3) To evaluate the developed model by comparing the estimated and actual machining error obtained from prediction models

1.3 Structure of Dissertation

This dissertation contains six chapters in which three sections of the details are organized and explained as follows; the first section, chapters 1 and 2, express the theoretical and previous methodological perspective through relevant literature. In the second section, chapters 3 and 4 will propose the machining error modelling framework, modelling concepts, experiment configuration, and machining error prediction models construction via the preliminary cases. Finally, in chapter 5, the evaluation experiment will be expressed to confirm the prediction models and the machining error results will be discussed. Chapter 6 is the conclusion and the further aspect of the research. The structure of the dissertation will show in **Fig. 1-3**.

Chapter 1 will provide an initiative to the study by first discussing the research background and context, followed by the purpose of the research and its outcome. Afterward, the structure of the dissertation will express.

Chapter 2 engages with the theoretical and methodological perspectives and previous studies on machining error prediction through the relevant theory and literature reviews.

Chapter 3 introduces the compositional modelling for the machining error prediction model. A mapping function of the complex machining phenomena led to the concept of modelling frameworks. Firstly, a framework for machining error modelling will be proposed for creating

the model. Then an evaluation framework will be investigated by a fundamental evaluation of the machining error model to confirm a good agreement of the measured machining error.

Chapter 4 proposes diverse machining error models based on elastomer end-milling. These machining error prediction models consist of conventional cutting conditions, mechanistic, and statistical. The concepts of modelling, experimental setup and configurations, preliminary experiment, model construction, and formula will systematically be described.

Chapter 5 expresses an evaluation experiment with the larger cases of machining conditions for evaluating the prediction models. Finally, the results of machining error will be discussed and compared.

Chapter 6 is the final chapter of this dissertation which will express the conclusion of this research. After that, the tendency of the research will be presented as a further aspect.

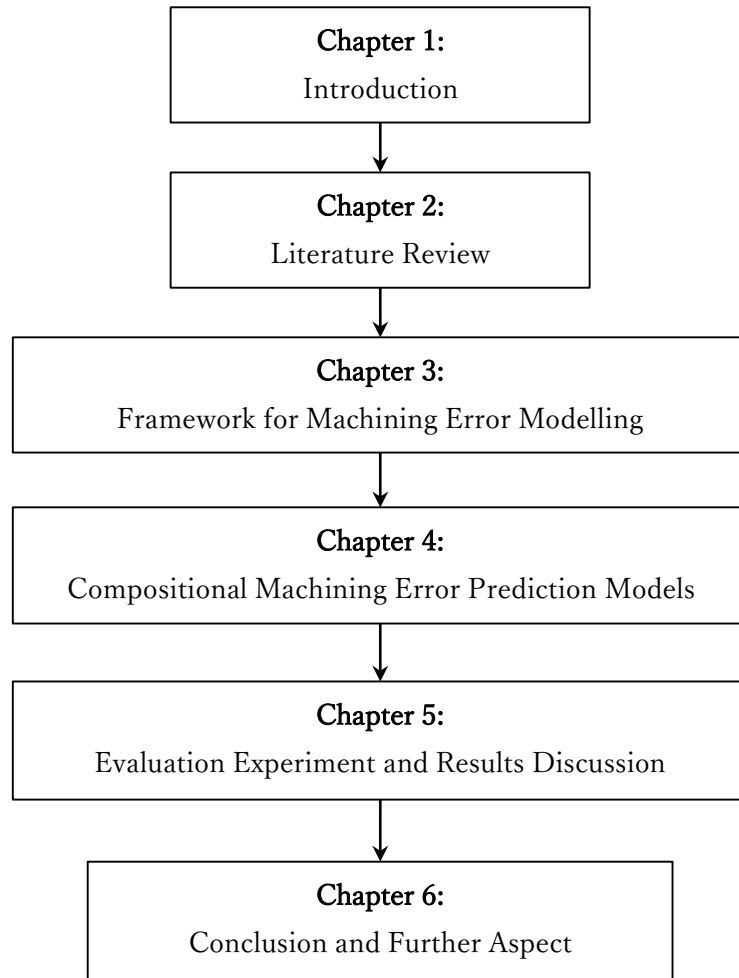


Fig. 1-3 Structure of the dissertation

2. Literature Review

This chapter engages with the theoretical and methodological perspectives and previous studies on machining error prediction through the relevant theory and literature reviews.

2.1 Small-lot Manufacturing

Small-lot production describes the manufacture of a small number of items of the same type and design. The production run varies from between three and one hundred items. Unlike industrial mass production, products are made in small numbers for a very limited market only. Production is considerably more expensive. Small lot productions are common in product design as well as in crafts [7-9]. A “limited edition” is produced in considerably greater numbers than a small lot production.

The lot size refers to the quantity of an item ordered for delivery on a specific date or manufactured in a single production run. In other words, lot size basically refers to the total quantity of a product ordered for manufacturing. A smaller lot of production is an important part of many lean manufacturing strategies. Inventory and development directly affect the lot size. There are other factors too, which are less evident but equally essential. A small lot size causes a reduction in variability in the system and ensures smooth production. It enhances quality, simplifies scheduling, reduces inventory, and encourages continuous improvement.

On the other hand, a product prototyping or non-mass production such as make-to-order (MTO) production needs to utilize machining methods [10, 28]. Particularly in the small-lot production of elastomeric parts, a reliable and accurate production method is eagerly desired [29-30]. In order to guarantee essential quality indexes such as surface roughness and machining error, a prediction model is highly required for reducing the cost and time of machining [15-16].

2.2 Machining Error

Machining is a subtractive manufacturing process that involves material removal. This method is usually in the form of chips removal from the workpiece. Machining using a cutting tool or energy source, the material has been removed from the workpiece. [31]

2.2.1 Machining Process Classification

In traditional machining, material removal is accompanied by the formation of chips, which is accomplished by using a cutting tool with cutting edges. On the other hand, nontraditional machining processes are chip-less material removal processes that involve energy usage for material cutting. The traditional machining operations include turning, drilling, milling, shaping/planning, broaching, grinding, and so on. Machining can be regarded as a system consisting of; workpieces, cutting tools, and equipment (machine tools). **Figure 2-1** shows the classification of machining process. [32]

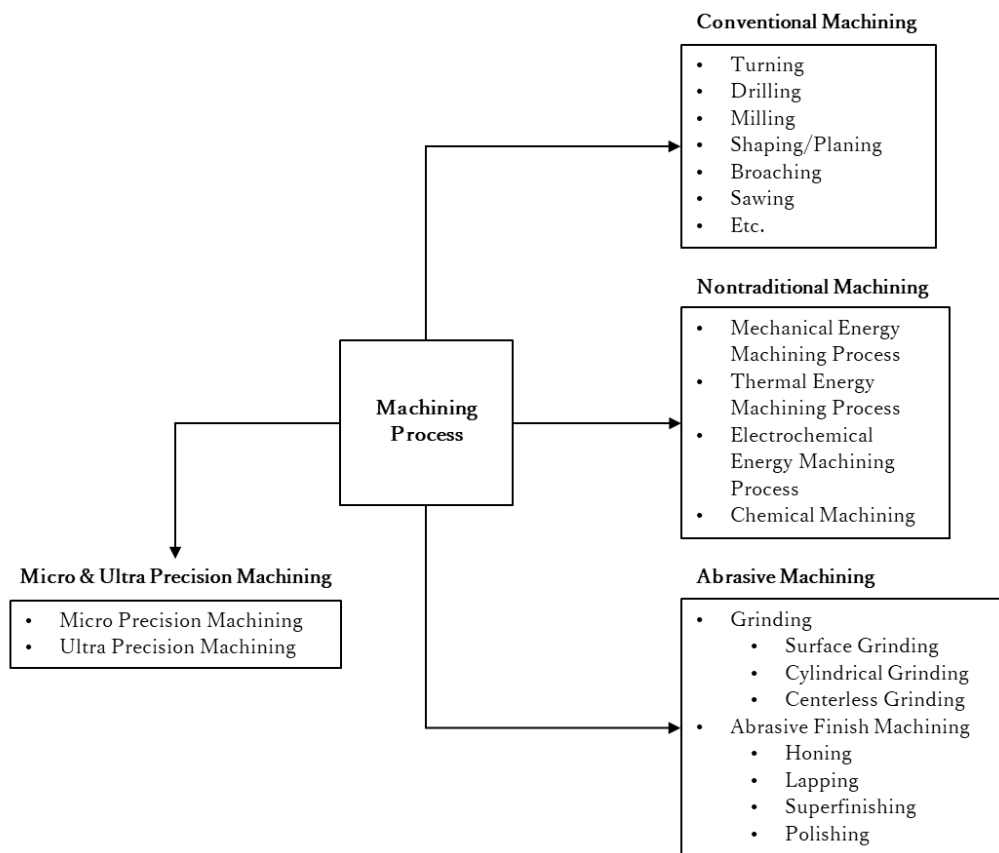
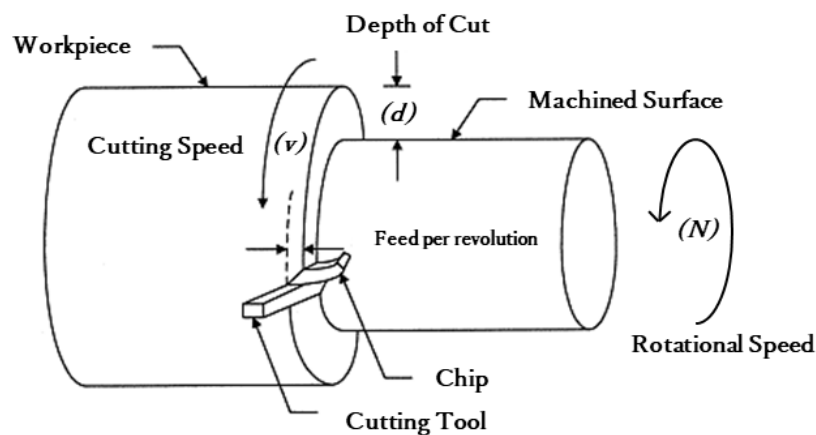


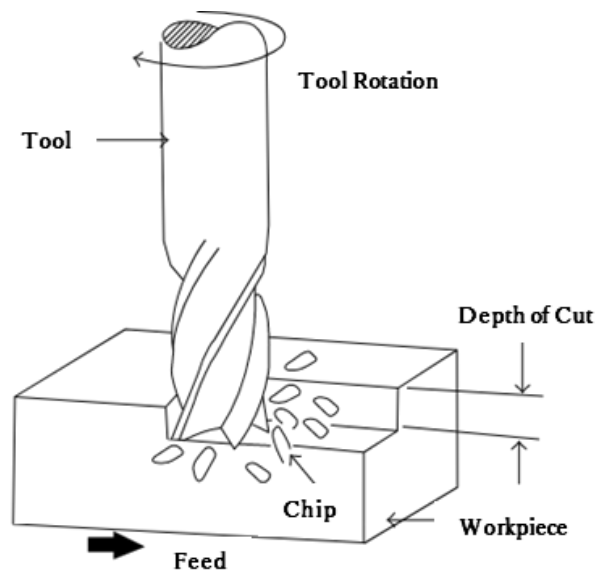
Fig. 2-1 Machining process classification

2.2.2 Conventional Machining Process

Conventional machining processes involve using machine tools, such as lathes, milling machines, drill presses, shapers, or others, with a sharp cutting tool that removes material to achieve the desired geometry. The cutting tool may be either a single-point tool or a multiple-point cutting tool. Notable examples of conventional machining processes include turning, drilling, milling, shaping, broaching, and so on.



a) Basic turning operation [33]



b) Basic milling operation [34]

Fig. 2-2 Conventional machining operation

Turning involves the removal of material from a rotating cylindrical workpiece using a single-point cutting tool; the latter has a feed motion. In machining, there exists a relative motion between tool and workpiece which is the primary motion called cutting speed, whereas the second motion is called a feed. There are three fundamental cutting conditions: cutting speed, feed, and depth of cut. Cutting speed is the greatest of the relative velocities of the cutting tool or workpiece. For example, in a turning machining operation, the surface speed of the workpiece is the cutting speed (v), usually expressed in m/min (see **Figure 2-2 a**). Feed (f) is the distance moved by the tool (or sometimes by the work) per revolution, usually expressed as mm/rev. Depth of cut (d) is the distance the cutting tool penetrates the work. Milling involves the use of a rotating cutter with multiple-point cutting edges; here, the cutting tool has speed motion, and the work has feed motion. (see **Figure 2-2 b**)

2.2.3 Machining Accuracy and Surface Quality

In conventional machining processes, it is often desirable to remove high stock from the bulk material (solid) as well as to achieve reasonably good surface quality. However, the achievement of both objectives in a single pass is not possible. Thus, machining is usually carried out in two steps with varying cutting conditions (cutting speed, feed, and depth of cut). The two steps in machining are (a) roughing pass and (b) finishing pass. In the roughing pass, a bulk amount of material is quickly removed from the workpiece as per the required feature. In this step, a higher feed rate and depth of cut are employed to achieve a high material removal rate from the work. The roughing pass creates a shape close to desired geometry but leaves some machining allowance (material unremoved) for finish cutting. The roughing pass cannot provide a good surface finish and close tolerance. This is why a finishing pass is carried out to improve surface finish, dimensional accuracy, and tolerance level; here, the feed rate and depth of cut are low. Thus, the material removal rate (MRR) is reduced in the finishing pass, but the surface quality is improved. [35-36]

2.2.4 Cutting Phenomena

The complex machining phenomena are influenced by varying cutting conditions, shape of workpiece, and material characteristics. Previously, there are three types of investigations to predict the complex phenomena. They are physics-based, data-centric and mechanistic approaches.

- **Physics-based Approach** - This approach based on the computational mechanics such as Finite Element Methodology (FEM) analysis. They are required only minimum numbers of preliminary experiments that expected to be applicable to various machining situation [37]. FEM based machining process models are used in research and industry for process design and optimization. They require a constitutive description of the material behavior to accurately model and predict process response [38].
- **Data-centric Approach** - Data-centric become popular recently, they require a huge amount of experimental data. In usual machining situation, it is difficult to measure physical information during the machining operation. In order to achieve accurate and stable prediction method with limited preliminary experiments, it is necessary to utilize empirical process knowledge effectively [39]. They utilize statistics to find direct relations between the machining conditions and values which represent phenomena. Furthermore, they also utilize preliminary experiment as much as possible to construct reliable phenomena model.
- **Mechanistic Approach** - This approach combines empirical knowledge and appropriate numbers of preliminary experiments [40]. Workpiece deformation and shape transfer error should be considered to formulate a mechanistic model of machining error in end-milling. It can be calculated by using FEM analysis when appropriate calculation model is prepared. This calculation process can be achieved based on established systematic procedure. In addition, the workpiece deformation field at continuous workpiece can be considered smooth distribution.

For predicting complex phenomena, data-centric approaches have been mainly investigated because they are expected to find direct information to control the phenomena. Anywise, these approaches cannot be adapted against machining variety such as different workpiece shape and different machining method. **Figure 2-3** shows the factors of cutting phenomena.

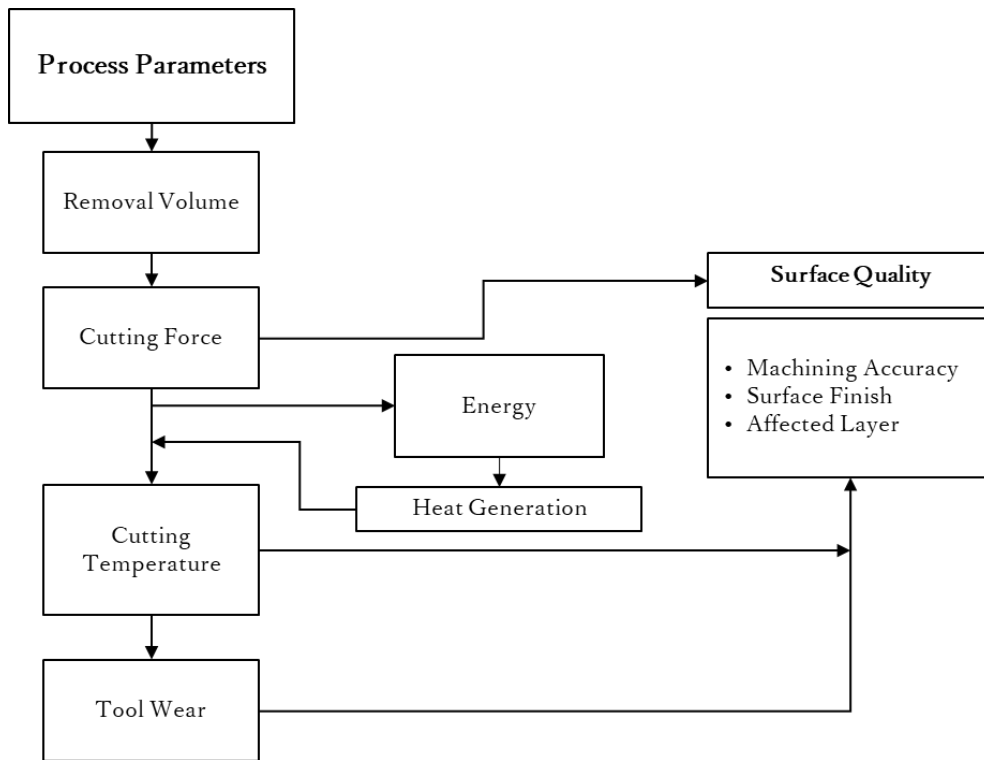


Fig. 2-3 Cutting Phenomena (modified from [41])

2.2.5 Orthogonal Cutting Model

The machining process is a complex 3D operation. A simplified 2D model of machining is available that neglects many geometric complexities, yet describes the process quite well. Orthogonal cutting uses a wedge-shaped tool in which the cutting edge is perpendicular to the cutting direction. As the tool is forced into the material, the chip is formed by shear deformation along a shear plane oriented at an angle ϕ (shear angle) with the surface of the workpiece. Along the shear plane, plastic deformation of work material occurs. The tool in orthogonal cutting has only two elements of geometry: (1) rake angle and (2) clearance angle. The rake angle α determines the direction of chip flow as it is formed, and the clearance angle provides a small clearance between the tool flank and the newly generated work surface. During cutting, the cutting edge of the tool is positioned at a certain distance below the original work surface. This corresponds to the chip thickness prior to chip formation [41]. **Figure 2-4** shows a simple two-dimensional orthogonal cutting model and the significant geometrical parameters involved in chip formation. This model assumes the tool as a single point characterized by rake angle (α) and clearance angle (β). The rake angle (α) is dominant in controlling the cutting forces, tool chip contact length, and vibrations. A small

value of the clearance angle (normally 6° - 7°) prevents the rubbing between the tool and the machined surface and hence controls wear on the tool and residual stresses on the machined surface. Shearing of un-deformed chip thickness (t) occurs on a plane defined by a shear angle (ϕ). The contact length (L_c) is the distance on the rake face of the tool at which the deformed chip (t_c) is in contact with the tool rake face i.e. it is a measure of the rake face surface over which the chip flows. This contact length can be further classified as the sum of sticking (L_{st}) and sliding (L_{sl}) lengths. The important theories based on the orthogonal cutting model which have paved the way for the analysis of the chip formation process include Merchant's model.

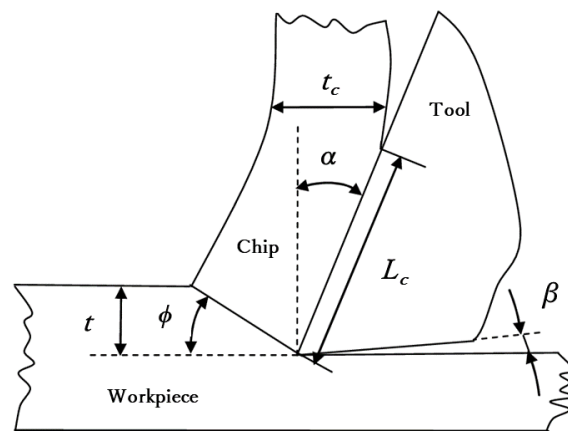


Fig. 2-4 Orthogonal cutting model [42]

2.2.6 End-milling Process

End-milling refers to a physical surface preparation process used to generate material chips by feeding a metal workpiece into a revolving cutter. End-milling is a practical and very common procedure in industrial fabrication applications.

End-milling is widely used in machining moulds and dies, as well as, various aircraft components. In order to ensure cutting quality, tool life prolongation, and productivity, accurate milling process analysis is critically necessary for beforehand process planning and adaptive controlling. During the entire milling process, cutting force is one of the most important issues, as well as an efficient and precise cutting force model, is thus crucial for selecting machining parameters such as feed rate and spindle speed.

Conventional milling process (up-cut), the metal is removed in the form of small chips by a cutter rotating against the direction of the travel of the workpiece. The chip thickness is

minimum at the beginning of the cut and maximum at the top of the cutting. The climb milling process (down-cut) claimed that there's less friction involved and consequently less heat is generated on the contact surface of the cutter and workpiece. The cutting tool moves in the same direction as the workpiece and removes the material. The process of up-milling and down-milling is illustrated in **Fig. 2-5**.

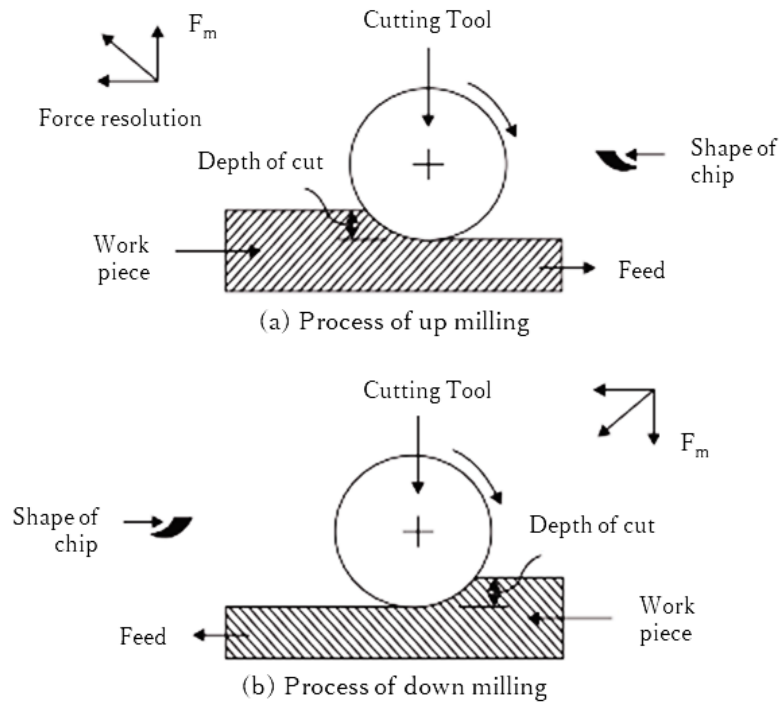


Fig. 2-5 Process of up-milling and down-milling [43]

2.2.7 Cutting Force and Deformation in Milling

A considerable amount of investigations has been directed toward the prediction and measurement of cutting forces. This is because cutting force is a result of the extreme conditions at the tool-workpiece interface and this interaction can be directly related to many other output variables such as generation of heat and consequently tool wear and quality of machined surface as well as chip formation process and the chip morphology. Measurement of forces becomes mandatory in certain cases say, adequate equations are not available, evaluation of the effect of machining parameters cannot be done analytically and theoretical models have to be verified. Several works are available in the literature that makes use of different types of dynamometers to measure the forces. The dynamometers being commonly used nowadays for measuring forces are either strain gauge or piezoelectric types. Though the

piezoelectric dynamometer is highly expensive, this has almost become standard for recent experimental investigations in metal cutting due to its high accuracy, reliability, and consistency. [44]

Estimation of forces acting between tool and work material is one of the vital aspects of mechanics of cutting process since it is essential for:

- Determination of the cutting power consumption
- Structural design of the machine-fixture-tool system
- Study of the effect of various cutting parameters on cutting forces
- Condition monitoring of both the cutting tools and machine tools

Analysis of force during machining includes the magnitude of cutting forces and their components and location of action of those forces as well as the pattern of the forces, say, static or dynamic. The Merchant's circle diagram is shown in **Fig. 2-6** with schematic representation of forces acting on a portion of continuous chip passing through the shear plane at a constant speed which is in a state of equilibrium.

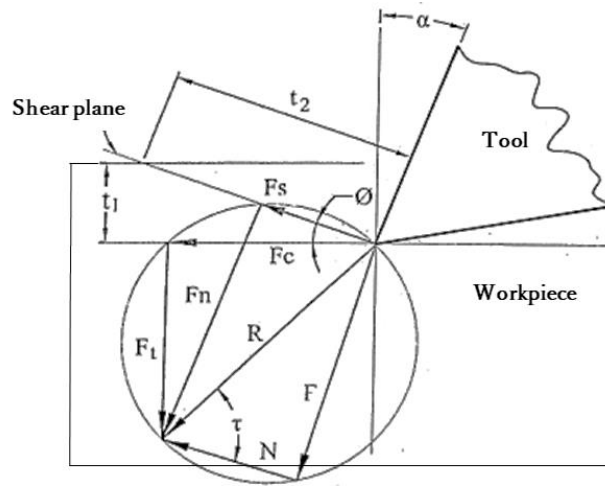


Fig. 2-6 Merchant's circle diagram [45]

F_s and F_n are called shear force and normal force, respectively, that act on the chip from workpiece side i.e. in the shear plane. F and N are friction force at chip-tool interface and force normal rake face, respectively, that act on the chip from the tool side i.e. in the chip-tool interface. These forces can be determined as follows:

$$F = F_c \sin \alpha + F_t \cos \alpha \quad \dots\dots (2-1)$$

$$N = F_c \cos \alpha + F_t \sin \alpha$$

$$F_s = F_c \cos \phi + F_t \sin \phi$$

$$F_n = F_c \sin \phi + F_t \cos \phi$$

Chip formation and its morphology are the key areas in the study of the machining process that provide significant information on the cutting process itself. The process variables such as cutting force, temperature, tool wear, machining power, friction between tool-chip interface, and surface finish are greatly affected by the chip formation process and chip morphology. Chip is formed due to the deformation of the metal lying ahead of the cutting tool tip by the shearing process. The extent of deformation that the workpiece material undergoes determines the nature or type of chip produced. The extent of deformation of chips again depends upon cutting tool geometry (positive or negative rake angle), workpiece material (brittle or ductile), cutting conditions (speed, feed, and depth of cut), and machining environment (dry or wet machining). [45]

For mechanical machining, the concept of similarity is fatal. If a product that looks similar is used in combination with other products, the defects will continue to magnify, causing the processing quality of the factory to fail to meet the high-end precision manufacturing requirements. We all know that the problem of workpiece deformation in machining centers is more difficult to solve, so we must first analyze the reasons for the deformation, and then take countermeasures. The causes of deformation from many reasons are as follows;

- The material and structure of the workpiece affect the deformation
- Deformation caused by workpiece clamping
- The deformation caused by the processing of the workpiece
- Stress and deformation after processing

However, the deformation of the workpiece due to cutting force induced accounts for the majority of machining errors, in the range of 40–70%. Therefore, many researchers have paid increasing attention to more efficient and accurate error prediction methods for low-rigidity parts [46]. In case of an end-mill with multiple cutting edges, **Figure 2-7** shows a schematic diagram when the j_{th} (cutting edge number) cutting edge is at the tool rotation angle θ . The instantaneous cutting forces of the cutting edge tangential force $F_{tj}(\theta)$, tool radial force $F_{rj}(\theta)$, and tool axial force $F_{aj}(\theta)$ are the cutting edge contact length (axis) corresponding to

the cutting width of two-dimensional cutting. It is expressed as follows using the direction cut amount (a), and the cut (cut thickness) $h(\theta)$. In the case of a straight-edged end-mill, $F_{aj}(\theta)$ does not occur because the influence of the bottom edge of the end-mill can be ignored when the assumption of two-dimensional cutting is established.

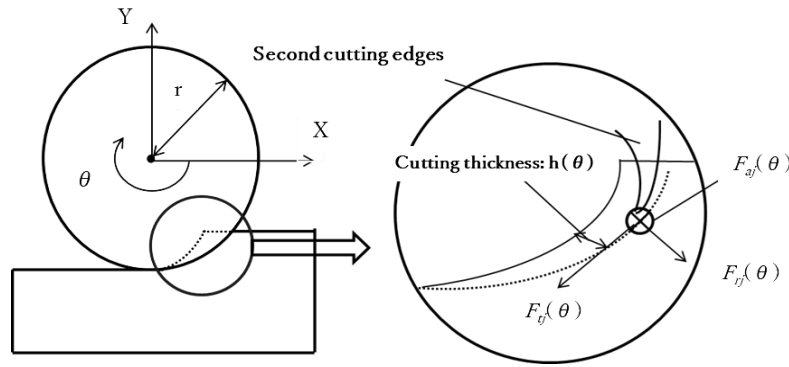


Fig. 2-7 Instantaneous cutting force in end-milling [47]

The cutting force prediction model used in the previous studies is for metal cutting. It can be expressed by the formula on the left using the axial depth of cut, the nominal depth of cut, the coefficient per unit area, and the coefficient per unit length, as shown in Fig. 2-8, and can be expressed in Eq. (2-2).

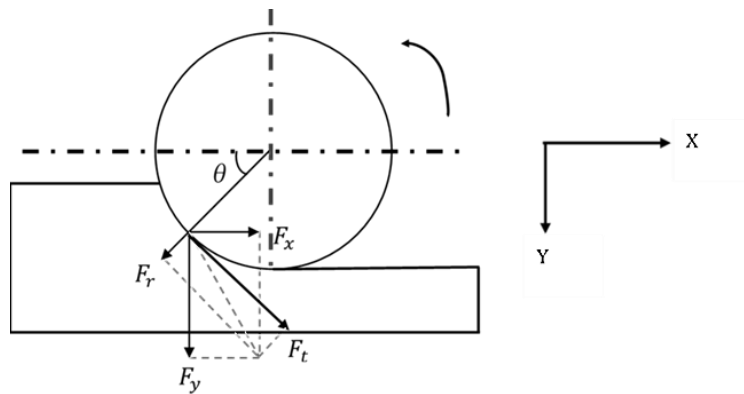


Fig. 2-8 Interrelationship of cutting force in end-milling [47]

$$\begin{aligned}
F_{tj}(\theta) &= K_{tc}ah(\theta) + K_{te}a & \dots\dots (2-2) \\
F_{rj}(\theta) &= K_{rc}ah(\theta) + K_{te}a \\
F_{aj}(\theta) &= K_{ac}ah(\theta) + K_{te}a \\
h(\theta) &= f_i \cos\theta
\end{aligned}$$

where; $F_{tj}(\theta)$; instantaneous cutting forces of the cutting edge tangential force (N/mm²), $F_{rj}(\theta)$; tool radial force (N/mm²), $a(\theta)$; axial depth of cut (mm), $h(\theta)$; thickness of cutting (mm), K_{tc} , K_{rc} , K_{te} , K_{re} are the cutting coefficients obtained by experiments.

The considerable rise in computer processing speeds makes it possible to incorporate the finite element methodology (FEM) for analyzing various aspects of the metal cutting process, thus overcoming most of the restrictive assumptions associated with analytical models. Many investigators have adopted FEM to gain a better understanding of the machining process. In this research we used ANSYS software for investigating the deformation of elastomer.

The finite element method is a numerical method seeking an approximated solution to a wide variety of engineering problems. The engineering problems are boundary value problems (or field problems) containing one or more dependent variables that must satisfy a differential equation everywhere within a known domain and satisfy specific conditions on the boundary of the domain. The field is the domain of interest, often representing a physical structure while the dependent variables of interest are called field variables. The specified value of a field variable on a field scope is called a boundary condition. Field variables may include displacement in solid mechanics' problems consisting of the temperature in heat flow problem velocity, fluid flow problems, etc. in FE modeling for physical problems. A few basic steps are required, which are common for any type of analysis, whether it is a structural problem heat flow, or fluid flow. [44-45]

2.3 Elastomer End-milling

Elastomers are widely used in various applications because of their excellent characteristics, including low elasticity, insulation performance, and flexibility. Because elastomeric parts are usually mass-produced consumables, moulding is applied in their fabrication. However, a small-lot fabrication of elastomeric parts is needed for variation products development;

personalized products, and trial products. Etc. In order to achieve an agile production of elastomeric parts, the end-milling of elastomers has begun to attract considerable attention.

The elastomer end-milling commence attracted considerable attention because of its excellent characteristics, uniquely elastic deformation, and difficulty controlling machining error. Since the standard metal machining processes are planned by assuming rigid workpiece and perfect shape transfer, elastomer's characteristics consist of low rigidity and different fracture mechanism causing large machining errors.

2.3.1 Cutting Force and Deformation Studies in Elastomer Milling

In the conventional metal end-milling, cutting force during the end-milling is one of the dominant factors to machining error. The cutting force causes the workpiece deformation, thermal formation, machine tool deflection, and tool wear. On the other hand, most elastomers have low rigidity then the relationship between cutting force and machining error is considered a fundamental characteristic. The chip formation mechanisms of elastomers are moderately different from those of metal milling.

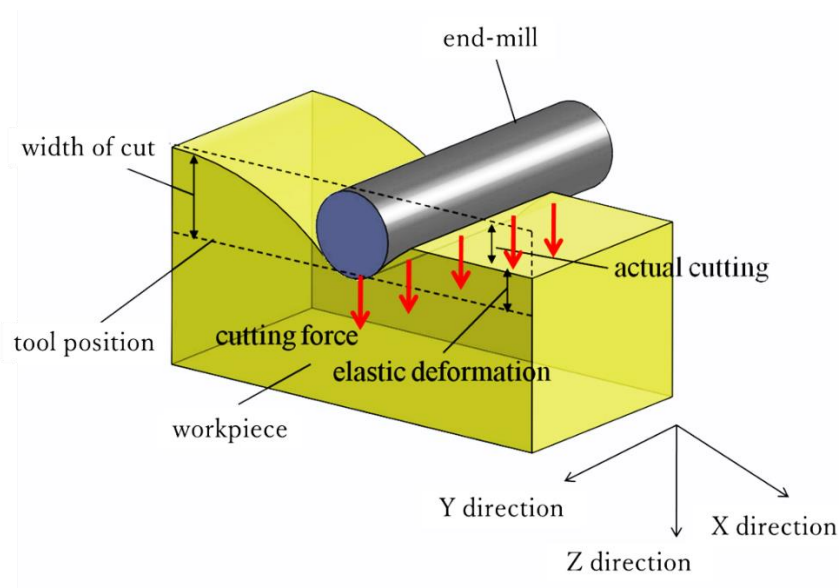


Fig. 2-9 Elastomer end-milling simulation model

Furthermore, the deformation of the workpiece dominantly affects the machining accuracy. These facts indicate that the problem to be tackled for the end-milling of soft objects or elastomers is to control the appropriate surface generation of the machined workpiece that can overcome by designing an optimized cutting tool shape and/or determining proper

machining conditions. Because of the large variety of elastomer objects, it is necessary to develop a systematic method to aggregate empirical cases to generate a mechanistic model of the surface generation process. There is little knowledge of those factors that are dominant to the error and required further knowledge. Therefore, a preliminary evaluation of the important factors is necessary [30]. **Figure 2-9** shows the simulation model for elastomer end-milling. **Figure 2-10** proposes the concepts of the experimental design to find machining errors based on elastomer end-milling.

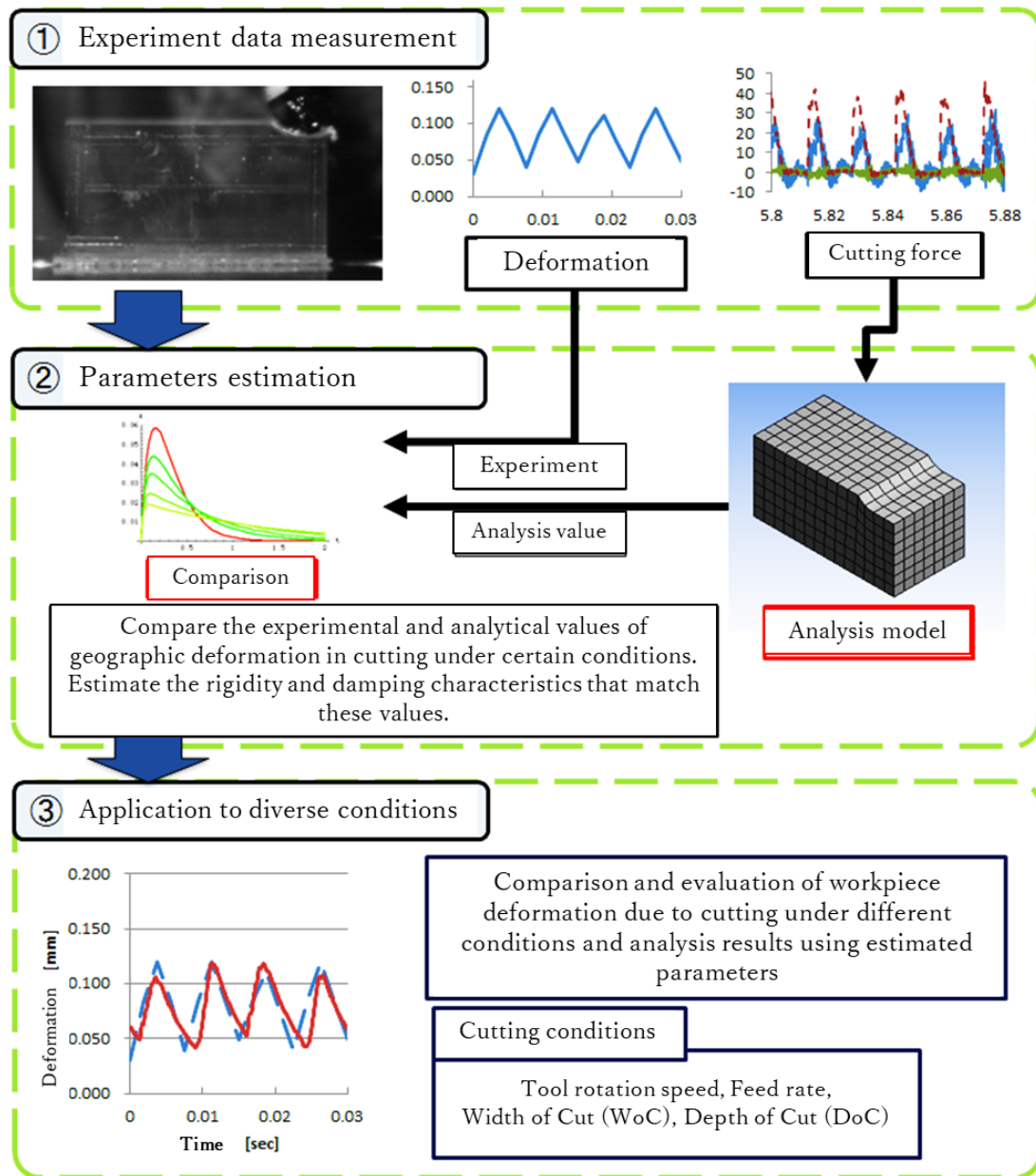


Fig. 2-10 Systematic model construction procedure

In previous research done on elastomers machining, machining error and stable work holding have been necessary obstacles to appropriate end-milling of elastomeric parts. These works became the main inspiration for this research are as follows;

Shih et al. [30] have reported that the extraordinary mechanical properties of elastomer, considerably enduring elongation and low thermal conductivity are capable of affect chip formation during machining significantly. In other words, tool wear is not a dominant factor for elastomer end-milling. Meanwhile, the accumulations of cutting heat and the influence of thermal effects are not a dominant factor of the error tendency have been reported [25]. Therefore, it is promising to improve the machining accuracy by considering the mechanistic surface generation model with the dominant factors such as cutting force, workpiece deformation, and machining conditions for elastomer end-milling. In 2008-2010, Teramoto K. et.al, have proposed a framework for machining the soft objects as well as the machining error in soft objects end-milling, respectively [15-16, 48]. In 2012, Kakinuma Y. et.al, studied the ultra-precision cryogenic machining of viscoelastic polymers [49], while Tsurimoto S. and Moriwaki T. studied the experiment on the cutting of silicone rubber under hydrostatic pressure [50]. In 2015, Nakamoto K. et.al, introduced the dexterous machining of soft objects by the means of a flexible clasper [51]. Similar to Kakinuma Y., in 2016 Putz M. studied the mechanism of cutting elastomers with cryogenic cooling as well [52]. In the same year, Funatani K. et.al, have proposed their research on the dexterous creation pattern of the urethane rubber [53].

2.3.2 Machining Error Studies in Elastomer End-milling

The machining error in the end-milling process has involved machining conditions, workpiece shape, and material removal characteristics. During the actual machining situation, workpiece shape and machining conditions such as depth of cut (DoC) and width of cut (WoC) are varied according to the machining process [25, 37, 54]. Furthermore, tool rotation speed and feed rate are sometimes adjusted to find the appropriate conditions when the new cutting tool, workpiece material, and/or different workpiece shape has to be applied. Regarding the workpiece deformation, the elastic analyses and measurement in the elastomer end-milling have been investigated by a similar method for metal end-milling [37-39].

Wu et al. (2017) [21] proposed a model based mechanistic for machining error prediction. The model which utilized machining knowledge for empirical model formulation was employed. By introducing a mathematical model which reflect process knowledge, stabile

calculation with limited experimental data. As mentioned in topic 2.2.4, thus, the deformation at cutting point can be presented by a function of a displacement of a neighborhood point of cutting point. On the other hand, the shape transfer error is complicated to model quantitatively because it is affected by a crack generation point, a trajectory of crack propagation, and slippage between cutting tool and workpiece. From the analysis of crack generation of elastomer, the indentation forces, an indentation depth, and a local stiffness are important factors for the crack generation. Because the indentation depth can be related to the local workpiece deformation, it is assumed that the shape transfer error is affected by the workpiece deformation, cutting force and the local stiffness of workpiece. Based on the extracted factors to explain the machining error for elastomer end-milling a simplified error model which can be applicable to statistical analysis was introduced.

In the experiment stage, a high-speed steel end-mill with a 6-mm diameter and a two-flute straight blade edged with a 20 μm roundness was applied on the machining center. Urethane rubber shore A90 hardness is employed as elastomer material because of its unique characteristics and mechanical properties. In addition, there are significantly difficult controlling chip separation and cutting phenomena [29-30]. The experiments have been conducted the pattern according to our previous study [55]. **Table 2-1** detailed this research instruments, materials and their specification. Then **Chapter 5** will explain of the setup and configurations of these instruments.

Table 2-1 Experimental instruments, materials and their specification



Instrument/Material	Specification
	Machining center: TOMINAGA Model D-Matric 24 Moving distance: 600 x 250 x 250 mm. Table size: x-axis 900 mm., y-axis 300 mm. Spindle: 40-4000 rpm. Speed: up to 6,000 mm/min.
	Power meter: Model 3-component force sensor 9327C: KISTLER Preloaded with a jig to enable measurement of cutting force Measurement range; X, Y direction: -1 to 1kN, Z direction: -4 to 4kN Sensor unit weight: 380g

Table 2-1 Experimental instruments, materials and their specification (cont.)

Instrument/Material	Specification
	Machine vice: IKEA-MISUMI Material: Cast iron WIKFB 150
	High speed camera: MotionXtra NR4-S2-IDT Sensor: CMOS-Polaris II Recording memory: 1.25 GB No. of Pixel: 1.0 Megapixel, 187.14 μm^2 pixel size Analysis software: Motion Studio
	Multi-function generator: A&D-AD-8623A Output frequency range: 0.3 Hz ~ 3 MHz Output wave form: Square Rise and fall time: 100 ns or less
	LED light source High-performance LED light source Used instead of the conventional halogen light source
	AC power supply unit output: KEYENCE Model: KZ U3 Power: DC24V1.4A
	Mirror For reflecting workpiece deformation observation recording by the HSS camera during machining

Table 2-1 Experimental instruments, materials and their specification (cont.)

Instrument/Material	Specification
	<p>Non-contact Laser Displacement Sensor: KEYENCE KS 1100</p> <p>High-precision shape measurement system with stage</p> <p>Pitch Measurement: 70 μm</p> <p>CCD laser displacement meter LK- GD500</p> 
	<p>Metallic base</p> <p>Double stick tape</p> <p>Use NITOMS'</p> <p>"Ultra-strong double-sided tape for polyethylene No.5015"</p> <p>to fix the work and base</p>
	<p>High speed steel (HSS-SKH57) end-mill: MISUMI</p> <p>Type: 2-flute straight-blade, Diameter: 6 mm.</p> <p>Tool length: 60 mm. Cutting length: 20 mm. Edge roundness: 20 μm</p> <p>Density: 8,160 kg/m^3, Young's modulus: 2.26e+05 MPa</p> <p>Poisson's Ratio: 0.29, Bulk Modulus: 1.7937e+05 MPa</p> <p>Shear Modulus: 87597 MPa,</p> <p>Tensile Yield Strength: 2.17e-15 MPa</p> <p>Tensile Ultimate Strength: 2.39e-15 MPa</p> <p>Isotropic Secant Coefficient of Thermal Expansion: 1.02e-05 $1/^{\circ}\text{C}$</p> <p>Isotropic Thermal Conductivity: 0.022 $\text{W/mm}\cdot^{\circ}\text{C}$</p> <p>Specific Heat Constant Pressure: 4.65e+05 $\text{mJ/kg}\cdot^{\circ}\text{C}$</p> <p>Isotropic Resistivity: 0.000832 ohm.mm</p>
	<p>Urethane rubber hardness shore A90</p> <p>Density: 1.15e-06 kg/m^3, Young's modulus: 98.778 MPa</p> <p>Poisson's Ratio: 0.49, Bulk Modulus: 1646.3 MPa</p> <p>Shear Modulus: 33.147 MPa</p> <p>k-Matrix Damping Multiplier: 0.0012</p> <p>Marker film</p> <p>MIRACLE's "Miracle Sheet Film Seal" to transfer the marker to the work</p>

During the machining process, a side view of the workpiece is reflected by a mirror and photographed by a high-speed camera for observing cutting behavior. These devices are detailed in **Table 2-1**. Regarding the machining observation, there are a bit uncut parts at the beginning of cutting, and there are a bit uncut parts at the end of machining because of the unique characteristic of elastomers which are difficult to machine. **Figure 2-11** shows the observation markers on the workpiece.

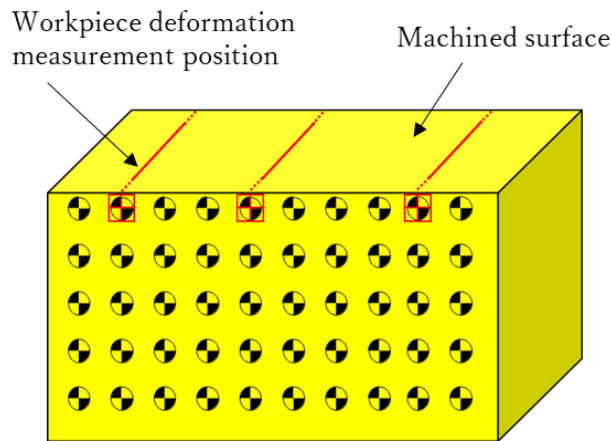


Fig. 2-11 Workpiece with marker film for machining observation

Because of the recording time limitation of the high-speed camera, the synchronized measurements are also limited. Therefore, all workpieces are divided into three sections then the machining experiments are conducted three times for each workpiece. The number of three markers indicated by the red marker as shown in **Fig. 2-11**, referred to the measured positions at each experiment. The distances of each point starting from the edge of the workpiece are 3 mm, 11 mm, and 17 mm, respectively.

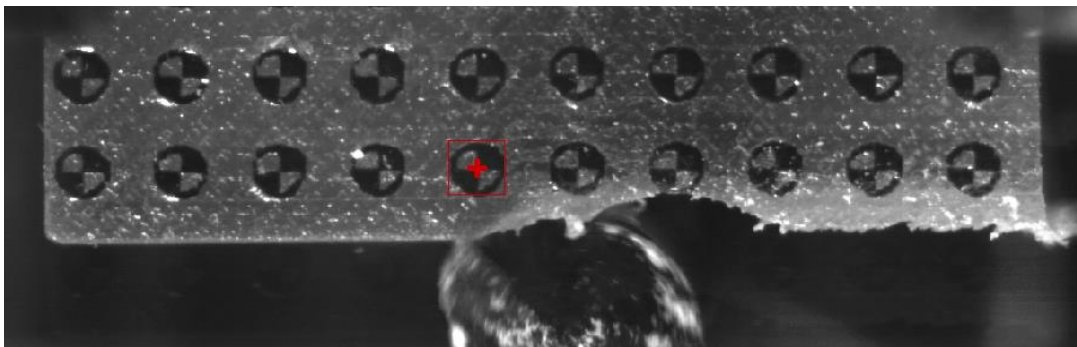


Fig. 2-12 Behavior observation during machining

Figure 2-12 expresses behavior observation during machining. A high-speed camera is employed to record workpiece deformations at the quasi-two-dimensional machining. From the recorded images, workpiece deformations at representative points are measured by using visual tracking of the marker. **Figure 2-13** shows the tracking screen using a software analyzer.

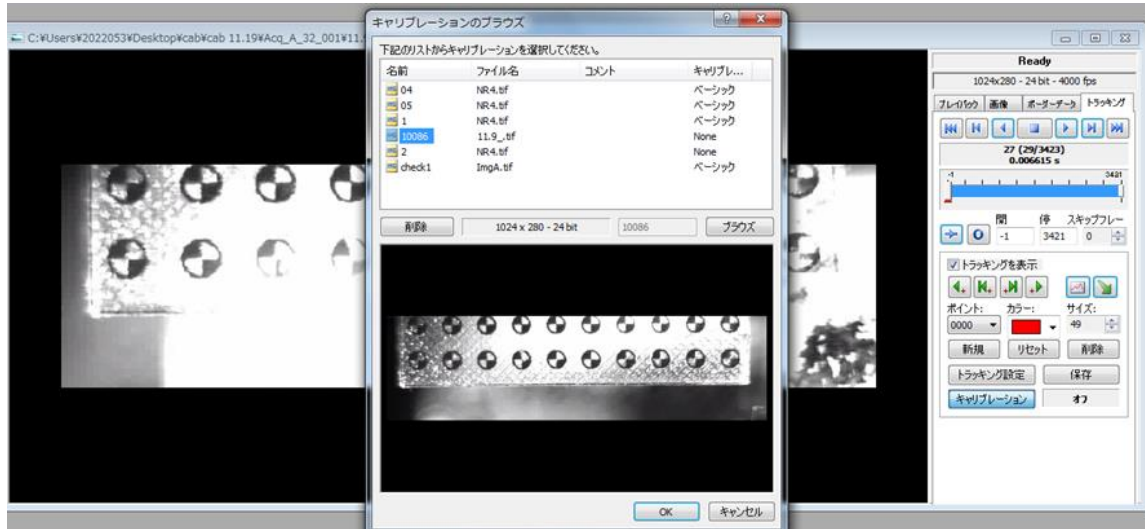


Fig. 2-13 Tracking screen using software analyzer

The machined workpiece was removed from the dynamometer after machining and placed on the measuring equipment. A schematic of the machining error measurement is shown in **Fig. 2-14**. A non-contact laser displacement sensor was utilized for measuring the machined workpiece surface. The average difference between the idealized surface and measured surface has been calculated. The synchronized measurement points are extracted corresponding to the machining error. The blank workpiece that is attached to the metallic base (see **Fig. 2-15**) has been measured thickness before machining. Subsequently, a laser displacement sensor with a spot size of 70 micrometers was used to scan the machined elastomers.

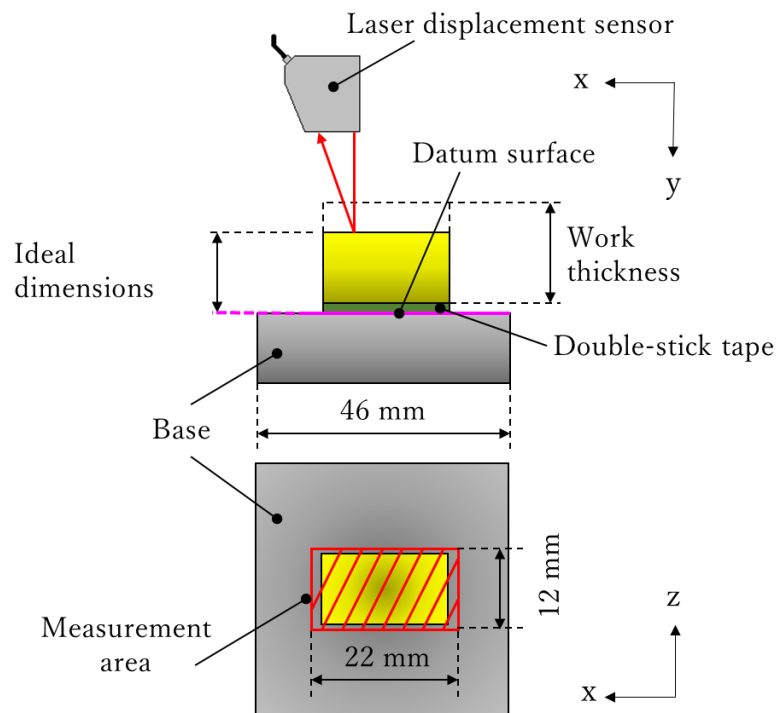


Fig. 2-14 Schematic of machining error measurement

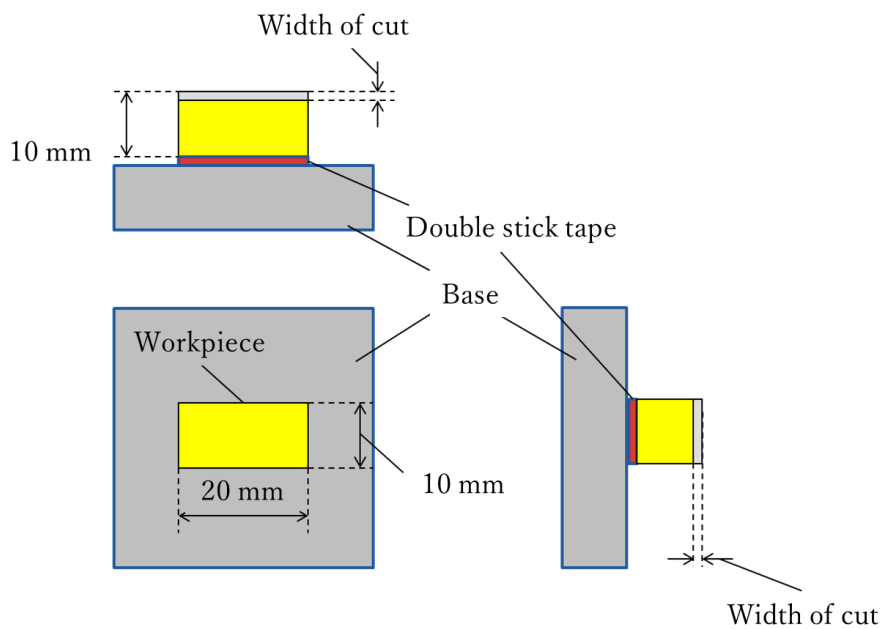


Fig. 2-15 Machining and measurement configuration

The surface of the metallic base was used as the reference (datum) surface for machining and measuring, as shown in **Fig. 2-16**. By comparing the before and after scanning thickness data of blank workpiece and machined surface, machining error has been estimated.

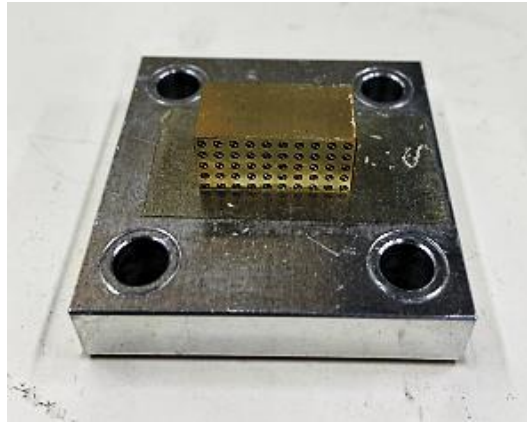


Fig. 2-16 Machined workpiece on a metallic base

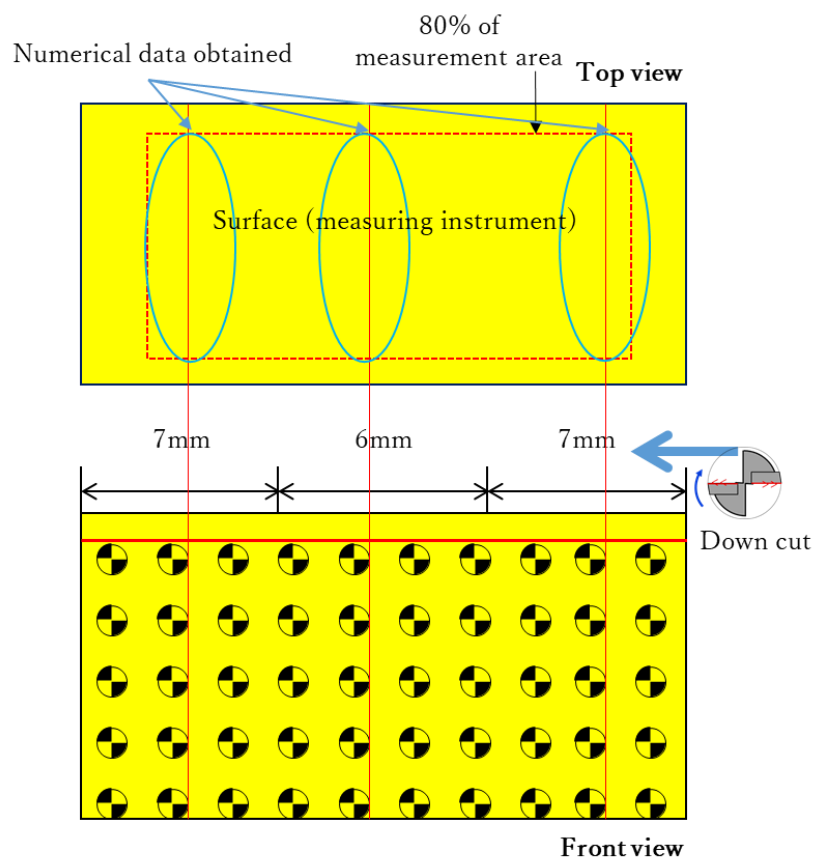


Fig. 2.17 Measurement area for machined workpiece

From obtained surface data, the machining error corresponding to the synchronized measurement points are extracted. As a machining error, average differences between the ideal surface and measured surface are calculated. Because of near edge areas have burr shape error, the machining errors are calculated by using the middle of profile curve (80% of workpiece width) as shown in **Fig. 2-17**. Afterward, obtained machined-surface data will be evaluated by a software analyzer and then recorded for the comparing process as illustrated in **Fig. 2-18** and **Fig. 2-19**, respectively.

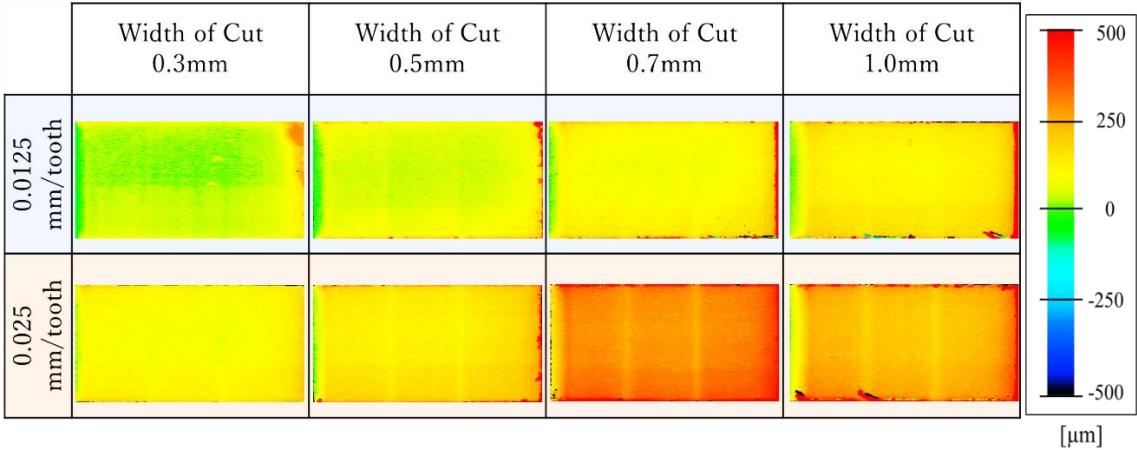


Fig. 2.18 Processed surface shape evaluation

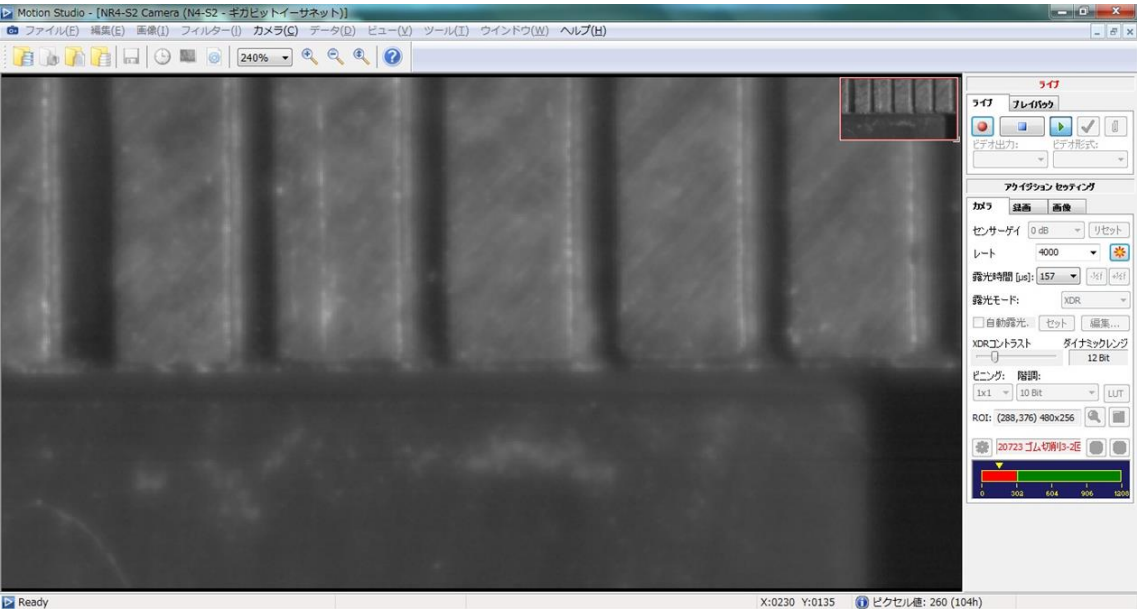


Fig. 2.19 Machining error measurement

2.4 Statistics Implementation

There are essential statistics approaches involved in this research. The main task of these statistics is distinguished into three divisions. First of all, the principal component analysis (PCA), is a part of machine learning which responded to the main criteria components' relationships to create a based-statistics machining error model in this research. Secondly, the correlation coefficient is a statistical method that computed the main effect of the significant coefficient values. Finally, the multiple regression analysis was used to calculate the solution on linear regression for comparing the model results.

2.4.1 Principle Component Analysis

Principal component analysis (PCA) is the main component of a problem in which several factors are considered. They are not treated individually but comprehensively. In other words, the comprehensive characteristics of some explanatory variables $x_1, x_2, x_3, \dots, x_p$ can be expressed by linear expressions such as $a_1x_1 + a_2x_2 + \dots + a_px_p$. This formula is called the main component. The number of principal components is equal to the number of variables contained in the data to be analyzed. Therefore, in this study, a total of 18 main components can be obtained. The names of each principal component are called the first principal component (PC1), the second principal component (PC2), and so on. [56-59]

Since the 81 data in this study deal with 18 variables, there are many numerical values, and it is difficult to see which processing conditions are affected. However, when the machining data is divided into several clusters, from the principal component analysis that it is inappropriate to apply a single prediction model, simple numerical values, and the degree of variation in each machining case, can be understood. The flow of principal component analysis is shown below;

- Data reading
- Standardization of experimental data
- Execution of principal component analysis
 - (1) Principal component score
 - (2) Plot of PC1 and PC2
 - (3) Plot of principal component score from PC1 to PC18
 - (4) Contribution rate/ cumulative contribution rate/ eigenvalue/ eigenvector of each principal component
 - (5) Plot of eigenvectors for each condition

The analysis contents will be explained in order. Since some of the 18 variables have different units, the standardization of experimental data is performed for the purpose of establishing a certain standard that allows the numerical values between each condition to be used in common.

The principal component score is the score of each principal component in each data, and the data is rotated based on the principal component axis. The value corresponding to the coordinates when it is set. A plot of the principal component scores with each principal component placed on the coordinate axes. Contribution rate indicates how much the information represented by the eigenvalue of a certain principal component occupies in all the information of the data. It means the variance composition ratio of the score of the principal component in the total variance of the entire variable. It represents the equation obtained in Eq. (2-3).

$$\text{Contribution Rate} = \frac{\text{Eigenvalue}}{(\text{Standard Deviation})^2} \times 100 \quad \dots\dots (2-3)$$

The cumulative contribution rate is the sum of the contribution rates of each main component in descending order. The component shows how much the amount of information that the data had is explained.

Eigenvalues are numerical values corresponding to each principal component. This eigenvalue corresponds to the variance of the principal components. It shows how much the main component holds the information of the original data. For $n \times n$ matrix, as following Eq. (2-4).

$$Ax = \lambda x \quad \dots\dots (2-4)$$

when there is a combination of "non-zero vector x " and "scalar λ " that satisfies $Ax = \lambda x$ is called the "eigenvector of A" and λ is called the "eigenvalue of A".

2.4.2 Correlation Coefficient

Correlation coefficients are used to measure how strong a relationship is between two variables. There are several types of correlation coefficient, but the most popular is Pearson's. Pearson's correlation (also called Pearson's R) is a correlation coefficient commonly used in

linear regression. If you're starting out in statistics, you'll probably learn about Pearson's R first. In fact, when anyone refers to the correlation coefficient, they are usually talking about Pearson's.

About n data $(x_1, y_1), (x_2, y_2), (x_3, y_3), \dots, (x_n, y_n)$. The value obtained by dividing the "covariance of x and y " by the "product of the standard deviation of x and the standard deviation of y ". It is called the correlation coefficient between x and y . **Eq. (2-5)** expresses the correlation coefficient r ($-1 \leq r \leq +1$) and the variable names.

$$r = \frac{\text{Covariance}}{SD_x \times SD_y} = \frac{s_{xy}}{s_x \times s_y} = \frac{\frac{1}{n} \sum_{i=1}^n (x_i - \bar{x})(y_i - \bar{y})}{\sqrt{\frac{1}{n} \sum_{i=1}^n (x_i - \bar{x})^2} \times \sqrt{\frac{1}{n} \sum_{i=1}^n (y_i - \bar{y})^2}} \quad \text{..... (2-5)}$$

where, r refers to correlation coefficient of x and y , s_{xy} refers covariance of x and y , s_x refers to the standard deviation of x , s_y refers to the standard deviation of y , while n is the total number of data, (x_i, y_i) refers to i^{th} data value, \bar{x} is an average of x , and \bar{y} is an average of y .

The purpose of calculating the correlation coefficient is to investigate how much the physical quantity that can be calculated by machining conditions and machining simulation correlates with the machining error, and the causal relationship between the machining error and other conditions is investigated. It should be noted that it is not a proof. [60]

2.4.3 Multiple Regression Analysis

Multiple regression analysis is a method of predicting the value of one objective variable by linearly combining two or more explanatory variables. However, it is assumed that the objective variable has error fluctuations and that the explanatory variables have no error fluctuations. [60]

Given p explanatory variables be $x_1, x_2, x_3, \dots, x_p$, and consider a matrix in which each measured value is arranged in each column as shown in **Eq. (2-6)**.

$$X = \begin{pmatrix} x_{11} & x_{12} & \dots & x_{1p} \\ x_{21} & x_{22} & & x_{2p} \\ \vdots & \vdots & \ddots & \vdots \\ x_{n1} & x_{n2} & \dots & x_{np} \end{pmatrix} \quad \text{..... (2-6)}$$

where; δ and the observed variables be $\delta_1, \delta_2, \delta_3, \dots, \delta_p$. The regression line in the same as the simple regression analysis at this time is a hyperplane on the p dimension in the multiple regression analysis. (as shown in **Eq. (2-7)**)

$$\delta = b_0 + b_1x_1 + b_2x_2 + \dots + b_px_p \quad \text{..... (2-7)}$$

where; δ is an objective variable, x_1, x_2, \dots, x_p are the explanatory variables, b_0 is a constant (intercept), and b_1, b_2, \dots, b_p are the regression coefficients.

The purpose of performing multiple regression analysis in this study is to formulate a model formula that compares the error rates of the calculated error and the measured error obtained from the calculation under the evaluation machining conditions with those of the conventional study.

3. Framework for Machining Error Modelling

This chapter introduces the compositional modelling for the machining error prediction model. A mapping function of the complex machining phenomena led to the concept of modelling frameworks. Firstly, a framework for machining error modelling will be proposed. Then the second framework, an evaluation of the machining error model framework, will be investigated as a fundamental evaluation of the machining error model to confirm a good agreement of the measured machining error.

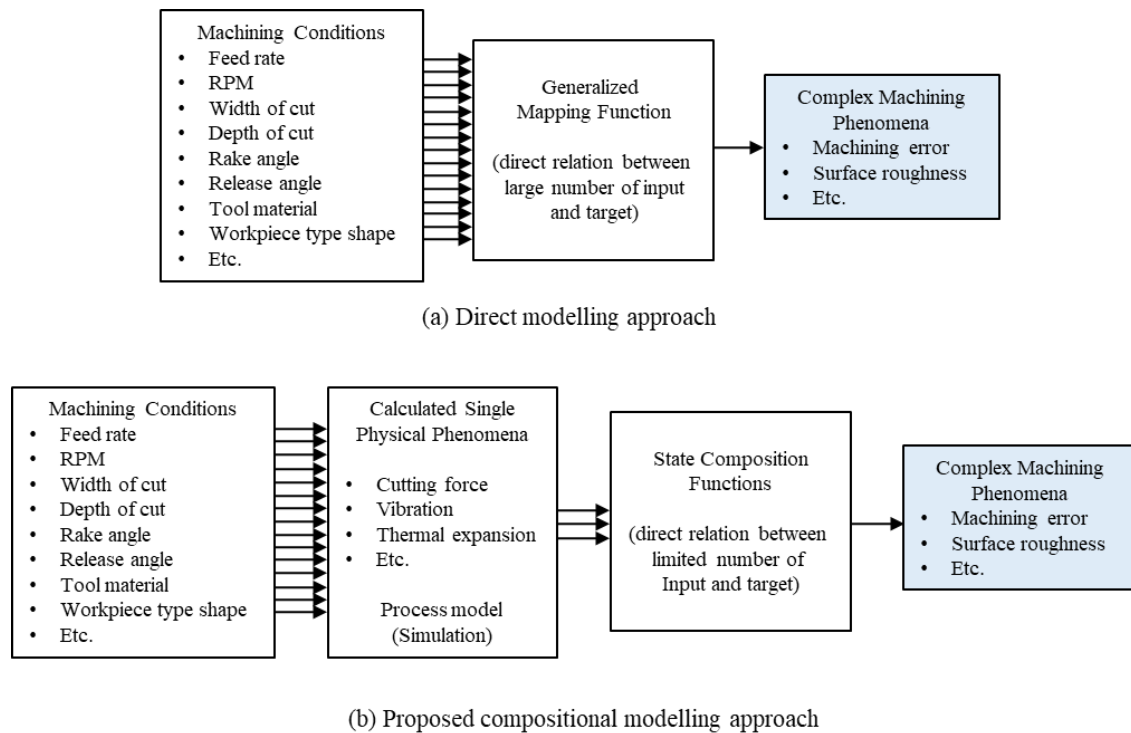


Fig. 3-1 A mapping function of compositional modelling

In order to adapt to the diversity of the machining process, this research considers state values to represent machining cases. As illustrated in **Fig. 3-1(a)**, conventional empirical models

utilize generalized functions which indicate direct relations between machining conditions and machining phenomena. [55]

From the mapping functions, many complex functions which contain a large number of model parameters are utilized. When the focused aspect is determined, a physics-based model can represent the machining process accurately with a minimum number of model parameters. It expects to represent the machining process with a small number of model parameters by composing these single aspect process descriptions, as shown in **Fig. 3-1(b)**.

The systematic model construction procedure is defined as follows.

1. Collecting candidates of model variables include machining condition and physical state values considering available process simulation.
2. Designing a preliminary experiment by known characteristics of material and cutting tool within the capability of experiment load.
3. Evaluating candidates of model variables based on the preliminary experiment.
4. Formulating a process model using selected model variables
5. Identifying the process model based on the preliminary experiment.
6. Utilize the identified model to predict machining situations at different machining situations from preliminary experiments.

3.1 A Framework of Machining Error Modelling

The frameworks involving the error prediction of complex physical phenomena for the manufacturing process have been previously proposed [61]. The compositional machining simulation and accuracy assured machining for a closed loop machining operation were introduced.

Based on the defined procedures, we propose a modelling framework to predict the machining error of elastomer end-milling. The frameworks involving the error prediction of complex physical phenomena for the manufacturing process are based on the previously proposed modelling concept [15]. The framework consists of two phases included the identification phase and the estimation phase. At the identification phase, limited cases of preliminary experiments are utilized to identify the process model. The identified model is used to predict actual machining situations that are different from the preliminary experiments. For designing preliminary experiments, it is assumed certain knowledge of the characteristics of

workpiece material and the cutting tool such as; the cutting force tendency, workpiece material characteristics, physical state values, and error generation mechanism. When the new material and/or cutting tool will be employed, some basic trials are necessary to grasp the characteristics. A schematic expression of the framework for identifying and utilizing the machining error model is illustrated in **Fig. 3-2**. The variations of workpiece materials and cutting tools are smaller than variations of machining conditions and workpiece shapes. Therefore, the framework is organized to achieve the versatility of various machining conditions and workpiece shapes.

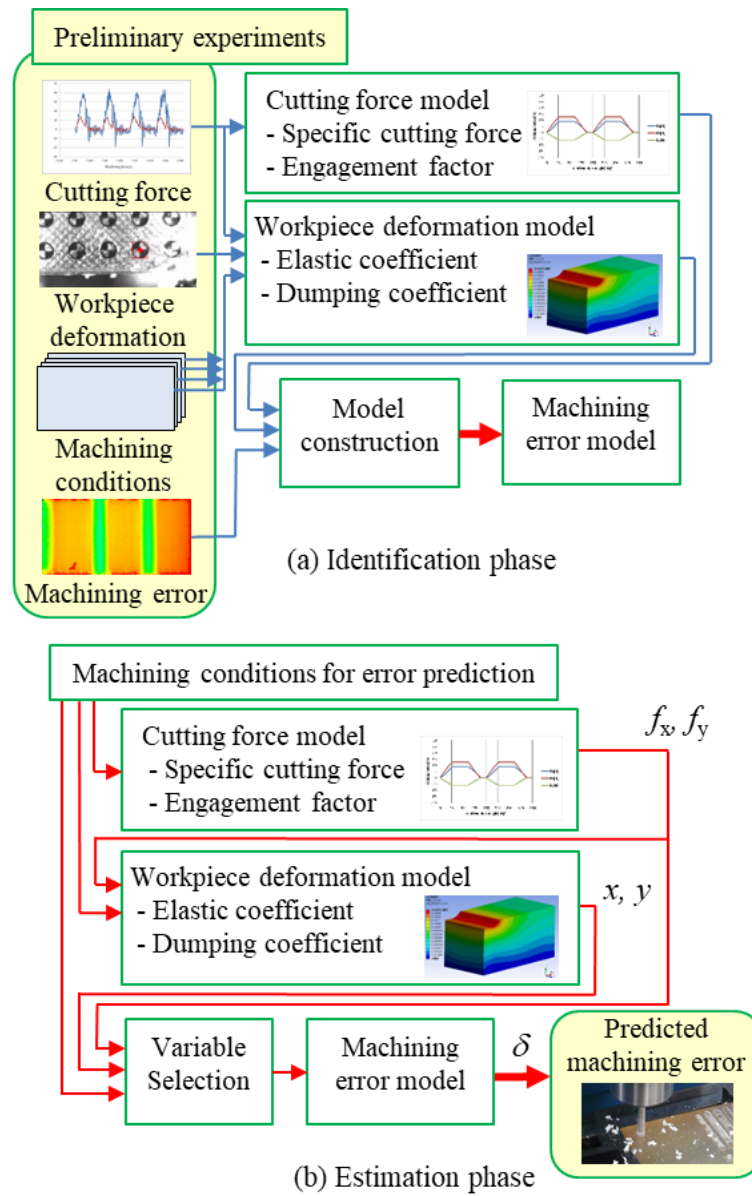


Fig. 3-2 Framework of machining error modelling

In order to compensate for influences of machining case variations, state values that included cutting force, workpiece deformation, and machining conditions are used for constructing the error model. Because the influence of workpiece materials and cutting tools are not considered in this framework, the parameter identification process is required when a new cutting tool and/or a workpiece material are employed for the machining process.

In the identification phase as demonstrated in **Fig. 3-2(a)**, the simplified preliminary experiments with the specialized machining equipment [25] are executed. It can measure instantaneous cutting force and workpiece displacement simultaneously at the different machining conditions. Furthermore, a simplified workpiece enables the evaluation of the machining error easily. The fundamental studies on machining have applied both a computational finite element methodology (FEM) and the experimental approach. For an initial effort of cutting force simulation, a standard discrete cutting force model has been used.

The conventional cutting force model assumes which total cutting force can be approximated as the sum of local cutting forces [62]. The coefficients for the end-mill are determined based on the average force-based determination method for cutting coefficients [63]. In order to investigate an error generation mechanism, the measurements of instantaneous workpiece deformation have been conducted. A quasi-two-dimensional cutting situation with the uniform fixture effect is constructed for machining. An image processing is employed to observe the actual displacements by using a pre-calculated calibration scale and origin [25]. From the observation, the obtained displacements can be used to estimate the mechanical property for FEM analysis to simulate workpiece deformation [54].

Based on the previous research, the physical state values such as cutting force and workpiece deformation can be calculated in principle. By using the data obtained from preliminary experiments, the model parameters for deformation analysis and cutting force prediction can be determined. Physical state values at every machining situation can be calculated using the identified process models. Machining conditions, physical state values, and their combined variables are candidates of model variables of machining error.

By utilizing the preliminary experiments, candidates of variables are evaluated and selected. An empirical model of machining error is constructed based on the selected variables. In the estimation phase as shown in **Fig. 3-2(b)**, the machining error of the actual machining situations will be reasonably calculated based upon the selected model variables and the identified machining error model.

3.2 Evaluation of Machining Error Model

In order to appraise the proposed framework, the cutting force model and the workpiece deformation model also must be estimated in principle. However, an evaluation of a combined model becomes complex, and it is difficult to find the problem when estimation is not moderately appropriate. Hence, an independent evaluating of the machining error model is investigated as a fundamental evaluation of the machining error model.

In case if the machining error calculated by the error model offers a good agreement of the measured machining error, the evaluating of the framework is equivalent to the evaluation of the cutting force model and workpiece deformation model that has been partially reported [25, 62]. Based on the independent evaluating of the machining error model, preliminary experimental data for the workpiece deformation and cutting force corresponding to the machining cases that are different from the parameter identification case are employed to calculate the machining error. **Figure 3-3** illustrates an outline of the evaluation procedure for the error model. The candidates of model variables are selected through the principle component analysis (PCA), and a machining error model is constructed as a linear model of the selected variables.

The constructed error model coefficients are identified initially by the measured parameters included the cutting force, the workpiece deformation, the machining conditions, and machining error. The responses of cutting force and workpiece deformation in the constructed model correspond to the evaluation cases are substituted by the measured cutting force and the measured workpiece deformation. By comparing the estimated machining error and the measurement machining error, this error modelling is evaluated reasonably.

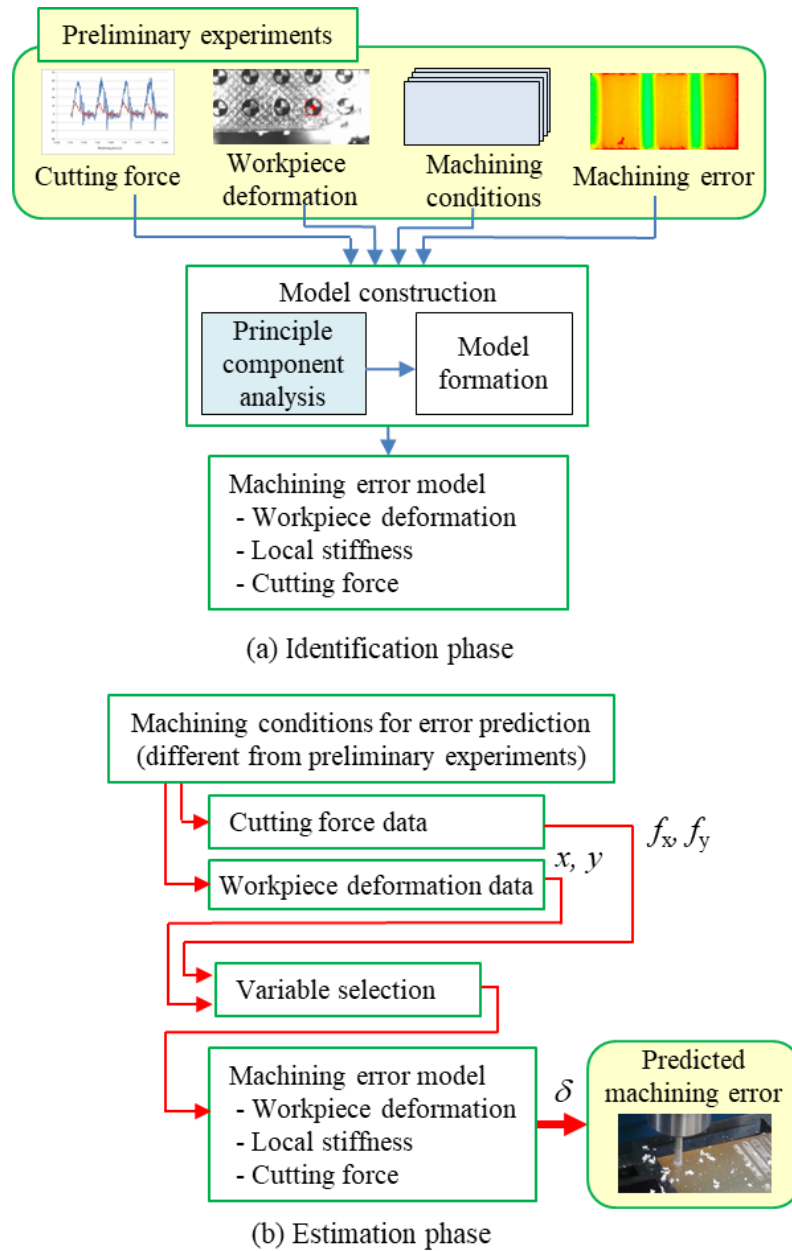


Fig. 3-3 Evaluation of machining error model

4. Compositional Machining Error Prediction Models

This chapter proposes the diverse machining error modelling based on elastomer end-milling. These machining error prediction models consist of the conventional cutting condition, mechanistic, and statistics model. The concepts of modelling, experimental setup, preliminary experiment, model construction, and their formula will be described, respectively.

The modelling of machining operations has been evolving as an essential engineering tool to simulate operation physics ahead of costly production trials of parts used in industry [22]. In order to achieve the appropriate machining, a model-based approach is widely desired to become an alternative to a conventional trial and error approaches concept. Regarding these reasons, the prediction models are continuously developed and evaluated by comparing predicted machining error with experimental results. Previously, a framework of the compositional machining simulation has been proposed for model-based precision machining [14-16, 55]. Since the standard metal machining processes are planned by assuming rigid workpiece and ideal chip removal, it is difficult to apply for elastomer end-milling because of low rigidity and different fracture mechanism. There have been many researches to predict the machining process, such as the analysis of workpiece deformation, chip separation, cutting force, including the soft materials [17-20, 25, 37-39, 51, 62-65]. Previously, the mechanistic approach model has been proposed for predicting machining error in elastomer end-milling [21]. However, the proposed mechanistic approach requires the heuristic introduction of an empirical model. By utilizing the statistics, the sensational data have been considered to construct the machining error model. The machining error in the end-milling process has involved machining conditions, workpiece shape, and material removal characteristics. During the actual machining situation, workpiece shape and machining conditions such as depth of cut and width of cut are varied according to the machining process [21-25, 62]. Furthermore, tool rotation speed and feed rate are sometimes adjusted to find the appropriate conditions when the new cutting tool, workpiece material, and/or different workpiece shape

has to be applied. Regarding the workpiece deformation, the elastic analyses and measurement in the elastomer end-milling have been investigated by a similar method for metal end-milling [37-39]. However, there have been a limited number of studies on the elastomer shape transferring error because the elastomer chip separation mechanism is entirely different from the metal mechanism [20, 26]. In the conventional metal end-milling, cutting force during the end-milling is one of the dominant factors to machining error. The cutting force causes the workpiece deformation, thermal formation, machine tool deflection, and tool wear. On the other hand, most elastomers have low rigidity then the relationship between cutting force and machining error is considered fundamental characteristics. The chip formation mechanisms of elastomers are moderately different from those of metal milling. Furthermore, the deformation of the workpiece dominantly affects the machining accuracy. These facts indicate that the problem to be tackled for the end-milling of soft objects or elastomers is to control the appropriate surface generation of the machined workpiece that can overcome by designing an optimized cutting tool shape and/or determining proper machining conditions. Because of the large variety of elastomer objects, it is necessary to develop a systematic method to aggregate empirical cases to generate a mechanistic model of the surface generation process. There is few knowledge of what factors are dominant to the error and needed more knowledge in further. Therefore, a preliminary evaluation of the important factors is necessary [15]. Shih et al. [27] have reported that the extraordinary mechanical properties of elastomer: considerably enduring elongation and low thermal conductivity are capable of affect chip formation during machining significantly. In other words, tool wear is not a dominant factor for elastomer end-milling. Meanwhile, the accumulations of cutting heat and the influence of thermal effects are not a dominant factor of the error tendency have been reported [25]. Therefore, it is promising to improve the machining accuracy by considering mechanistic surface generation model with the dominant factors such as cutting force, workpiece deformation, and machining conditions for elastomer end-milling. The analysis target uses the data obtained in the experiments from previous research [21], and the machining experiments are carried out under several conditions. In addition, in this study, the 18 variables described below are the targets of the analysis items. Specifically, for machining error (M.E.), 3 workpiece conditions (width, height, length), 4 machining conditions (rpm, feed rate, width of cutting (WoC), depth of cutting (DoC)), and 10 physical quantities during machining (x , $1/x$, f_x , $1/f_x$, f_x/x , y , $1/y$, f_y , $1/f_y$, f_y/y) are associated. To construct the prediction models, a systematic procedure for creating the preliminary experiment which conducted the appropriate machining factors for parameters estimation is proposed.

4.1 Experimental Setup and Configurations

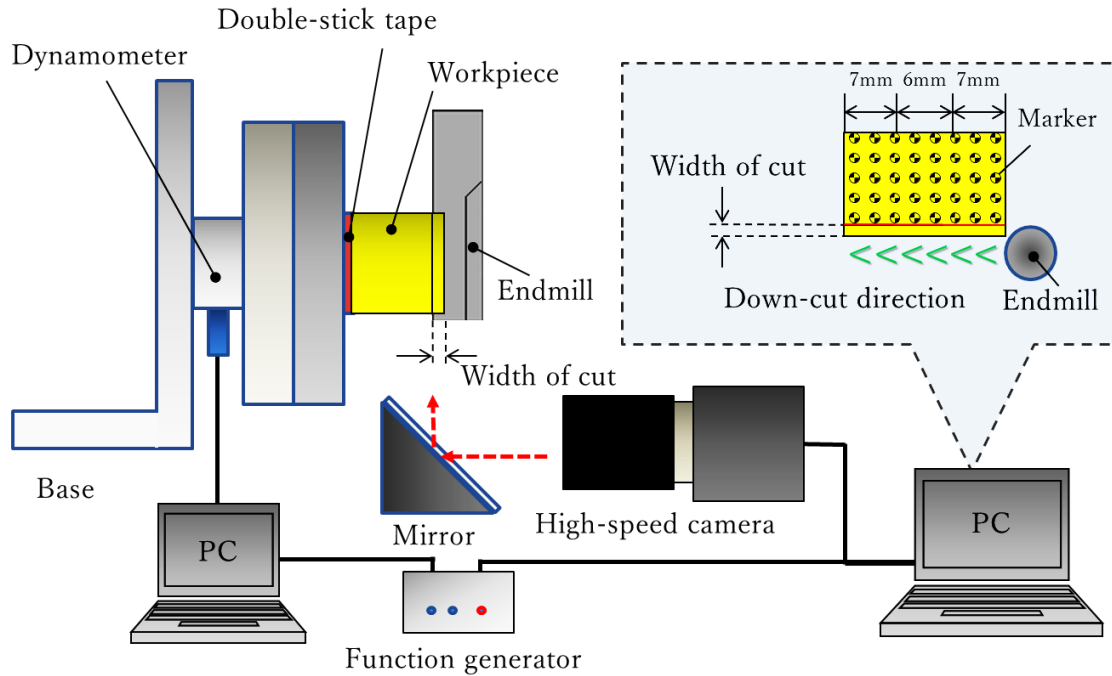


Fig. 4-1 Instruments setup schematic

Figure 4-1 represents a schematic diagram of the experimental setup and configurations in which the instruments are detailed in **Chapter 2**.

Concerning the experimental configuration, the workpiece was stuck by double-side tape on a metallic base which was seized together with the dynamometer. In the experiments, there are no effects on the thickness of double-stick tape which were evaluated and confirmed based on their stability and uniformity. The workpiece has been operated by the down-cutting method while a mirror is applied to observe the cutting behavior as a side view reflection during the machining process. Meanwhile, the workpiece deformation is monitored by the recorded moving images under the image processing method using a synchronized transmitting trigger signal from a function generator and a high-speed camera. In actual machining, the machining configuration is shown in **Fig. 4-1**, and an actual experimental setup is shown in **Fig. 4-2**.

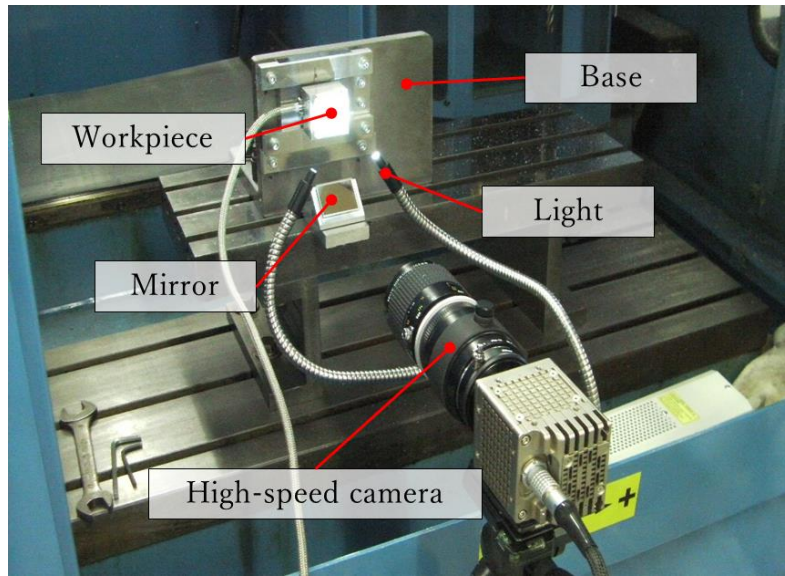


Fig. 4-2 Actual experimental setup

4.2 Preliminary Experiment

Initially, a preliminary experiment is conducted to obtain the data for model identification. In order to identify the machining error model, machining experiments of elastomer end-milling with various machining conditions are designed to obtain the cutting forces, the workpiece deformation, and the machining error. All machining cases, and machining directions are down cut. The concept of the preliminary experiment creation is mentioned in topic 2.3.1 and the systematic procedures are appeared.

Table 4-1 Machining conditions for preliminary experiment

Conditions	1	2	3	4	5	6
Machining direction	Down cut					
Width of cut (W) [mm]	1.0	0.5	0.7	1.0		
Depth of cut (D) [mm]	5.0	10.0				
Rotational speed (R) [rpm]	4000				2000	4000
Feed Rate (F) [mm/tooth]	0.0125				0.025	
Workpiece width (A) [mm]	5.0	10.0				
Workpiece height (H) [mm]	10.0					20.0
Workpiece length (L) [mm]	20.0					

For the machining industry, little preparation for the experiment is a desirable requirement due to a necessity to avoid costly and time-consuming trials. **Table 4-1** shows the machining condition for the preliminary experiment in elastomer end-milling cases. This experiment is the central part of a proposed framework for error modelling introduced in the previous chapter. There are 6 preliminary experiments for the processing performed in three sections; the early stage, middle stage, and final stage. Therefore, the total is 18 machining cases for this preliminary experiment. For the results of the machining error of the preliminary experiment, the comparison plot of regression proposed models will be shown in **Fig. B-1** to **Fig. B-3, Appendix B**.

4.3 Conventional Cutting Conditions Model

Due to using preliminary experiments obtained data, model parameters for deformation analysis, cutting force prediction, and coefficients of the empirical models are determined. From the machining error modelling framework, in the estimation phase, the machining error of the actual machining situations will be calculated, based on the identified cutting force model, workpiece deformation model, and machining error model.

In order to evaluate the proposed framework, the simplified evaluation cases are investigated by using reported machining cases [21]. One is a direct modelling case, and the other is a proposed compositional modelling case. For the direct conventional cutting conditions modelling case, only the cutting conditions are introduced as an error model variable. Four machining conditions are considered for model construction: width of cut (WoC), depth of cutting (DoC), feed rate of cutting, and rotational speed of the spindle, then the machining error can be formulated as follows;

$$\delta = \alpha_1 W + \alpha_2 D + \alpha_3 R + \alpha_4 F + \alpha_5 \quad \text{..... (4-1)}$$

where W represent width of cut, D represent depth of cut, R represent rotational speed of spindle, F represent feed rate of cutting and $\alpha_1 \cdots \alpha_5$ are model coefficients, and δ is machining error.

4.4 Mechanistic Model

The mechanistic modeling for machining error in elastomer end-milling has been introduced by Wu, et.al [21]. The model which utilized machining knowledge for empirical model formulation was employed. By introducing a mathematical model which reflect process knowledge, stable calculation with limited experimental data. As mentioned in topic 2.2.4, thus, the deformation at cutting point can be presented by a function of a displacement of a neighborhood point of cutting point. On the other hand, the shape transfer error is complicated to model quantitatively because it is affected by a crack generation point, a trajectory of crack propagation, and slippage between cutting tool and workpiece. From the analysis of crack generation of elastomer, the indentation forces, an indentation depth, and a local stiffness are important factors for the crack generation. Because the indentation depth can be related to the local workpiece deformation, it is assumed that the shape transfer error is affected by the workpiece deformation, cutting force and the local stiffness of workpiece.

The model applied machining knowledge for the empirical model formulation was employed. By proposing the mathematical model which reflects process knowledge, the offered model is applicable of skipping evaluating the complicated phenomena of elastomer [23-24, 54]. Based upon the empirically extracted factors to explain machining error for elastomer end-milling phenomena, a simplified error model that able to apply to statistical analysis was introduced [21]. Regarding the empirical assumptions, the machining error can be formulated the mechanistic model as follows;

$$\delta = \beta_1 x + \beta_2 y + \beta_3 f_x + \beta_4 f_y + \beta_5 \frac{f_x}{x} + \beta_6 \frac{f_y}{y} + \beta_7 \quad \text{..... (4-2)}$$

where x and y represent the displacements of the neighborhood point, f_x and f_y represent cutting forces at a surface generation moment, and $\beta_1 \dots \beta_7$ are model coefficients, and δ is machining error. The cutting forces have normalized by an axial depth of cut. An approximate local stiffness of the workpiece is the fifth and the six-term on the right side of **Eq. 4-2**. Because the displacements and the cutting force can be predicted before machining when the appropriate model parameters have been identified, the machining error can be predictable.

4.5 Statistical Model

Regarding the mentioned model, the essential variables are obtained from the insight observation of humans. This method can be achieved by human heuristics that cannot be confirmed the applicability in advance. For this main reason, it is necessary to establish a more systematic methodology to evaluate the candidates of the model variables. As the application of the statistical technique to the variables' evaluation, the principal component analysis (PCA) statistical method, used in exploratory data analysis and for making predictive models [56-59], is employed for analyzing the error model that is related machining error and variables such as machining conditions (depth of cut (DoC), width of cutting (WoC), feed rate of cutting (F), and rotational speed of the spindle) and physical state values (cutting force and/or workpiece deformations). The correlation between both machining conditions and physical state values to the machining error is considered from the statistical aspect that can select the priority related variables for model formation. Based on this idea, the systematic model construction procedure is defined as follows;

The purpose of the principal component analysis of this study is to confirm whether the data are separated into clusters. Therefore, we do not reduce the principal components according to the results and continue to pursue the analytical principal components. However, the idea is that 70% to 80% of the total information should be covered. Because the number of principal components is adopted, the contribution rates are increased from the top, and the cumulative contribution rate reaches 70% to 80%.

According to acquired cutting force, workpiece deformation, and machining error, the principal component analysis (PCA) is instructed to recognize the priority relations of machining conditions and physics-based parameters that are important for constructing an error model. PCA has become a dimensional reduction method to reduce the dimensionality of large data sets by condensing a set of variables into a smaller one that preserves the amount of data from the large. Obviously, reducing the number of variables in a data set decreases accuracy, but the method in dimensional reduction is to trade a little accuracy for simplicity. In this study, the following 18 components that can be utilize in actual experiment are evaluated. There are multiple numerical values, and determining which parameters have a significant influence; [55, 66]

1. Machining error (M.E.)
2. Workpiece conditions; width (A), height (H), and length (L)

3. Machining conditions; rotational speed (R), feed rate (F), width of cutting (W), and depth of cutting (D)
4. Physical state values; displacement terms of neighborhood point; (x) , $(1/x)$, (y) , $(1/y)$ and cutting force terms at a surface generation moment; (f_x) , $(1/f_x)$, (f_x/x) , (f_y) , $(1/f_y)$, (f_y/y)

Since some of the 18 variables have different units, the standardization of experimental data is performed to establish a certain standard that allows the numerical values between each condition to be used in common. Initially, standardization is employed as the first step of the PCA procedures. Then covariance matrix, eigenvectors, and eigenvalues are computed. The aim is to utilize the feature vector formed using the eigenvectors of the covariance matrix, to reorient the data from the original axes to the ones represented by the principal components (PC). The total contribution rate of each PC is equal to 1 then the data percentage can be rearranged. By ranking eigenvectors in order of eigenvalues, in descending order highest to lowest, the principal components in order of significance are obtained.

Regarding PCA is employed for constructing this model, so the general-purpose Python programming language is utilized for executing the parameter components analysis. Furthermore, since characters other than alphanumeric characters written in the table are not displayed, all characters are rewritten to alphanumeric characters. Since performing an analysis method, the lengths are all the same and not included in the analysis.

However, the Python programming language needed to perform statistical analysis for coding on the scientific computing assist platform, which is used in this research as follows;

- Python version 3.8 (32-bit)
- Visual Studio Code
- Anaconda Prompt (Anaconda version 3)

Visual Studio Code and Anaconda Prompt (Anaconda 3) Coordinate and activate. Then call Python in the terminal. The program is always executed while interacting with Python. The coding of the PCA model generated will be proposed in **Appendix C**, and the machining error as CSV data analyzed will be introduced in **Appendix A**. Principal component analysis by Python is shown in **Fig. 4-3**.

```

48 # PCA の固有値
49 pd.DataFrame(pca.explained_variance_, index=["PC{}".format(x + 1) for x in range(len(dfs.columns))])
50
51 # PCA の固有ベクトル
52 pd.DataFrame(pca.components_, columns=df.columns[1:], index=["PC{}".format(x + 1) for x in range(len(dfs.columns))])
53
54 # 第1主成分と第2主成分における観測変数の寄与度をプロットする
55 plt.figure(figsize=(8,8))
56 for x, y, name in zip(pca.components_[0], pca.components_[1], df.columns[1:]):
57     plt.text(x,y,name,fontsize=15)
58
59 plt.scatter(pca.components_[0], pca.components_[1], alpha=0.8)
60 plt.grid()
61 plt.xlabel("PC1",fontsize=18)
62 plt.ylabel("PC2",fontsize=18)
63 plt.show()

```

Fig. 4-3 Example of program coding for PCA approach

```

>>> # 行列の標準化
... dfs = df.iloc[:, 1:].apply(lambda x: (x-x.mean())/x.std(), axis=0)
>>> dfs.head(81)

```

	width	height	position	m.e	rpm	x	1/x	...	1/y	fy	1/fy	fy/y	feedrate	WoC	DoC
0	0.414447	-0.697411	-1.217161	-0.374044	-2.084629	0.186792	-0.430965	...	1.154124	1.198780	-0.923629	3.806746	1.115749	-1.584878	0.414447
1	0.414447	-0.697411	0.000000	-1.039619	-2.084629	-0.353182	-0.238102	...	0.716088	-0.139330	-0.260907	1.247352	1.115749	-1.584878	0.414447
2	0.414447	-0.697411	1.217161	-1.065967	-2.084629	-0.307521	-0.259531	...	0.643083	-0.026415	-0.334543	1.289880	1.115749	-1.584878	0.414447
3	0.414447	-0.697411	-1.217161	0.103898	-2.084629	-0.059945	-0.366677	...	-0.159982	-0.276594	-0.187271	-0.145752	-0.862010	0.554707	0.414447
4	0.414447	-0.697411	0.000000	-0.264818	-2.084629	-0.520745	-0.130956	...	-0.269491	0.178338	-0.481814	-0.101936	-0.862010	0.554707	0.414447
...
76	0.414447	-0.697411	0.000000	0.574974	0.473779	-0.308568	-0.259531	...	-0.232988	0.281545	-0.555450	0.008894	1.115749	-0.729044	0.414447
77	0.414447	-0.697411	1.217161	0.551021	0.473779	-0.568710	-0.080098	...	-0.305994	0.864499	-0.776357	0.065597	1.115749	-0.729044	0.414447
78	0.414447	-0.697411	-1.217161	1.169009	0.473779	-0.015750	-0.366677	...	-0.379000	1.525378	-0.997264	0.072041	1.115749	0.554707	0.414447
79	0.414447	-0.697411	0.000000	1.044453	0.473779	-0.381667	-0.216673	...	-0.379000	1.624120	-0.997264	0.118435	1.115749	0.554707	0.414447
80	0.414447	-0.697411	1.217161	1.333486	0.473779	-0.798482	0.233340	...	-0.415503	1.689066	-0.997264	0.099104	1.115749	0.554707	0.414447

```

[81 rows x 18 columns]

```

Fig. 4-4 Standardization of target data (factor_analysis.csv)

Figure 4-4 demonstrates the standardization of the numerical values of the target data (factor_analysis.csv), and **Figure 4-5** expresses the scores of each principal component with a total of 81 data.

```

>>> # 主成分分析の実行
... pca = PCA()
>>> feature = pca.fit(dfs)
>>>
>>> # データを主成分空間に写像
... feature = pca.transform(dfs)
>>>
>>> # 主成分得点
... pd.DataFrame(feature, columns=["PC{}".format(x + 1) for x in range(len(dfs.columns))]).head(81)

```

	PC1	PC2	PC3	PC4	PC5	PC6	PC7	...	PC12	PC13	PC14	PC15	PC16	PC17	PC18
0	-0.076682	3.821374	-1.877936	3.217428	-0.438630	1.284698	0.076404	...	-0.534775	-0.412998	0.557451	-0.292723	-0.329946	0.136108	0.477384
1	0.335291	2.671270	-0.518429	2.887105	-0.634851	0.129403	-0.291948	...	-0.364710	0.075401	0.251496	-0.029747	0.246125	-0.077134	-0.157361
2	0.102057	3.005647	0.114956	3.181140	-0.776578	-0.386757	0.397003	...	-0.040594	0.017572	0.724581	-0.076256	0.197672	0.054501	-0.181547
3	-0.447008	0.215946	-0.749933	0.965676	-1.110211	-0.601418	-1.962405	...	-0.103628	0.104286	-0.816966	-0.134482	0.289359	-0.107588	0.057233
4	-0.941494	1.064266	0.599262	1.581579	-1.502019	-1.055765	-1.294897	...	0.057006	0.051480	-0.318381	-0.041913	0.032597	0.077038	-0.030416
...
76	-0.064664	0.594025	-0.454255	-0.020225	1.766426	-0.066310	-0.083595	...	0.203830	-0.062728	-0.278553	-0.128418	0.037799	-0.036612	-0.046278
77	-0.189812	1.020519	0.312218	-0.157939	2.147948	-0.646013	0.522285	...	0.415775	-0.018930	-0.147804	0.037509	-0.125138	0.145306	0.050251
78	-1.297155	0.169952	-0.781554	-0.486300	2.160670	0.264863	-0.735825	...	-0.233761	-0.270139	-0.148787	0.085649	-0.037962	0.000644	-0.138023
79	-1.194135	0.549806	0.002572	-0.354029	2.185171	-0.301386	-0.071119	...	-0.045434	-0.154779	-0.123892	0.206299	-0.030605	0.034316	-0.007292
80	-1.126798	0.837600	1.037808	-0.374652	2.387166	-0.637488	0.467457	...	0.190346	-0.224934	-0.241442	0.230400	-0.074434	0.006933	0.118972

```

[81 rows x 18 columns]

```

Fig. 4-5 Calculation of principal component score

Figure 4-6 plots the principal component scores of the first and second principal components. In the plots of PC1 and PC2, the points are not locally concentrated, and there are variations. **Figure 4-7** shows the plotting of the principal component scores from PC1 to PC18. In the plotting of the principal components, there are almost widely scattered.

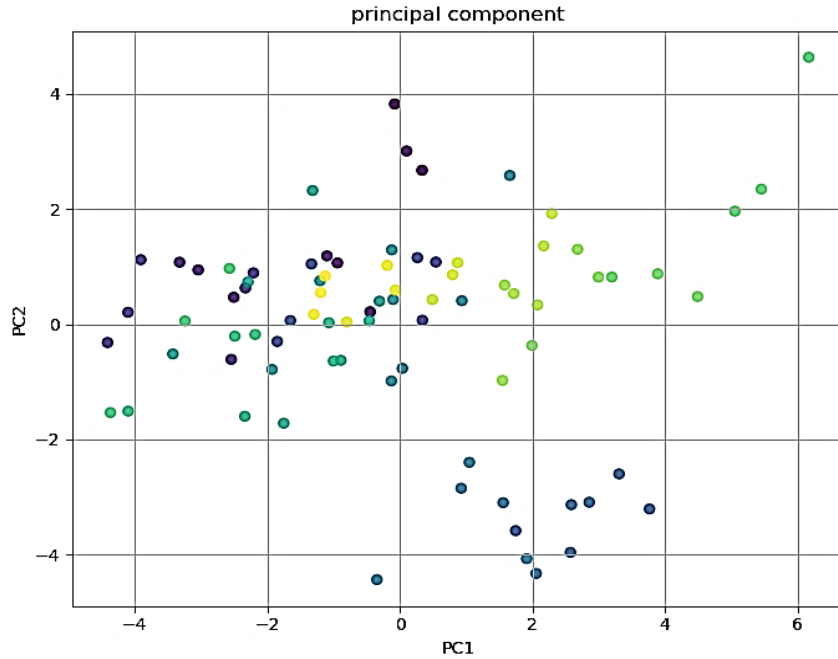


Fig. 4-6 A plot of principal component score

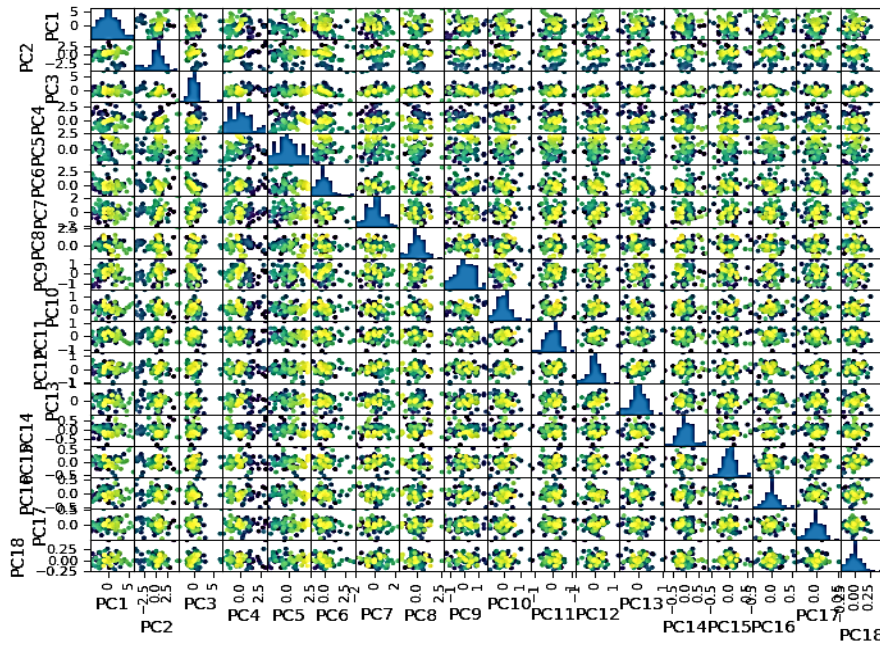


Fig. 4-7 All principal component score plot

PC1 was 0.318 (about 32%) and PC2 was 0.182 (about 18%). The total up to PC7 is 0.901 (about 90%). After PC10, the ratio of each main component is 1% or less, and the total of PC10 to PC18 is 0.041, which is about 4%. **Figure 4-8** summarizes each contribution rate in a pie chart.

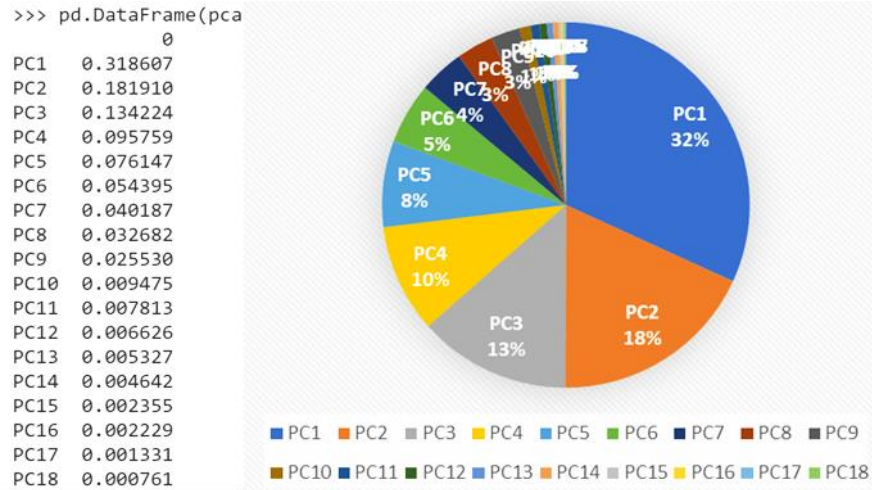


Fig. 4-8 Contribution rate from PCA

Figure 4-9 presents the contribution rate of each principal component when the total contribution rate is 1, and the percentage of the data can be explained by one principal component axis.

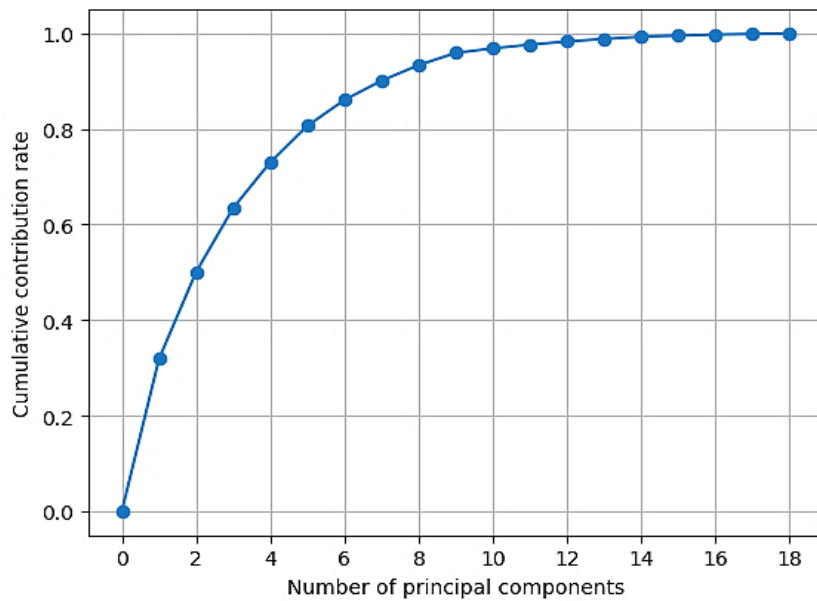


Fig. 4-9 Cumulative contribution rate of main components

Furthermore, **Fig. 4-9** is a line graph showing the sum of these contribution ratios in descending order. The slope of the line segment connecting the contribution ratio is reduced greatly after PC10.

```
>>> # PCA の固有値
... pd.DataFrame(pca.explained_variance_, index=["PC{}".format(x + 1) for x in range(len(dfs.columns))])
0
PC1    5.734922
PC2    3.274386
PC3    2.416041
PC4    1.723659
PC5    1.370642
PC6    0.979103
PC7    0.723373
PC8    0.588267
PC9    0.459539
PC11   0.140638
PC12   0.119267
PC13   0.095878
PC14   0.083561
PC15   0.042391
PC16   0.040121
PC17   0.023964
PC18   0.013703
```

Fig. 4-10 The eigenvalues of main components

The eigenvalues in this study are shown in **Fig. 4-10**, and the eigenvectors are shown in **Fig. 4-11**.

```
>>> # PCA の固有ベクトル
... pd.DataFrame(pca.components_, columns=df.columns[1:], index=["PC{}".format(x + 1) for x in range(len(dfs.columns))])
width height position m.e rpm x 1/x ... 1/y fy 1/fy fy/y feedrate WoC DoC
PC1 -0.146341 -0.236239 0.042092 -0.332076 0.170018 -0.271115 0.136754 ... 0.279311 -0.309869 0.289872 0.183969 -0.182118 -0.235868 -0.129880
PC2 0.434921 -0.030884 0.146668 -0.196286 -0.159852 -0.157096 0.131348 ... 0.239678 0.248035 -0.325253 0.373367 0.079393 -0.274786 0.408649
PC3 -0.145303 -0.028685 0.414252 0.009878 0.021004 -0.318064 0.501857 ... -0.194056 0.083654 -0.027743 -0.176818 -0.015972 0.215720 -0.171299
PC4 -0.269252 -0.401776 0.002338 0.059289 -0.469539 -0.133595 -0.170405 ... 0.099745 -0.026579 0.147773 0.153566 0.267963 -0.107807 -0.284173
PC5 -0.018410 -0.356616 0.069282 0.230207 0.236326 -0.181954 -0.030515 ... -0.137827 0.255710 -0.138079 -0.070220 0.616264 -0.183815 -0.019559
PC6 -0.076084 0.105890 -0.441609 0.226479 0.151724 0.319007 0.356281 ... 0.290137 -0.070982 0.156848 0.234587 0.253688 -0.188240 -0.092239
PC7 -0.173806 0.435699 0.533432 0.076616 0.376871 -0.015113 -0.195178 ... 0.300999 0.062597 0.048193 0.275016 0.146028 -0.049025 -0.195280
PC8 -0.107734 -0.189159 -0.246555 0.072276 0.075732 -0.111380 -0.017322 ... 0.199847 0.405659 -0.246067 0.404094 -0.246844 0.550451 -0.231859
PC9 0.075261 -0.066730 -0.326820 -0.228282 0.556366 -0.159333 -0.131551 ... -0.251079 0.020030 -0.055593 -0.088592 0.093749 -0.020942 -0.039759
PC10 0.047598 -0.306643 0.132518 0.440261 0.235564 -0.043575 -0.054458 ... 0.185107 -0.231348 0.272745 0.015859 -0.016141 0.347544 0.554158
PC11 -0.228243 0.104484 0.123278 0.303516 -0.176293 0.306166 0.108358 ... -0.300549 -0.099111 -0.199179 0.231671 0.037300 -0.015434 0.064772
PC12 0.317534 -0.471067 0.260361 0.180547 0.178899 0.377641 0.078175 ... 0.074768 -0.070449 -0.192342 -0.091549 -0.348982 -0.235540 -0.335123
PC13 -0.355357 -0.222085 0.101204 -0.426897 -0.034813 0.180040 -0.011686 ... 0.115310 -0.247524 -0.247020 -0.005603 0.144933 0.168196 0.271935
PC14 -0.052810 -0.140576 0.141820 -0.384380 0.185438 0.513119 0.083256 ... -0.194693 0.090943 0.036452 0.175449 0.185631 0.180960 0.004982
PC15 0.106397 -0.039605 0.083085 -0.153815 -0.117783 0.224385 0.163368 ... 0.187022 0.530960 0.529740 -0.258935 0.075374 0.096520 0.049073
PC16 0.508909 0.065483 0.070064 -0.081971 -0.139946 0.052156 -0.276295 ... 0.134793 -0.317722 0.001353 -0.030353 0.349518 0.388665 -0.309128
PC17 -0.163763 -0.088075 0.085558 0.003683 0.011651 0.118846 -0.602859 ... -0.108145 0.260622 0.148910 0.055557 -0.213050 -0.192467 0.089399
PC18 0.246635 -0.054653 0.055713 -0.034062 -0.026194 -0.093611 0.072289 ... -0.523402 -0.082546 0.402173 0.548631 -0.033875 0.026080 -0.012137
```

Fig. 4-11 Eigenvectors for each principal component condition

```
... plt.figure(figsize=(8,8))
<Figure size 1600x1600 with 0 Axes>
>>> for x, y, name in zip(pca.components_[0], pca.components_[1], df.columns[1:]):
...     plt.text(x,y,name)
...
Text(-0.14634142547418832, 0.4349214395164109, 'width')
Text(-0.23623942702332143, -0.030883791244498932, 'height')
Text(0.04209155344302808, 0.14666785131741666, 'position')
Text(-0.3320761330488562, -0.19628593779916934, 'm.e')
Text(0.1700182139895515, -0.1598522576523324, 'rpm')
Text(-0.27111509693070707, -0.1570962480171663, 'x')
Text(0.136754345791658, 0.13134845081427676, '1/x')
Text(-0.2569760466183433, 0.12505184431654787, 'fx')
Text(0.30512952435889057, -0.09224884657442238, '1/fx')
Text(0.014174016179340793, 0.16753310138970945, 'fx/x')
Text(-0.3642830207035207, -0.13109815001121689, 'y')
Text(0.2793112497794358, 0.23967771354934414, '1/y')
Text(-0.3098694104684405, 0.2480349612654255, 'fy')
Text(0.2898723138174459, -0.32525310297415616, '1/fy')
Text(0.18396879408372024, 0.3733665639167007, 'fy/y')
Text(-0.18211763435443606, 0.07939298993443168, 'feedrate')
Text(-0.23586844691486036, -0.27478649120262966, 'WoC')
Text(-0.12987966719120156, 0.40864881312209644, 'DoC')
>>> plt.scatter(pca.components_[0], pca.components_[1], alpha=0.8)
<matplotlib.collections.PathCollection object at 0x1B8EFB30>
>>> plt.grid()
>>> plt.xlabel("PC1")
Text(0.5, 0, 'PC1')
>>> plt.ylabel("PC2")
Text(0, 0.5, 'PC2')
>>> plt.show()
```

Fig. 4-12 Coordinated eigenvectors of variables related to PC1 and PC2

In **Fig. 4-12**, the values of the eigenvectors of each condition related to PC1 and PC2 are identified at the coordinate points.

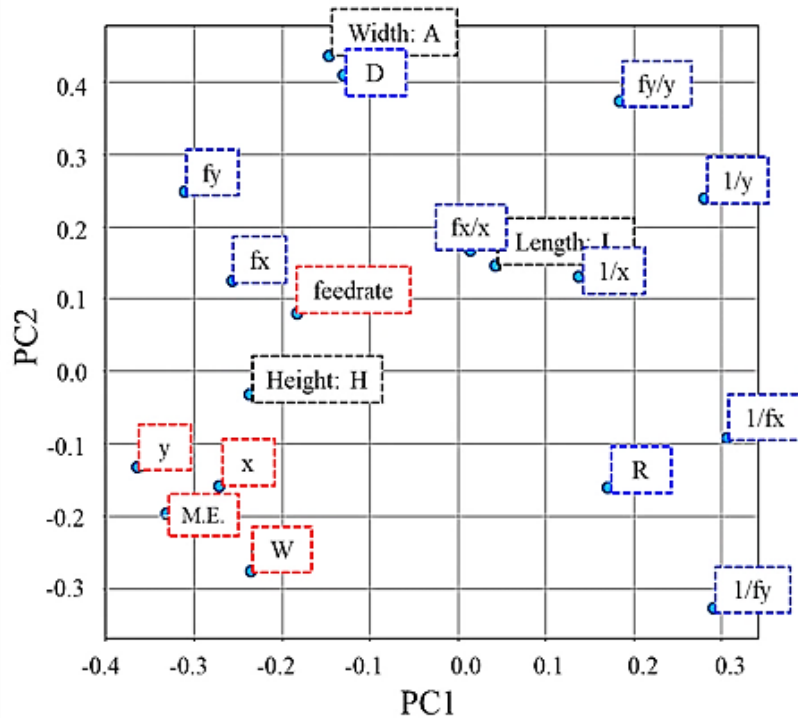


Fig. 4-13 Principal Component observed variable contribution

Figure 4-13 shows the plot of principal component scores by comparing the first and second PC (PC1 versus PC2). From PCA plotting, there are variations from every component in which the scores are not concentrated in one area, locally. Machining error is the target objective which principal component scores and eigenvector can determine the influence related variables are displacement y , x , the width of cut: W , and feed rate; F . Width, height, and length ($A \times H \times L$) are workpiece conditions that should be avoided considering to apply the error model to various workpiece shape. Based on the PCA approach, the influential variables are selected then the machining error model called the statistical model can be formulated the hybrid machining conditions and physic-based model as follows;

$$\delta = \gamma_1 x + \gamma_2 y + \gamma_3 W + \gamma_4 F + \gamma_5 \quad \text{..... (4-3)}$$

where x and y represent displacements of the neighborhood point, W represent width of cut, F represent feed-rate of cutting and $\gamma_1 \dots \gamma_5$ are model coefficients, and δ is machining error.

Furthermore, the correlation coefficients and the multiple regression analysis are applied to determine the coefficients and linear regression results of **Eq. (4-1)** to **Eq. (4-3)** for comparison, respectively.

4.6 Machining Error Calculation

For analyzing the data obtained from the experiments, two statistical methods are used in this study as the data analyzer consisted of;

- Correlation coefficient
- Multiple regression analysis

The correlation coefficient method is used as a data analyzer for all 18 machined data obtained from preliminary experiments. The purpose of using is to determine the model's coefficients which affected their factors as shown in the prediction model equations. In order to identify the comparison of the proposed prediction models as the linear regression results, the data of the evaluation experiments will be performed using the multiple regression analysis. The

calculated error and the measurement error will be performed by correlation plotting to obtain a linear approximate straight line.

4.6.1 Model Coefficient Calculation

This analysis stage deals with the preliminary experiment in which there are six conditions for the processing performed in three sections; the early stage, middle stage, and final stage. Therefore, the total is 18 machining cases for this preliminary experiment. By using the correlation coefficient analysis, the data obtained from the preliminary experiments are computed by the data analyzer software. The results of the calculated coefficients are shown in **Table 4-2**. These coefficients will be substituted in the model equation for predicting the calculation of machining error in the next step.

Table 4-2 Machining error prediction model's variable coefficients

Conventional model		Mechanistic model		Statistical model	
Variable	Coefficient (α)	Variable	Coefficient (β)	Variable	Coefficient (γ)
W	115.828	x	0.512	x	0.368
D	1.256	y	0.137	y	0.262
R	0.00389	f_x	2.019	W	87.697
F	7714.154	f_y	0.823	F	4195.756
<i>Interception*</i>	-104.715	f_x/x	-25.134	<i>Interception*</i>	-32.807
		f_y/y	-13.679		
		<i>Interception*</i>	73.808		

* The intercept value is a constant at the final term of the equation

4.6.2 Multiple Regression Calculation

The purpose of using the multiple regression analysis is to identify the comparison of the proposed prediction models as the linear regression results. From the machining conditions, there are 21 evaluation experiments for the processing performed in three sections; the early stage, middle stage, and final stage. Therefore, the total is 63 machining cases for this evaluation experiment. After calculating the machining error from model equations by variables substitution, the data of the evaluation experiments are calculated using this analysis by the data analyzer software. The calculated machining error and the measurement machining error are computed to identify a plot of linear regression correlation. These correlation plots of the proposed models will be illustrated in the next chapter. From the assumption of the model formula and specify the data to be used for executing the

regression analysis. The multiple regression analysis results of the conventional cutting conditions, the mechanistic, and the statistical model are shown in **Table 4-3** to **Table 4-5**. The normal probability plot of the proposed models is shown in **Fig. 4-14** to **Fig. 4-16**.

Table 4-3 Multiple regression analysis of the conventional model

Regression Statistics								
Multiple R	0.710879							
R Square	0.505349							
Adjusted R Square	0.49724							
Standard Error	33.12819							
Observations	63							
ANOVA								
	df	SS	MS	F	Significance F			
Regression	1	68394.02	68394.02	62.31934	6.69E-11			
Residual	61	66946.08	1097.477					
Total	62	135340.1						
	Coefficients	Standard Error	t Stat	P-value	Lower 95%	Upper 95%	Lower 95.0%	Upper 95.0%
Intercept	63.69801	13.4136	4.748762	1.28E-05	36.87585	90.52016	36.87585	90.52016
M.E.	0.562219	0.071219	7.89426	6.69E-11	0.419808	0.704629	0.419808	0.704629

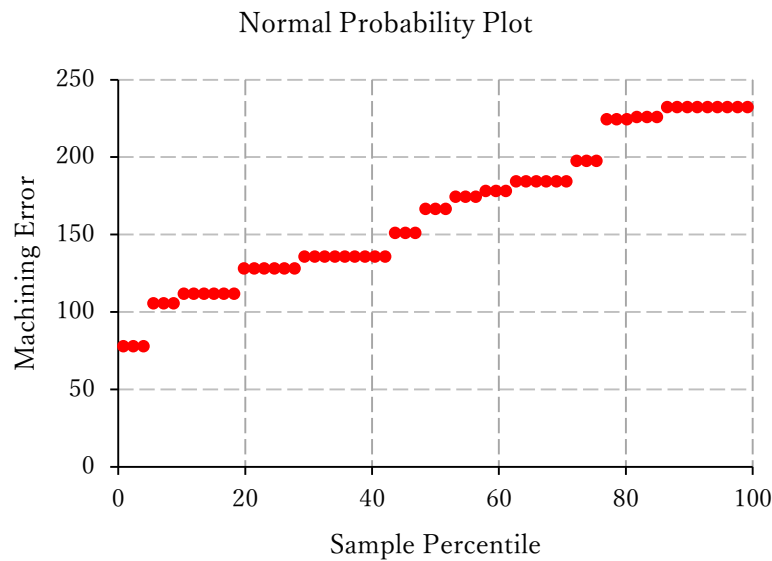


Fig. 4-14 Normal probability of the conventional model

Table 4-4 Multiple regression analysis of the mechanistic model

Regression Statistics								
Multiple R	0.61851							
R Square	0.382555							
Adjusted R Square	0.372433							
Standard Error	40.89061							
Observations	63							
ANOVA								
	df	SS	MS	F	Significance F			
Regression	1	63193.59	63193.59	37.79426	6.59E-08			
Residual	61	101994.6	1672.042					
Total	62	165188.1						
	Coefficients	Standard Error	t Stat	P-value	Lower 95%	Upper 95%	Lower 95.0%	Upper 95.0%
Intercept	69.53454	16.55661	4.199806	8.84E-05	36.42755	102.6415	36.42755	102.6415
M.E.	0.540422	0.087906	6.147704	6.59E-08	0.364642	0.716201	0.364642	0.716201

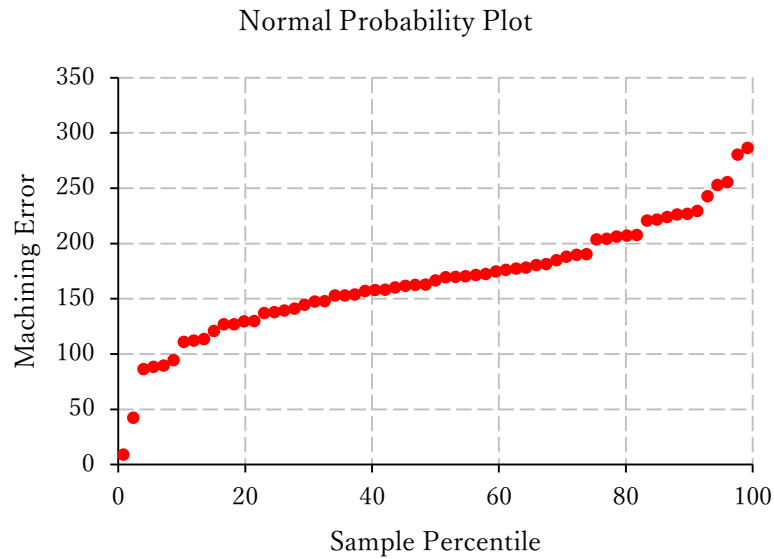


Fig. 4-15 Normal probability of the mechanistic model

Table 4-5 Multiple regression analysis of the statistical model

Regression Statistics								
Multiple R	0.894271							
R Square	0.79972							
Adjusted R Square	0.796437							
Standard Error	18.95126							
Observations	63							
ANOVA								
	df	SS	MS	F	Significance F			
Regression	1	87479.8	87479.8	243.5744	5.68E-23			
Residual	61	21908.17	359.1503					
Total	62	109388						
	Coefficients	Standard Error	t Stat	P-value	Lower 95%	Upper 95%	Lower 95.0%	Upper 95.0%
Intercept	49.23481	7.673366	6.416325	2.31E-08	33.89097	64.57865	33.89097	64.57865
M.E.	0.635843	0.040741	15.60687	5.68E-23	0.554376	0.71731	0.554376	0.71731

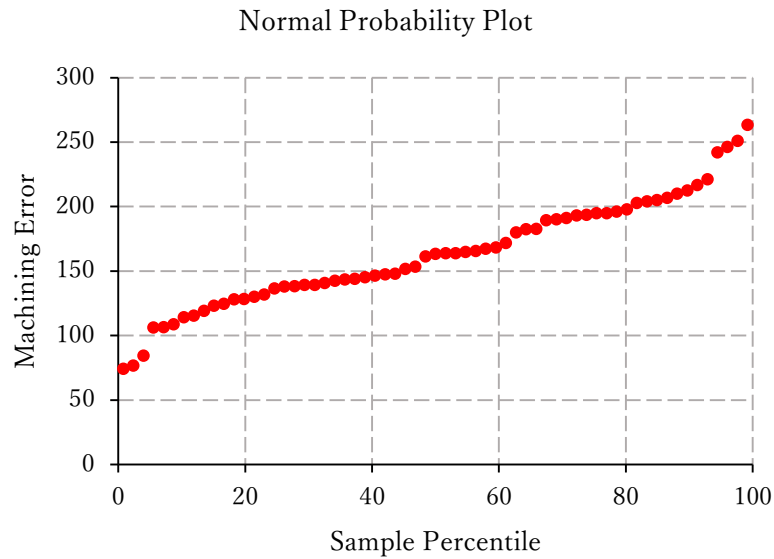


Fig. 4-16 Normal probability of the statistical model

5. Evaluation Experiment and Results Discussion

This chapter expressed the evaluation experimental to evaluate machining errors based on elastomer end-milling. The evaluation experiment consisting of diverse machining conditions and various workpiece dimensions will be proposed. Finally, the results of machining error will be discussed and compared.

5.1 Evaluation Experiment

Regarding the preliminary experiment which is used for identifying the machining error model in the framework for machining error modelling, Afterward, the machining conditions which different from the preliminary experiments are prepared as shown in **Table 5-1**.

To evaluate the proposed framework of machining error modelling, the cutting force model and the workpiece deformation model must also be investigated in principle. However, an evaluation of the combined model becomes complex, and it is difficult to find the problem when the estimation is not appropriate. Hence, an independent evaluation of the machining error model is investigated as a basic evaluation of the machining error model. If the machining error calculated with the error model shows good agreement with the measured machining error, thus the evaluation of the framework is equivalent to evaluating the cutting force model and workpiece deformation model that has been partially reported [25, 64].

The number of machining conditions with three cases of each is designed for actual machining situation experiments. Then the measured cutting force and workpiece deformation are used to calculate to determine the machining error. There are 21 evaluation experiments for the processing performed in three sections; the early stage, middle stage, and final stage. Therefore, the total is 63 machining cases for this evaluation experiment.

Table 5-1 Machining conditions for evaluation experiment

#	Width of cut (W) [mm]	Depth of cut (D) [mm]	Rotational speed (R) [rpm]	Feed Rate (F) [mm/tooth]	Width x Height x Length (A x H x L) [mm]
1	0.3	10.0	4000	0.0125	10x10x20
2				0.0250	
3	0.5		2000		
4					
5	0.7		4000		
6	5.0	0.0094		5x10x20	
7		0.0188			
8		0.0250			
9	1.0	10.0	4000	0.0094	10x15x20
10				0.0125	10x10x20
11					10x15x20
12		2000			
13		4000	0.0188	10x10x20	
14			0.0250		
15		2000		10x15x20	
16					
17		4000	0.0094	10x20x20	
18			0.0125		
19			0.0188		
20					
21					

5.2 Machining Error Prediction Results

To evaluate the machining operations, the measured cutting force and workpiece deformation acquired from the evaluation experiments were used to calculate the machining error as the estimated error. The estimated error can be compared with the measured machining errors. The experimental data for workpiece deformation and cutting force corresponding to machining cases which different from parameter identification case, are employed to calculate machining error. The coefficients of the direct error model are identified based on machining

conditions and measured machining error. The coefficients of the proposed error model are identified by measured cutting forces, workpiece displacements, and machining error. A coefficient correlation approach is employed to identify the coefficients. Then the multiple regression analysis is conducted to execute the plot of a linear regression model for comparing the calculated machining error from the model and the actual experimental results. The identified error models are used to calculate the machining error for different machining conditions. **Figure 5-1, 5-2, and 5-3** show comparisons between measured machining error and calculated machining error. The proposed models show good agreement to the measured error.

5.2.1 Machining Error of Conventional Model

A simplified evaluation case is a direct modelling case. For the direct modelling case, only cutting conditions are introduced as the error model variables. Four machining conditions: depth of cut, width of cut, feed rate of cutting, and rotation speed of the spindle are considered for model constructing. This machining error model formulation, **Eq. 4-1**. The measured machining error results in comparison to this model are shown in **Fig. 5-1**.

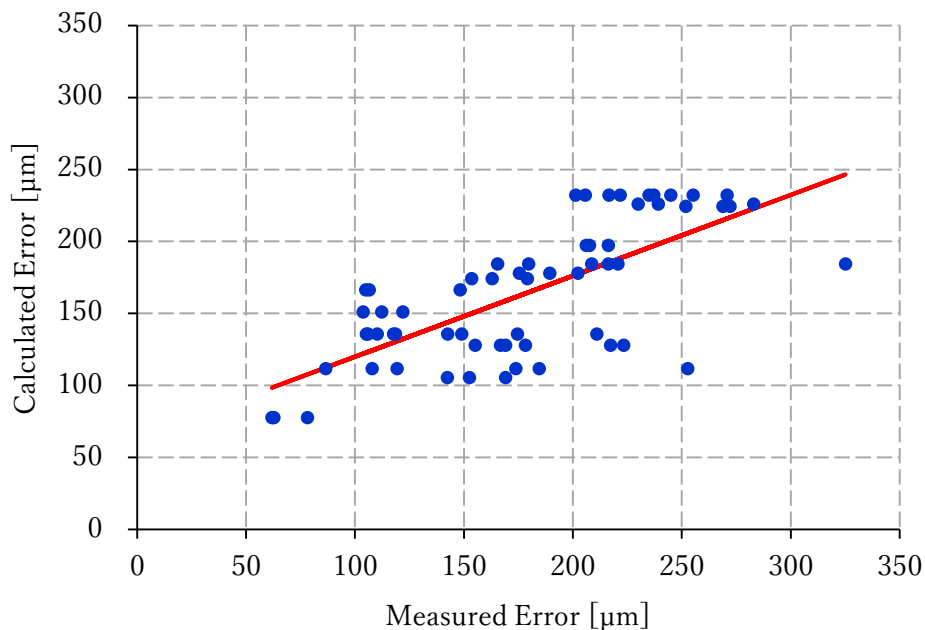


Fig. 5-1 Measured machining error comparison of the conventional model

From **Fig. 5-1**, the linear regression model for comparing the machining error results between the model calculation and actual machining results has been shown. It can be found that the different error of estimated and actual machining is 19.20%

5.2.2 Machining Error of Mechanistic Model

The mechanistic modeling for machining error in elastomer end-milling has been introduced by Wu, et.al. [21]. The model utilized machining knowledge for empirical model formulation was employed. By introducing a mathematical model which reflects process knowledge, and stable calculation with limited experimental data. The deformation at the cutting point can be presented by a displacement function of a neighborhood of the cutting point. On the other hand, the shape transfer error is complicated to model quantitatively because it is affected by a crack generation point, a trajectory of crack propagation, and slippage between the cutting tool and workpiece. From the analysis of the crack generation of elastomer, the indentation forces, an indentation depth, and a local stiffness are important factors for the crack generation. Because the indentation depth can be related to the local workpiece deformation, it is assumed that the shape transfer error is affected by the workpiece deformation, cutting force, and the local stiffness of the workpiece. Based on the extracted factors to explain the machining error for elastomer end-milling a simplified error model can be applied. A comparison of machining error results by mechanistic model (**Eq. 4-2**) is shown in **Fig. 5-2**.

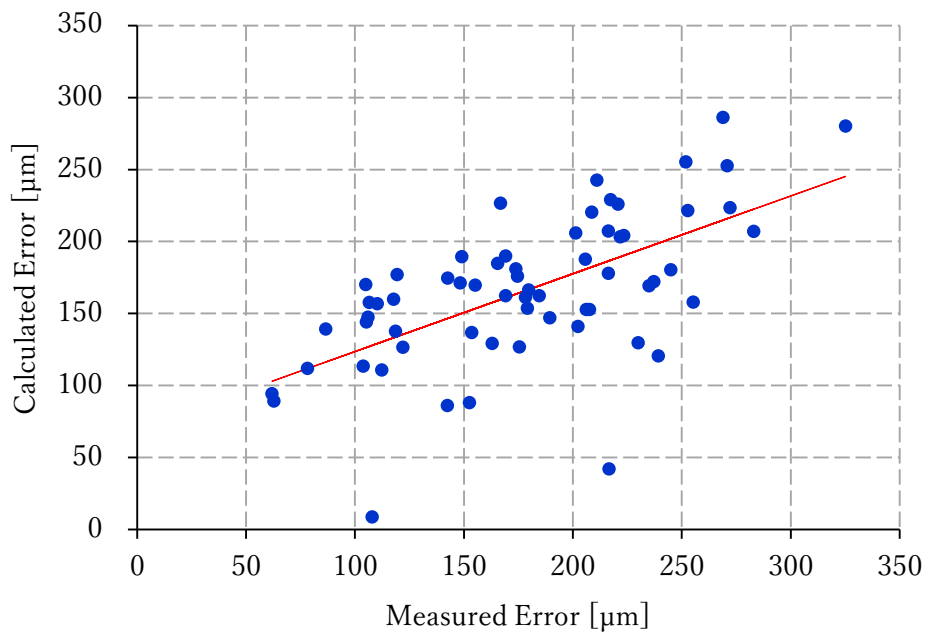


Fig. 5-2 Measured machining error comparison of the mechanistic model

From **Fig. 5-2**, the linear regression model for comparing the machining error results between the model calculation and actual machining results has been shown. It can be found that the different error of estimated and actual machining is 24.18%

5.2.3 Machining Error of Statistical Model

In this model, the essential variables are obtained from the insight observation of humans. This method can be achieved by human heuristics that cannot be confirmed the applicability in advance. For this main reason, it is necessary to establish a more systematic methodology to evaluate the candidates of the model variables. As the application of the statistical technique to the variables' evaluation, the principal component analysis (PCA) statistical method, used in exploratory data analysis and for making predictive models [56], is employed for analyzing the error model related to machining error and variables such as machining conditions (depth of cut, width of cut, feed rate of cutting, and rotational speed of the spindle) and physical state values (cutting force and/or workpiece deformations). The correlation between both machining conditions and physical state values to the machining error is considered from a statistical aspect that can select the priority related variables for model formation. Based on this idea, the statistic model can be constructed as **Eq. 4-3**, previous chapter.

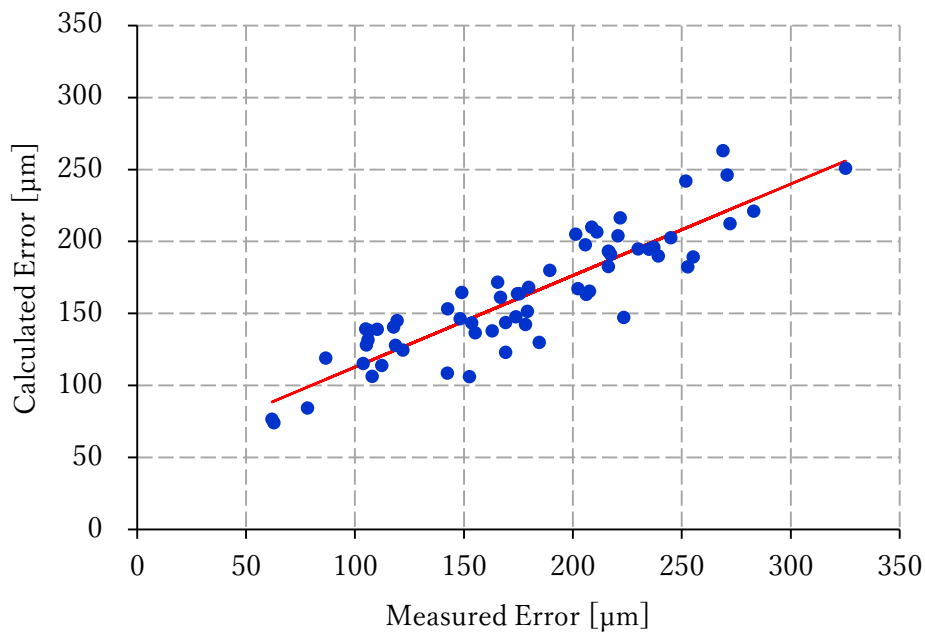


Fig. 5-3 Measured machining error comparison of the statistical model

From **Fig. 5-3**, the linear regression model for comparing the machining error results between the model calculation and actual machining results has been shown. It can be found that the different error of estimated and actual machining is 14.79%

5.3 Results Discussion

A comparison of the calculated (estimated) error results and measured error results of the mentioned evaluation experiments (21 conditions with 3 cases of each operation) are shown in **Table 5-2**.

Table 5-2 Comparison of machining error

Experiment	Proposed Model	Conventional (α)	Mechanistic (β)	Statistical (γ)
Preliminary	Difference of	11.39	12.38	7.84
Evaluation	machining error (%)	19.20	24.18	14.79

From the obtained information of **Table 5-2**, presents a comparison of the machining error results between the conventional cutting conditions model (α), mechanistic model (β) and the statistical model (γ) in this research.

In the case of preliminary experiments which purposed to identify coefficient and construct the models, the average differences between the measurement machining error and the estimation machining error of the proposed error models were approximately 11.39%, 12.38%, and 7.84%, respectively. (see **Fig. B-1** to **Fig. B-3** in **Appendix B**)

Regarding the evaluation experiment, the average differences between the measurement machining error and the estimation machining error of the proposed error models were approximately 19.20%, 24.18%, and 14.79%, respectively. These results indicate that the proposed machining error models can be reasonably predicted when physical state values are appropriately predicted. **Figure 5-1** and **Figure 5-2** show the comparison of the machining error results obtained from the proposed conventional and mechanistic models. The error rates of both the maximum difference and distribution become large. **Figure 5-3** shows good agreement with the different machining error rate predictions than previous models, due to the PCA-based variables selection has been considered by the significant variable component relationship. These indicate that the proposed empirical models of machining error can estimate reasonable prediction when cutting force simulation and analysis of workpiece deformation predict the appropriate values.

6. Conclusion and Further Aspect

This chapter is the final chapter of this dissertation which will express the conclusion of this research. Afterward, the tendency of the research will be presented as a further aspect.

6.1 Conclusion

In this research, the conventional direct empirical modelling, mechanistic modelling, and statistical modelling of machining error were investigated. Using a quasi-two-dimensional cutting on an elastomer was a case study to predict the machining error. The results of the proposed models can be expressed by comparing the calculated and the measured machining error.

The proposed models were constructed by considering the variables of machining error from the cutting force measured in the experiment, the workpiece deformation, and the machining conditions. The correlation coefficient and multiple regression analysis were employed to create the model. The proposed models' accuracy was evaluated to confirm the validity of the results in the evaluation experiment.

In order to express the model results more clearly, the proposed models were compared. The systematic procedures were introduced as the modeling framework to construct and identify these error models. From the experimental evaluation, the feasibility of the proposed framework has been confirmed.

In the case of a suitable approach, it is appropriate to construct an effective data-centric model without only human insights. From these case studies of the machining error prediction, the proposed procedure can instruct the construction of a suitable error model in the end-milling.

6.2 Further Aspect

The further aspect of research could target to improve more prediction accuracy of the machining error model. Firstly, designing a more precise preliminary experiment. Secondly, conduct data collection in a larger amount of machining experiments for evaluation. Next, consider changing for complex workpiece shape, the tool type, and other materials.

In addition, improving cutting force analysis and workpiece deformation in order to obtain more accuracy in error prediction is also necessary. Only conventional estimation is exactly insufficient. Therefore, the new theoretical formulas for cutting force prediction examining the appropriate release face contact length and uncut amount portion (residual) to define the suitable coefficients are currently studied.

Bibliography

- [1] J. Lin, M.M. Naim, L. Purvis, and J. Gosling, "The extension and exploitation of the inventory and order based production control system archetype from 1982 to 2015", *International Journal of Production Economics*, Vol.192, pp.135-152, 2017.
- [2] S. Mittal, M.A. Khan, D. Romero, and T. Wuest, "Smart manufacturing: Characteristics, technologies and enabling factors", *Proceedings of the Institution of Mechanical Engineers Part B Journal of Engineering Manufacture*, Vol.233, No.5, pp.1342-1361, 2019.
- [3] C. Siedler, P. Langlotz, and J.C. Aurich, "Identification of interactions between digital technologies in manufacturing System", *52nd CIRP Conference on Manufacturing Systems*, Vol.81, pp.115-120, 2019.
- [4] R. Oberle, S. Schorr, L. Yi, M. Glatt, D. Bahre, and J.C. Aurich, "A Use Case to Implement Machine Learning for Life Time Prediction of Manufacturing Tools", *53rd CIRP Conference on Manufacturing Systems*, Vol.93, pp.1484-1489, 2020.
- [5] K.D. Thoben, S. Wiesner, and T. Wuest, "Industries 4.0 and Smart Manufacturing - A Review of Research Issues and Application Examples", *International Journal of Automation Technology*, Vol.11, No.1, pp.4-16, 2017.
- [6] W. Drossel, I. Dani, and R. Wertheim, "Biological transformation and technologies used for manufacturing of multifunctional metal-based parts", *16th Global Conference on Sustainable Manufacturing - Sustainable Manufacturing for Global Circular Economy*, Vol.33, pp.115-122, 2019.
- [7] S.M. Bazaz, M. Lohtander, and J. Varis, "The prediction method of tool life on small lot turning process - Development of Digital Twin for production", *30th International Conference on Flexible Automation and Intelligent Manufacturing (FAIM2021)*, Vol.51, pp.288-295, 2020.
- [8] T.F. Carmon, and S. Nahmias, "A preliminary model for lot sizing in semiconductor manufacturing", *International Journal of Production Economics*, Vol.35, No.1-3, pp.259-264, 1994.
- [9] C. Kato, N. Hiraiwa, T. Arai, and J. Yanagimoto, "Multi-station molding machine for attaining high productivity in small-lot productions", *CIRP Annals, Manufacturing Technology*, Vol.67, pp. 293-296, 2018.

-
- [10] Y. Altintas, "Manufacturing Automation", Cambridge, UK: Cambridge University Press, 2000.
 - [11] H. Narita, and H. Fujimoto, "Analysis of Environmental Impact due to Machine Tool Operation", International Journal of Automation Technology, Vol.3, No.1, pp.49-55, 2009.
 - [12] K. Shirase, and K. Nakamoto, "Simulation Technologies for the Development of an Autonomous and Intelligent Machine Tool", International Journal of Automation Technology, Vol.7, No.1, pp.6-15, 2013.
 - [13] H. Pils, F. Klocke, and D. Lung, "Experimental Investigation on Friction under Metal Cutting Conditions", International Journal of Wear, Vol.310, pp.63-71, 2014.
 - [14] S. Takata: Generation of Machining Scenario and Its Applications to Intelligent Machining Operation, CIRP Annals, 42, 1, (1993) 531-534.
 - [15] K. Teramoto, J. Kaneko, T. Ishida, and Y. Takeuchi, "A Framework of Compositional Machining Simulation for Versatile Machining Simulation", Journal of Advanced Mechanical Design, Systems, and Manufacturing, Vol.2, No.4, pp.668-674, 2008.
 - [16] K. Teramoto, Y. Kuroishi, and M. Yamashita, "A Framework for Machining of Soft Objects", Proceeding of 5th International Conference on Leading Edge Manufacturing in 21st Century (LEM21), pp.365-368, 2009.
 - [17] S. Ratchev, W. Huang, and A.A. Becker, "Milling Error Prediction and Compensation in Machining of Low-rigidity Parts", International Journal of Machine Tools and Manufacture, Vol.44, No.15, pp.1629-164, 2004.
 - [18] N. Takahashi and J. Shinozuka, "Contributions of High-speed Cutting and High Rake Angle to the Cutting Performance of Natural Rubber", International Journal of Automation Technology, Vol.8, No.4, pp.550-560, 2014.
 - [19] K. Ichikawa, H. Saito, J. Kaneko, Y. Okuma, and K. Horio, "Estimation Method of Machining Error on Low Rigidity Workpiece for Tool Posture Planning", International Journal of Automation Technology, Vol.11, No.6, pp.964-970, 2017.
 - [20] C. T. McCarthy, M. Hussey, and M. D. Gilchrist, "On the Sharpness of Straight Edge Blades in Cutting Soft Solids: Part I - Indentation Experiments", Journal of Engineering Fracture Mechanics, Vol.74, No.14, pp.2205-2224, 2007.
 - [21] Z. Wu, K. Teramoto, T. Araki, and H. Matsumoto, "Research on Mechanistic Modeling of Machining Error for Model-based Elastomer End-milling", Proceeding of 9th International Conference on Leading Edge Manufacturing in 21st Century (LEM21), pp. 104-108, 2017.

-
- [22] Y. Altintas, P. Kersting, D. Biermann, E. Budak, B. Denkena, and I. Lazoglu, "Virtual Process Systems for Part Machining Operation", *CIRP Annals, Manufacturing Technology*, Vol.63.2, pp. 585-605, 2014.
- [23] S. R. Lavoie, R. Long, and T. Tang, "A Rate-Dependent Damage Model for Elastomers at Large Strain", *Extreme Mechanics Letters*, Vol.8, pp.114-124, 2016.
- [24] R. Brighenti, F. J. Vernerey, and F. Artoni, "Rate-Dependent Failure Mechanism of Elastomers", *International Journal of Mechanical Sciences*, Vol.130, pp.448-457, 2017.
- [25] K. Teramoto, S. Kudo, and Y. Furuya, "In-process Observation of Workpiece Deformation in Elastomer Endmilling", *Proceeding of 7th International Conference on Leading Edge Manufacturing in 21st Century (LEM21)*, pp.259-262, 2013.
- [26] A. Kobayashi, "Special Machining Methods of Nonmetallic Materials", Education, Chijinshokan, 1965. (in Japanese)
- [27] A. J. Shih, J. Luo, M. A. Lewis, and J. S. Strenkowski, "Chip Morphology and Force in End Milling of Elastomers", *ASME, Journal of Manufacturing Science and Engineering*, Vol.126, No.1, pp.124-130, 2004.
- [28] K. Morikawa, K. Takahashi, and D. Hirotani, "Make-to-stock Policies for a Multistage Serial System under a Make-to-Order Production Environment", *International Journal of Production Economics*, Vol.147, pp.30-37, 2014.
- [29] M. Jin and M. Murakawa, "High-Speed Milling of Rubber (1st Report), Fundamental Experiments and Considerations for Improvement of Work Accuracy", *Journal of Japan Society for Precision Engineering*, Vol.64, No.6, pp.897-901, 1998. (in Japanese).
- [30] A.J. Shih, M.A. Lewis, and J.S. Strenkowski, "End Milling of Elastomers - Fixture Design and Tool Effectiveness for Material Removal", *ASME, Journal of Manufacturing Science and Engineering Transactions*, Vol.126, pp.115-123, 2004.
- [31] W.F. Hastings, P. Mathew, P.L.B. Oxley, and H. Ford, "A machining theory for predicting chip geometry, cutting forces etc. from work material properties and cutting conditions", *Proceeding of the Royal Society A - Mathematical, Physical, and Engineering Sciences*, Vol.371, No.1747, 1980.
- [32] Y. Ito, and T. Matsumura, "Theory and Practice in Machining Systems", Springer, SZ: Springer International Publishing, 2017.
- [33] W.H. Yang and Y.S. Tarng, "Design Optimization of Cutting Parameters for Turning Operations based on the Taguchi Method", *Journal of Materials Processing Technology*, Vol.84, No.1-3, pp.122- 129, 1998.

-
- [34] M. Nurhaniza, M.K.A.M. Ariffin, F. Mustapha, and B.T.H.T. Baharudin, "Analyzing the Effect of Machining Parameters Setting to the Surface Roughness during End Milling of CFRP - Aluminium Composite Laminates", *International Journal of Manufacturing Engineering*, Vol.2016, pp.1-9, 2016.
- [35] T. Childs, K. Maekawa, T. Obikawa, and Y. Yamane, "Metal Machining - Theory and Applications", John Wiley & Son, NY, 2000.
- [36] Z. Huda, "Machining Processes and Machines Fundamentals, Analysis, and Calculations", Taylor & Francis CRC Press, NY, 2021.
- [37] J. Yan and J.S. Strenkowski, "A Finite Element Analysis of Orthogonal Rubber Cutting", *Journal of Materials Processing Technology*, Vol.174, No.1-3, pp.102-108, 2006.
- [38] P.F. Zelaia and S.N. Melkote, "Statistical Calibration and Uncertainty Qualification of Complex Machining Computer Models", *International Journal of Machine Tools and Manufacture*, Vol.136, pp.45-61, 2019.
- [39] J.W. Sutherland and R.E. DeVor, "An Improvement Method for Cutting Force and Surface Error Prediction in Flexible End Milling System", *Journal of Manufacturing Science and Engineering*, ASME, Vol.108, No.4, pp.269-279, 1986.
- [40] J. Wang, Y. Ma, L. Zhang, R.X. Gao, and D. Wu, "Deep learning for smart manufacturing: Methods and applications", *Journal of Manufacturing Systems*, Vol.48, Part C, pp.144-156, 2018.
- [41] T. Matsumura, "Orthogonal Cutting Model and Cutting Force", *Handbook*, Japan Society of Precision Engineering (JSPE), 2019. (in Japanese)
- [42] M. Fahad, P.T. Mativenga, and M.A. Sheikh, "An investigation of multilayer coated (TiCN/Al₂O₃-TiN) Tungsten Carbide Tools in High Speed Cutting using a Hybrid Finite Element and Experimental Technique", *Proceedings of the Institution of Mechanical Engineers, Part B: Journal of Engineering Manufacture*, Vol. 225, No.10, pp.1835-1850, 2011.
- [43] T. Matsumura, and S. Tamura, "Cutting Force Model in Milling with Cutter Runout", *Proceeding of 16th CIRP Conference on Modelling of Machining Operations*, Vol.58, pp.566-571, 2017.
- [44] A. Priyadashini, S.K. Pal, and A.K. Samantaray, "Finite Element Modeling of Chip Formation in Orthogonal Machining", *Statistical and Computational Techniques in Manufacturing*, Springer Berlin Heidelberg, DE, 2012.
- [45] ASM Handbook, Volume 16-Machining, ASM International Handbook Committee, ASM International, 1989.

-
- [46] G. Ge, Z. Du, and J. Yang, "Rapid Prediction and Compensation Method of Cutting Force-induced Error for Thin-walled Workpiece", *International Journal of Advance Manufacturing Technology*, Vol. 106, pp.5453–5462, 2020.
- [47] K. Nakamoto and Y. Takeuchi, "Lecture Handbook: Basics of Production Processing Software Learned with Excel", *Nikkan Kogyo Shimbun*, pp.75-97, 2011. (in Japanese)
- [48] K. Teramoto and D. Watanabe, "Analysis of Machining Error in Soft Objects End-milling", *Proceeding of International Symposium on Flexible Automation*, 2010.
- [49] Y. Kakinuma, S. Kidani, and T. Aoyama, "Ultra-precision Cryogenic Machining of Viscoelastic Polymers", *CIRP Annals*, Vol.61, No.1, pp.79-82, 2012.
- [50] S. Tsurimoto and T. Moriwaki, "Experimental Study on Cutting of Silicone Rubber under Hydrostatic Pressure", *Journal of the Japan Society for Precision Engineering*, Vol.78, No.9, pp.782-786, 2012. (in Japanese)
- [51] K. Nakamoto, T. Iizuka, and Y. Takeuchi, "Dexterous Machining of Soft Objects by Means of Flexible Clamper", *International Journal of Automation Technology*, Vol.9, No.1, pp.83-88, 2015.
- [52] M. Putz, M. Dix, M. Neubert, and T. Schmidt, "Mechanism of Cutting Elastomers with Cryogenic Cooling", *CIRP Annals*, Vol.65, No.1, pp.73-76, 2016.
- [53] K. Furitani, K. Nakamoto, A. Beaucamp, and Y. Takeuchi, "Dexterous Creation of Soccer-Ball Pattern by Using Urethane Rubber", *International Journal of Automation Technology*, Vol.10, No.2, pp.239-243, 2016.
- [54] Y. Furuya, K. Teramoto, and S. Kudo, "Modeling Deformation in Elastomer End-milling", *Proceedings of JSPE Autumn Conference 2013*, pp.125-126, 2013. (in Japanese)
- [55] A. Chainawakul, K. Teramoto, Z. Wu, and T. Katsube, "Proposal of a Framework for Empirical Modeling of Complex Machining Phenomena", *Proceeding of 18th International Conference on Precision Engineering (ICPE2020)*, pp.47-48, 2020.
- [56] I. T. Jolliffe, "Principle Component Analysis", NY, Springer Press, 2002.
- [57] J.T. Bernard, and B. Cote, "The Measurement of the Energy Intensity of Manufacturing Industries: A Principal Components Analysis", *Journal of Energy Policy*, Vol.33, No.2, pp.221-233, 2005.
- [58] Y. Tan, J. Zhang, X. Li, Y. Xu, and C.Y. Wu, "Comprehensive Evaluation of Powder Flowability for Additive Manufacturing using Principal Component Analysis", *Journal of Powder Technology*, Vol.393, pp.154-164, 2021.

-
- [59] Q. Liu, Z. Gui, S. Xiong, and M. Zhan, “A Principal Component Analysis Dominance Mechanism Based Many-objective Scheduling Optimization”, *Journal of Applied Soft Computing*, Vol.113, Part B, pp.1-11, 2021.
 - [60] D.C. Montgomery and G.C. Runger, “Applied Statistics and Probability for Engineers 6th Edition”, John Wiley & Sons, Inc., NY, 2011.
 - [61] F. Hiramatsu and K. Teramoto, “FEM Simulation of Chip Separation Process in Elastomer End-milling”, *Proceeding of Hokkaido Conference Japan Society of Precision Engineering*, pp.7-8, 2016. (in Japanese)
 - [62] K. Teramoto, T. Kunishima, and H. Matsumoto, “Analysis of Cutting Force in Elastomer End-Milling”, *International Journal of Automation Technology*, Vol.11, No.6, pp.958-963, 2017.
 - [63] H. Narita. “A Determination Method of Cutting Coefficients in Ball End Milling Forces Model”, *International Journal of Automation Technology*, Vol.7, No.1, pp.39-44, 2013.
 - [64] K. Teramoto, D. Wu, K. Ota, and R. Hayashi, “A framework of Accuracy Assured Machining for Smart Manufacturing”, *Memoirs of Muroran Institute of Technology*, Vol.65, pp.35-39, 2015.
 - [65] M. Yang, and H. Park, “The prediction of cutting force in ball-end milling”, *International Journal of Machine Tools and Manufacture*, Vol.31, No.1, pp.45-54, 1991.
 - [66] A. Chainawakul, K. Teramoto, and H. Matsumoto, “Statistical Modelling of Machining Error for Model-based Elastomer End-milling” *International Journal of Automation Technology*, Vol.15, No.6, pp.852-859, 2021.

Appendix

Appendix A: Machining Error Results

Table A-1 Machining error obtained from preliminary experiments

#	WP size	M/C	M.E	RPM	x	y	fx/h	fy/h	$fx/(x*h)$	$fy/(y*h)$	F	DoC	WoC
1	10x10x20	begin	225.14	2000	104.350	91.350	1.715	7.281	0.016	0.080	0.025	10	1
2		middle	195.09	2000	50.500	129.475	3.943	6.224	0.078	0.048	0.025	10	1
3		end	252.67	2000	46.900	130.750	3.533	7.108	0.075	0.054	0.025	10	1
4	5x10x20	begin	150.26	4000	53.125	51.919	1.589	3.702	0.030	0.071	0.013	5	1
5		middle	121.26	4000	35.415	34.273	2.017	4.064	0.057	0.119	0.013	5	1
6		end	116.58	4000	29.858	57.417	1.947	4.184	0.065	0.073	0.013	5	1
7	10x20x20	begin	293.75	4000	237.188	165.388	1.712	5.674	0.007	0.034	0.025	10	1
8		middle	205.38	4000	96.331	143.275	1.678	8.055	0.017	0.056	0.025	10	1
9		end	197.09	4000	34.590	104.650	2.433	7.876	0.070	0.075	0.025	10	1
10	10x10x20	begin	58.88	4000	30.515	4.904	0.832	2.828	0.027	0.017	0.013	10	0.3
11		middle	56.16	4000	13.535	9.715	0.735	2.105	0.054	0.046	0.013	10	0.3
12		end	40.95	4000	15.827	8.467	0.697	2.061	0.044	0.041	0.013	10	0.3
13	10x10x20	begin	123.31	4000	51.294	43.044	0.704	2.907	0.014	0.148	0.013	10	0.7
14		middle	97.22	4000	14.148	27.915	0.570	3.584	0.040	0.078	0.013	10	0.7
15		end	100.15	4000	8.563	32.500	0.748	3.798	0.087	0.086	0.013	10	0.7
16	10x10x20	begin	149.56	4000	51.071	53.038	0.613	2.975	0.012	0.178	0.013	10	1
17		middle	120.79	4000	28.506	38.356	0.621	5.510	0.022	0.070	0.013	10	1
18		end	126.31	4000	13.787	54.894	0.535	5.170	0.039	0.106	0.013	10	1

Table A-2 Machining error obtained from evaluation experiments

#	WP size	M/C	M.E	RPM	x	y	fx/h	fy/h	$fx/(x*h)$	$fy/(y*h)$	F	DoC	WoC
1	10x10x20	begin	148.27	2000	69.475	33.125	1.804	2.780	0.026	0.084	0.025	10	0.5
2		middle	106.59	2000	43.700	33.125	2.341	3.123	0.054	0.094	0.025	10	0.5
3		end	104.94	2000	45.875	39.300	2.416	3.346	0.053	0.085	0.025	10	0.5
4	10x10x20	begin	178.2	2000	57.700	52.325	1.750	4.106	0.030	0.078	0.013	10	1
5		middle	155.11	2000	35.700	60.800	2.995	4.982	0.084	0.082	0.013	10	1
6		end	169.11	2000	59.100	55.725	2.981	5.313	0.050	0.095	0.013	10	1
7	10x15x20	begin	217.3	2000	140.200	122.400	1.702	4.961	0.012	0.041	0.013	10	1
8		middle	166.84	2000	81.800	90.500	3.647	5.371	0.045	0.059	0.013	10	1
9		end	223.38	2000	55.050	74.750	3.757	5.174	0.068	0.069	0.013	10	1
10	10x15x20	begin	268.91	2000	178.475	143.250	2.972	6.243	0.017	0.044	0.025	10	1
11		middle	251.79	2000	112.450	155.125	2.889	6.891	0.026	0.044	0.025	10	1
12		end	272.08	2000	46.275	135.175	3.314	8.118	0.072	0.060	0.025	10	1
13	10x10x20	begin	117.66	4000	55.175	49.475	1.819	4.119	0.033	0.083	0.013	10	1
14		middle	105.29	4000	30.375	36.800	2.387	4.728	0.079	0.128	0.013	10	1
15		end	105.99	4000	25.125	57.000	1.831	5.888	0.073	0.103	0.013	10	1
16	10x10x20	begin	221.72	4000	82.875	99.575	2.183	5.230	0.026	0.053	0.025	10	1
17		middle	205.68	4000	56.700	64.650	1.505	8.557	0.027	0.132	0.025	10	1
18		end	234.91	4000	18.075	107.400	2.320	8.172	0.128	0.076	0.025	10	1
19	5x10x20	begin	169.07	4000	50.505	38.240	6.605	3.093	0.131	0.081	0.009	5	1
20		middle	152.56	4000	11.188	29.313	1.472	3.464	0.132	0.118	0.009	5	1
21		end	142.47	4000	7.988	43.100	1.580	4.434	0.198	0.103	0.009	5	1
22	5x10x20	begin	189.46	4000	82.321	60.008	1.460	3.479	0.018	0.058	0.019	5	1
23		middle	175.42	4000	28.392	74.383	1.702	5.800	0.060	0.078	0.019	5	1
24		end	202.39	4000	37.935	74.148	2.695	6.033	0.071	0.081	0.019	5	1
25	5x10x20	begin	283.08	4000	101.012	91.288	1.702	5.064	0.017	0.055	0.025	5	1
26		middle	239.24	4000	33.769	67.160	2.822	6.533	0.084	0.097	0.025	5	1
27		end	229.91	4000	38.454	79.413	2.421	7.855	0.063	0.099	0.025	5	1
28	10x15x20	begin	119.28	4000	93.031	62.906	1.575	3.196	0.017	0.051	0.009	10	1
29		middle	86.53	4000	42.044	34.604	1.647	3.652	0.039	0.106	0.009	10	1
30		end	107.87	4000	3.231	41.400	1.641	4.510	0.508	0.109	0.009	10	1
31	10x15x20	begin	174.52	4000	105.079	66.981	0.916	3.689	0.009	0.055	0.013	10	1
32		middle	110.25	4000	40.327	64.067	1.517	5.298	0.038	0.083	0.013	10	1
33		end	118.58	4000	18.921	52.104	2.363	5.466	0.125	0.105	0.013	10	1

Table A-2 Machining error obtained from evaluation experiments (cont.)

#	WP size	M/C	M.E	RPM	x	y	fx/h	fy/h	$fx/(x*h)$	$fy/(y*h)$	F	DoC	WoC
34	10x15x20	begin	208.7	4000	134.856	100.994	1.632	4.909	0.012	0.049	0.019	10	1
35		middle	165.4	4000	56.858	64.233	1.991	6.810	0.035	0.106	0.019	10	1
36		end	179.65	4000	66.431	37.877	2.149	3.919	0.032	0.103	0.019	10	1
37	10x15x20	begin	270.83	4000	142.442	129.113	2.065	6.977	0.014	0.054	0.025	10	1
38		middle	201.3	4000	58.225	90.450	2.369	7.786	0.041	0.086	0.025	10	1
39		end	216.59	4000	3.825	120.692	2.168	6.825	0.567	0.057	0.025	10	1
40	10x20x20	begin	252.69	4000	170.644	96.113	1.223	3.545	0.007	0.037	0.009	10	1
41		middle	173.77	4000	87.756	80.550	1.391	4.165	0.016	0.052	0.009	10	1
42		end	184.62	4000	60.450	50.500	1.702	4.247	0.028	0.084	0.009	10	1
43	10x20x20	begin	210.99	4000	179.519	126.131	1.800	3.584	0.010	0.028	0.013	10	1
44		middle	148.95	4000	95.788	83.531	1.763	3.660	0.018	0.044	0.013	10	1
45		end	142.54	4000	54.867	97.510	1.557	5.109	0.028	0.052	0.013	10	1
46	10x20x20	begin	325.13	4000	212.913	147.585	1.901	5.607	0.009	0.038	0.019	10	1
47		middle	220.76	4000	122.756	95.000	1.848	6.278	0.015	0.066	0.019	10	1
48		end	216.29	4000	91.879	98.056	2.258	4.919	0.025	0.050	0.019	10	1
49	10x10x20	begin	78.17	4000	43.796	17.894	0.803	2.740	0.018	0.065	0.013	10	0.5
50		middle	62.791	4000	12.729	22.454	0.575	2.610	0.045	0.086	0.013	10	0.5
51		end	61.86	4000	20.648	20.800	0.434	2.157	0.021	0.096	0.013	10	0.5
52	10x10x20	begin	122	4000	43.900	37.698	0.885	2.658	0.020	0.142	0.025	10	0.3
53		middle	103.7	4000	24.935	28.902	1.143	3.231	0.046	0.089	0.025	10	0.3
54		end	112.3	4000	26.723	21.631	1.282	3.387	0.048	0.064	0.025	10	0.3
55	10x10x20	begin	179.2	4000	60.817	50.129	1.168	4.189	0.019	0.120	0.025	10	0.5
56		middle	163	4000	24.225	49.525	1.077	4.705	0.044	0.105	0.025	10	0.5
57		end	153.6	4000	31.369	60.544	1.212	3.975	0.039	0.152	0.025	10	0.5
58	10x10x20	begin	216.3	4000	69.400	89.573	1.107	5.648	0.016	0.159	0.025	10	0.7
59		middle	207.7	4000	45.831	57.237	1.176	5.181	0.026	0.110	0.025	10	0.7
60		end	206.2	4000	33.406	66.396	1.095	6.304	0.033	0.105	0.025	10	0.7
61	10x10x20	begin	244.9	4000	59.813	79.431	0.978	7.577	0.016	0.105	0.025	10	1
62		middle	237.1	4000	42.344	78.444	1.089	7.767	0.026	0.101	0.025	10	1
63		end	255.2	4000	22.435	80.942	1.096	7.892	0.049	0.103	0.025	10	1

Appendix B: Preliminary Experiment Machining Error Results

In the case of preliminary experiments which purposed to identify coefficient and construct the models, the average differences between the measurement machining error and the estimation machining error of the conventional cutting conditions, the mechanistic, and the statistical models were approximately 11.39%, 12.38%, and 7.84%, respectively.

Table B-1 Multiple regression analysis of the conventional model for preliminary

Regression Statistics	
Multiple R	0.941833
R Square	0.887049
Adjusted R Square	0.879989
Standard Error	22.693727
Observations	18

ANOVA	df	SS	MS	F	Significance F
Regression	1	64712.55	64712.55	125.65	5.4856E-09
Residual	16	8240.08	515.01		
Total	17	72952.64			

	Coefficients	Standard Error	t Stat	P-value	Lower 95%	Upper 95%	Lower 95.0%	Upper 95.0%
Intercept	16.5069	12.7418	1.2955	0.2135	-10.5045	43.5183	-10.5045	43.5183
m. error	0.8870	0.0791	11.2096	0.0000	0.7193	1.0548	0.7193	1.0548

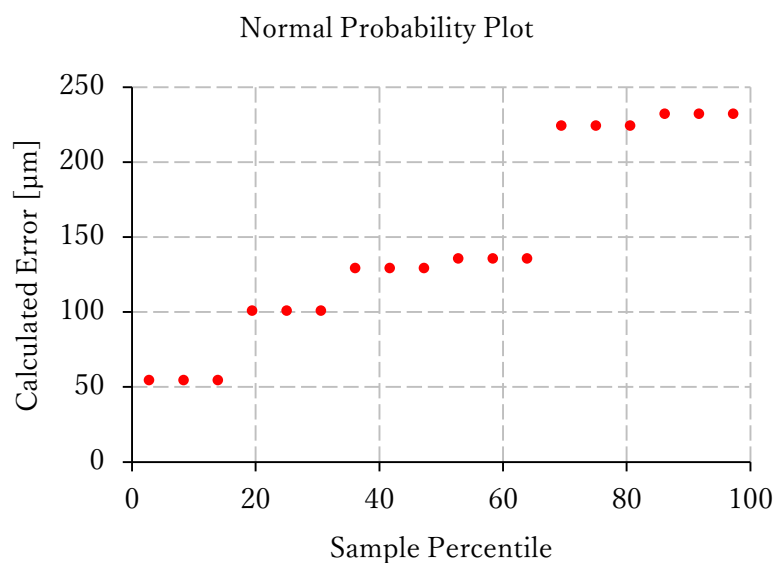


Fig. B-1 Normal probability of the conventional model for preliminary

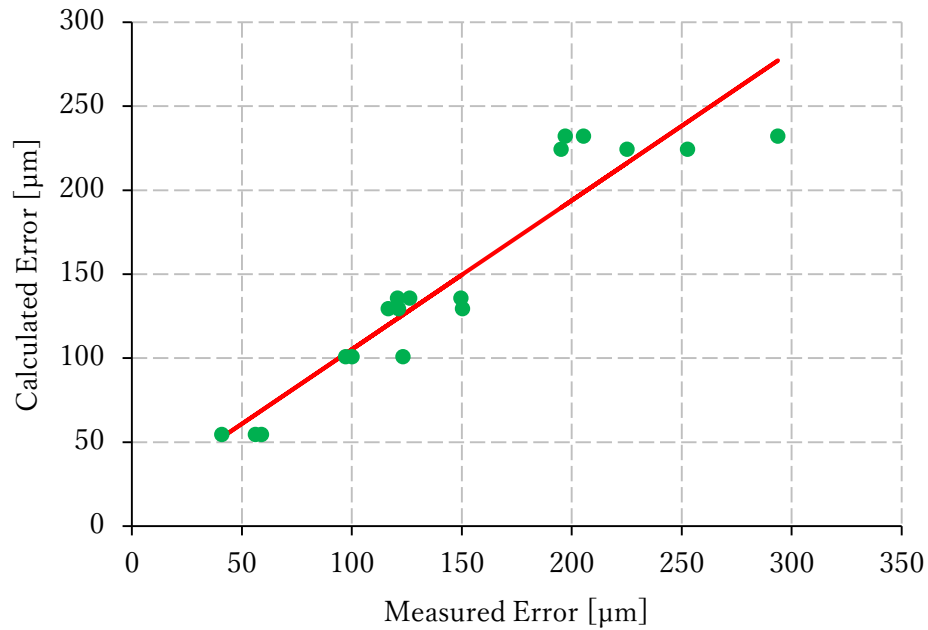


Fig. B-2 Preliminary machining error comparison of the conventional model

Table B-2 Multiple regression analysis of the mechanistic model for preliminary

Regression Statistics	
Multiple R	0.97091
R Square	0.94267
Adjusted R Square	0.93909
Standard Error	16.66695
Observations	18

ANOVA	df	SS	MS	F	Significance F
Regression	1	73082.47	73082.47	263.09	2.35231E-11
Residual	16	4444.60	277.79		
Total	17	77527.06			

	Coefficients	Standard Error	t Stat	P-value	Lower 95%	Upper 95%	Lower 95.0%	Upper 95.0%
Intercept	8.3783	9.3580	0.8953	0.3839	-11.4597	28.2162	-11.4597	28.2162
m. error	0.9427	0.0581	16.2200	0.0000	0.8195	1.0659	0.8195	1.0659

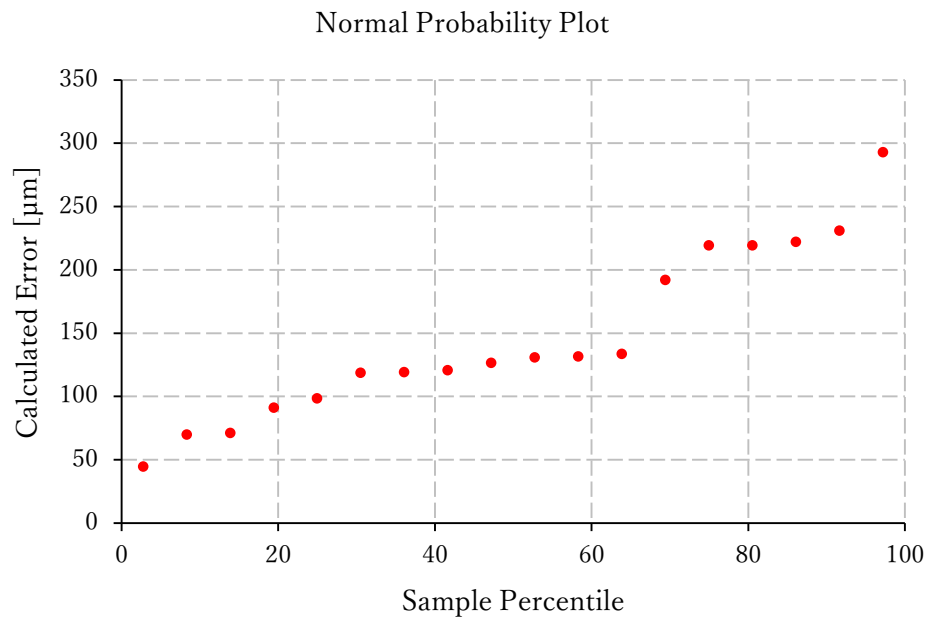


Fig. B-3 Normal probability of the mechanistic model for preliminary

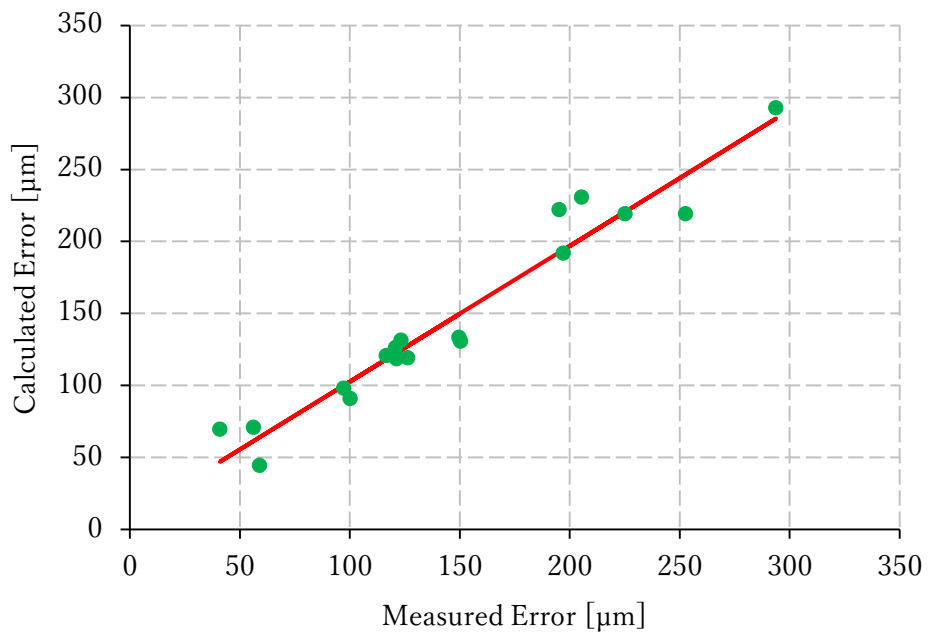


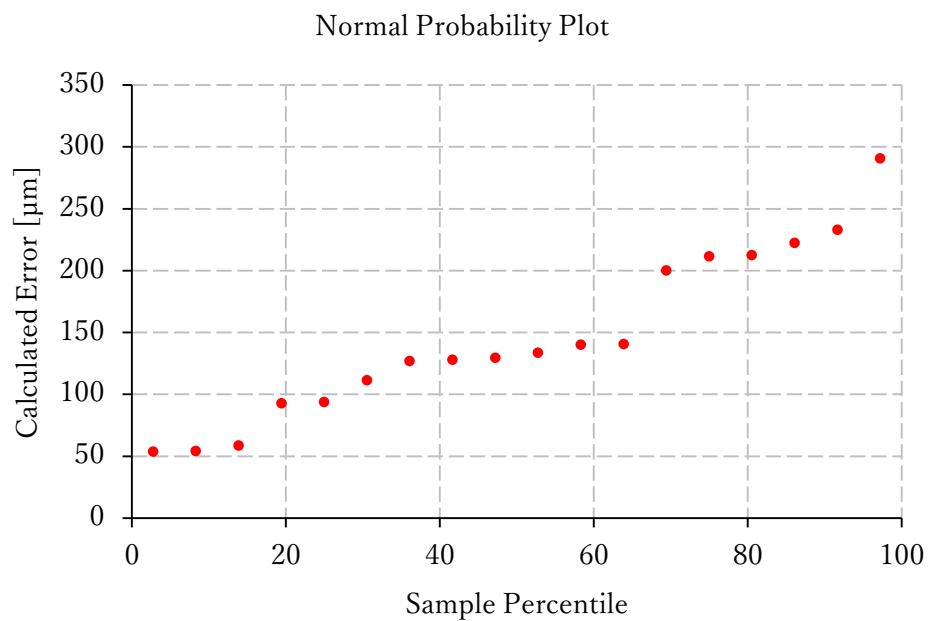
Fig. B-4 Preliminary machining error comparison of the mechanistic model

Table B-3 Multiple regression analysis of the statistical model for preliminary

Regression Statistics	
Multiple R	0.97685
R Square	0.95423
Adjusted R Square	0.95137
Standard Error	14.98287
Observations	18

ANOVA	df	SS	MS	F	Significance F
Regression	1	74886.37	74886.37	333.59	3.86022E-12
Residual	16	3591.78	224.49		
Total	17	78478.15			

	Coefficients	Standard Error	t Stat	P-value	Lower 95%	Upper 95%	Lower 95.0%	Upper 95.0%
Intercept	6.6883	8.4124	0.7951	0.4382	-11.1452	24.5218	-11.1452	24.5218
m. error	0.9542	0.0522	18.2644	0.0000	0.8435	1.0650	0.8435	1.0650

**Fig. B-5** Normal probability of the statistical model for preliminary

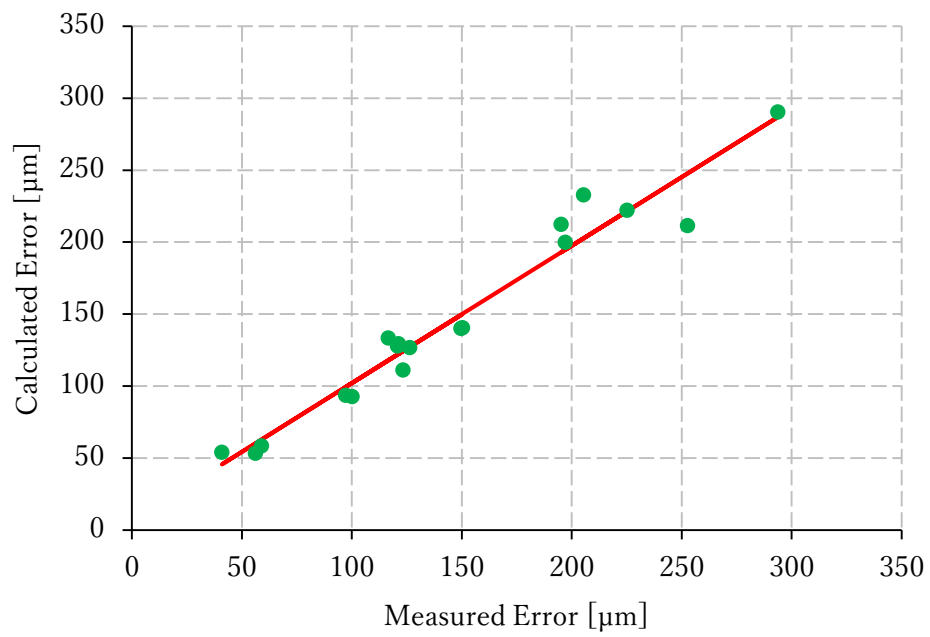


Fig. B-6 Preliminary machining error comparison of the statistical model

Appendix C: PCA Programming

Table C-1 PCA source code using Python

```
# pip install factor-analyzer
# pip install matplotlib scipy scikit-learn

import pandas as pd
import numpy as np
from sklearn.decomposition import PCA #主成分分析
import matplotlib.pyplot as plt

df = pd.read_csv('E:\Python\reference\factor_analysis.csv')

# 行列の標準化
dfs = df.iloc[:, 1:].apply(lambda x: (x-x.mean())/x.std(), axis=0)
dfs.head(81)

# 主成分分析の実行
pca = PCA()
feature = pca.fit(dfs)

# データを主成分空間に写像
feature = pca.transform(dfs)

# 主成分得点
pd.DataFrame(feature, columns=[
    "PC{}".format(x + 1) for x in range(
        len(dfs.columns))
]).head(81)
```

(Plot with first and second principal components)

```
plt.figure(figsize=(8,8))
plt.scatter(feature[:, 0], feature[:, 1], alpha=0.8, c=list(df.iloc[:, 0]))
plt.grid()
plt.title("principal component")
plt.xlabel("PC1")
plt.ylabel("PC2")
plt.show()

from pandas import plotting
plotting.scatter_matrix(
    pd.DataFrame(feature, columns=[
        "PC{}".format(x + 1) for x in range(len(dfs.columns))
    ]), figsize=(8,8), c=list(df.iloc[:, 0]), alpha=0.9
)

plt.show()

pd.DataFrame(
    pca.explained_variance_ratio_,
    index=["PC{}".format(x + 1) for x in range(len(dfs.columns))]
)

# 累積寄与率を図示する
import matplotlib.ticker as ticker
plt.gca().get_xaxis().set_major_locator(
    ticker.MaxNLocator(integer=True)
)

plt.plot([0] + list(
    np.cumsum(pca.explained_variance_ratio_)
), "-o")
plt.xlabel("Number of principal components")
plt.ylabel("Cumulative contribution rate")
plt.grid()
plt.show()
```


(PCA eigenvalues coding)

```
pd.DataFrame(  
    pca.explained_variance_,  
    index=["PC{}".format(x + 1) for x in range(len(dfs.columns))]  
)  
  
# PCA の固有ベクトル  
pd.DataFrame(pca.components_,  
    columns=df.columns[1:],  
    index=["PC{}".format(x + 1) for x in range(len(dfs.columns))]  
)  
  
# 第 1 主成分と第 2 主成分における変数の固有ベクトルをプロットする  
plt.figure(figsize=(8,8))  
for x, y, name in zip(pca.components_[0], pca.components_[1], df.columns[1:]):  
    plt.text(x,y,name)  
  
plt.scatter(pca.components_[0], pca.components_[1], alpha=0.8)  
plt.grid()  
plt.xlabel("PC1")  
plt.ylabel("PC2")  
plt.show()
```

Publication

International Journal

- Adirake Chainawakul, Koji Teramoto, and Hiroki Matsumoto. “Statistical Modelling of Machining Error for Model-Based Elastomer End-Milling”, International Journal of Automation Technology (IJAT), 2021, Vol. 15, No. 6, pp. 852-859.

International Conference

- Adirake Chainawakul, Koji Teramoto, Zejian Wu, Takahiro Katsube. “Proposal of a Framework for Empirical Modelling of Complex Machining Phenomena”, The 18th International Conference on Precision Engineering (ICPE2020), November, 2020.